Hilal ONAY

M.S. Thesis In Chemistry

July - 2009

SYNTHESIS AND CHARACTERIZATION OF NOVEL AMINO FUNCTIONALIZED PORPHYRAZINES

by

Hilal ONAY

July 2009

SYNTHESIS AND CHARACTERIZATION OF NOVEL AMINO FUNCTIONALIZED PORPHYRAZINES

by

Hilal ONAY

A thesis submitted to

the Graduate Institute of Sciences and Engineering

of

Fatih University

in partial fulfillment of the requirements for the degree of

Master of Science

in

Chemistry

July 2009
Istanbul, Turkey

APPROVAL PAGE

I certify that this thesis satisfies all the requirements as a thesis for the degree of Master of Science.

Assoc. Prof. Metin TÜLÜ
Head of Department

This is to certify that I have read this thesis and that in my opinion it is fully adequate, in scope and quality, as a thesis for the degree of Master of Science.

Assist. Prof. Ramazan ÖZTÜRK
Supervisor

Examining Committee Members

Assist. Prof. Ramazan ÖZTÜRK ……..

Assist. Prof. Burak ESAT ……..

Assist. Prof. Sadık GÜNER ……..

It is approved that this thesis has been written in compliance with the formatting rules laid down by the Graduate Institute of Sciences and Engineering.

Assoc. Prof. Nurullah ARSLAN

Director

July 2009

SYNTHESIS AND CHARACTERIZATION OF NOVEL AMINO FUNCTIONALIZED PORPHYRAZINES

Hilal ONAY

M. S. Thesis - Chemistry
July 2009

Supervisor: Assist. Prof. Ramazan ÖZTÜRK

ABSTRACT

Porphyrazines are constitutionally tetraazaanalogues of porphyrins and they have a characterisric central core with N atoms bridging the pyrrole rings instead of the CH groups present in the porphine and porphyrin skeleton. The fused heterocyclic groups on the peripheral positions, such as five membered selenodiazole (TSeDPz) provide a different electronic distribution for the porphyrazine macrocyclic core. The annulated 1,2,5-selenodiazole rings in the porphyrazine macrocycle, which can easily undergo different transformations, open up a new synthetic approach to octaaminoporphyrazines.

In this study, we have prepared the tetrakis(selenodiazole)porphyrazinato magnesium TSeDPzMg molecule from the tetramerization of 3,4-dicyano-1,2,5 selenodiazole ligand in propanol. After the demetallation of TSeDPzMg in the presence of trifluoroaceticacid, the metal free porphyrazine, $TSeDPzH_2$, has been prepared in resonable yield. The vanadyl complex has been prepared by the treatment of $TSeDPzH_2$ with $VOSO_4.5H_2O$ in DMSO. The All spectroscopic data and ESR measuments confirm the proposed vanadyl complex.

The tetrakis(cyclohexyl pyrazino)porphyrazine in which the porphyrazine molecule is annulated with six membered rings on the pepriferies was prepared by two different methods.In the first method, we first used H_2S in pyridine to open the annulated 1,2,5-selenodiazole rings in the porphyrazine macrocycle, in which the deselenation processes at the annulated selenodiazole rings in symmetrical and low-symmetry macrocycles and the formation of vicinal diamino functionalities have allowed the pyrazino groups formation by addition of 1,2 cyclohexadione porphyrazine macrocycles by ring reclosure. In the second method, 2,3-dicyano-5,6-cyclohexapyrazine ligand has been prepared and macrocylized in propanol and gave the pyrazino porphyrazine molecule in good yield. All spectroscopic data(FT-IR, UV and MALDI Mass) confirms the structure of the molecule.

Keywords: Porphyrazine, tetrakis, selenodiazole, pyrazino

YENİ AMİNO FONKSİYONLU PORFİRAZİNLERİN SENTEZİ VE KARAKTERİZASYONU

Hilal ONAY

Yüksek Lisans Tezi - Kimya
Temmuz 2009

Tez Yöneticisi: Yrd. Doç. Dr. Ramazan Öztürk

ÖZ

Porfirazinler porfirinlerin tetraazaanalogları olup porfin ve porfirin yapısındaki pirol halkalarını birbirine bağlayan CH gruplarının yerine N atomu ihtiva ederler. Bu nedenle de halka merkezi karakteristik bir yapıya sahiptir. Porfirazin molekülüne periferal konumlarda bağlanan beşli halka yapısındaki heterosiklik selenodiazol grupları, makrosiklik yapının halka merkezindeki elektron dağılımına normal porfirazin yapısından farklı bir özellik kazandırır. Bu yapıdaki 1,2,5-selenodiazol halkaları, kolayca farklı yapılara dönüştürülebilir özelliği ile oktaaminoporfirazin sentezine yeni bir yaklaşım getirmiştir.

Bu çalışmada, propanol içerisinde 3,4-disiyano-1,2,5 selenodiazol ligandının tetramerizasyonu ile tetrakis(selenodiazol)porphyrazinato magnezyum (TSeDPzMg) molekülü elde edildi. Daha sonra, sentezlenen porfirazin trifloroasetik asit ile metalsiz hale çevrilerek, iyi bir verimle ($TSeDPzH_2$) eldesi sağlandı. Hazırlanan metalsiz porfirazin DMSO içerisinde $VOSO_4.5H_2O$ ile muamele edilmek suretiyle vanadilli porfirazin kompleksi sentezlenerek, istenilen kompleksin elde edildiği çeşitli spektroskopik metodlar ve EPR ölçümleriyle doğrulandı.

Daha sonraki aşamada ise, periferal konumlarda altı halkalı heterosiklik gruplar ihtiva eden tetrakis(siklohekzilpirazino)porfirazin iki farklı metodla sentezlendi. Birinci metotta, piridin içerisindeki TSeDPzMg süspansiyonundan H_2S gazı geçirilerek açılan 1,2,5-selenodiazol halkalarından selenyum atomunun ayrılması sağlandı. Böylelikle elde edilen ürüne eklenen 1,2-siklohekzadion, oluşan komşu diamino uçlarına altılı halka oluşturacak şekilde bağlandı.

İkinci metotta ise, hazırlanan 2,3-disiyano-5,6-siklohekzapirazin ligandı propanol içerisinde tetramer haline getirilerek iyi bir verimle pirazino porfirazin elde edildi. Oluşan molekül çeşitli spektroskopik metodlarla (FT-IR, UV and MALDI Mass) karakterize edildi.

Anahtar kelimeler: Porfirazin, Tetrakis, selenodiazol, pirazino

ACKNOWLEDGEMENT

I am indebted to my research advisor Dr. Ramazan Öztürk for his personnel and professional guidance, kind help, unfailing suggestions and moral boosting. I also express my appreciation to our chairman Dr. Metin Tülü and all other professors.

With a deep sense of gratitude I acknowledge the support and encouragement of Anjum & Javed Kolkar, Pınar, Tevhide, Bahar, Sümeyye, Nürüfe, Fatma, Azize and all my other friends.

I appreciate whole-heartedly the encouragement given to me by my parents throughout my studies and deep sense of affection of my sister Neval and my brother Sunusi. Words are insufficient to express my appreciation and love to them.

TABLE OF CONTENTS

LIST OF FIGURES

LIST OF TABLES

LIST OF SYMBOLS AND ABBREVIATIONS

SYMBOL/ABBREVIATION

PH_2 : Porphine molecule
PzH_2 : Metal-free Porphyrazine
PzM : Metal complex of porphyrazine
PcH_2 : Metal-free Phthalocyanine
PcM : Metal complex of Phthalocyanine
MPA : Metalloporphyrazine
HMDS : Hexamethyldisilazane
PDT : Photo Dynamic Therapy
OL : Optical Limiting
TTDPzM : Metal complex of Tetrakis(thiadiazole)porphyrazine
TSeDPzM : Metal complex of Tetrakis(selenodiazole)porphyrazine
$TTDPzH_2$: Metal-free Tetrakis(thiadiazole)porphyrazine
$TSeDPzH_2$: Metal-free Tetrakis(selenodiazole)porphyrazine
OAPzMg : Octaaminoporphyrazinato Magnesium
$[(Pyz)_4PzM]$: Metal complex Tetrapyrazino porphyrazine
TSeDPzVO : Vanadyl Tetrakis(selenodiazole)prphyrazine
TCPyzPz : Tetrakis(cyclohexyl pyrazino)porphyrazine
p-TSA : Paratoluenesulfonic acid
DAMN : Diaminomaleonitrile
Py : Pyridine
DMF : Dimthylformamide
DMSO : Dimethylsulfoxide
HOMO : High Occupied Molecular Orbital
LUMO : Low Unoccupied Molecular Orbital

FT-IR : Fourier Transform Infrared

EPR : Electron Paramagnetic Resonance

λ_{ex} : Excitation wavelenght

CHAPTER 1

INTRODUCTION

1.1 GENERAL INFORMATIONS ABOUT TETRAPYRROLIC MACROCYCLES

Porphyrins and porphyrazines are the two main classes of tetrapyrrolic ring systems which are derived from the basic porphine molecule ([PH_2], Fig.1.1). Porphyrazines are constitutionally tetraazaanalogues of porphyrins since they have a porphyrazine-type central core with N atoms bridging the pyrrole rings instead of the CH groups present in the porphyrin skeleton ([PzH_2], Fig. 1.1). Porphyrazines are derived exclusively from synthetic laboratory work, whereas porphyrins are either naturally occurring molecular systems or original synthetic products. The best known and most widely studied class of porphyrazines are the phthalocyanines which contain benzenoid rings fused to the macrocyclic periphery (tetrabenzoporphyrazines; exemplified in Fig.1.1 as [PcM] with Pc=phthalocyaninato dianion, $C_{32}H_{16}N_8^{2-}$, and M=bivalent non-transition or first-row transition metal ion) [1].

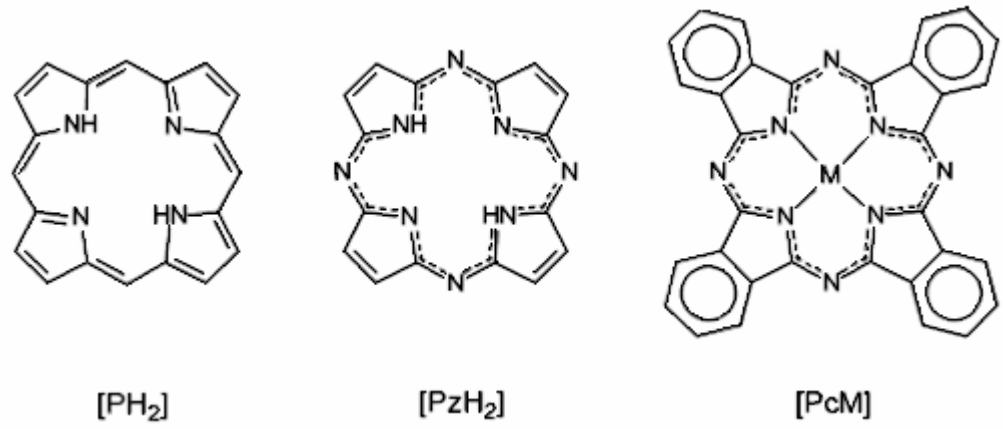

Figure 1.1 Porphine (unsubstituted porphyrin) [PH_2], porphyrazine [PzH_2] and phthalocyanine [PcM]

All porphyrins, porphyrazine-type macrocycles share a common substructure which consists of four pyrrolic subunits. Like porphyrins, porphyrazines also contain a 22-π electron system, and this feature imports porphyrazines wide range of extraordinary properties such as the ability to absorb visible light, to mediate the conversion of absorbed light to other forms of chemical and physical energy, and to enhance thermodynamic and kinetic stability [2]. These conjugated systems assume many resonance forms and can accept substituents at a number of positions. A porphyrin has 12 positions available including eight β positions and four *meso*-positions (Fig. 1.2), whereas porphyrazines, phthalocyanines, and naphthalocyanines have 8, 16 and 24 positions available for substitution, respectively. So far, many photosensitisers bearing numerous and bulky substituents have been synthesized in literature [3-5].

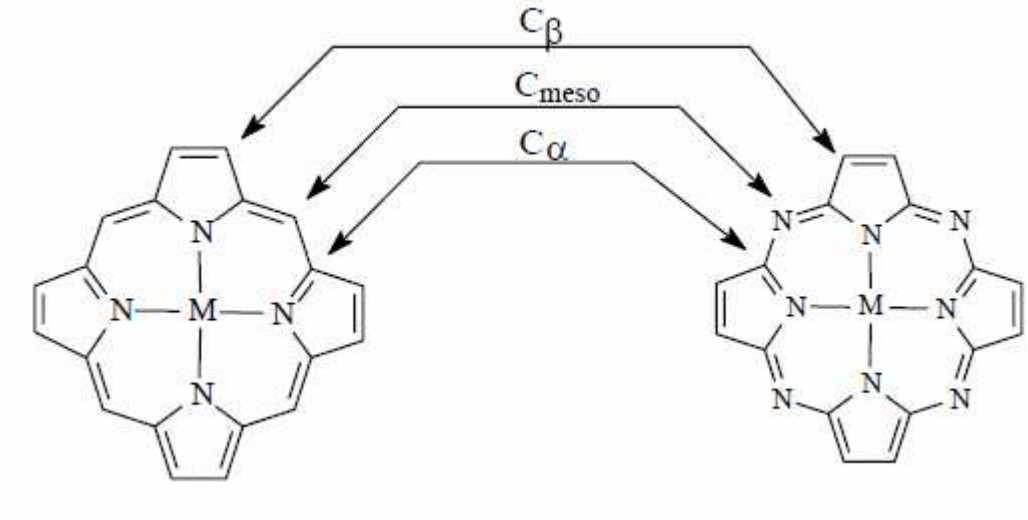

porphyrin *porphyrazine*

Figure 1.2 Positions of carbon atoms in the macrocycles [2]

1.2 PORPHYRAZINES

Porphyrazines and their structural analogs belong to a broad class of macroheterocyclic tetrapyrrole systems that are constitutionally tetraaza analogues of porphyrins. These porphyrins are of considerable interest because their representatives are components of the most important natural compounds (hemoglobin (Fig. 1.3), myoglobin, cytochromes, chlorophylls, and others) and are involved in such vital processes including photosynthesis, cell respiration, and electron transport.

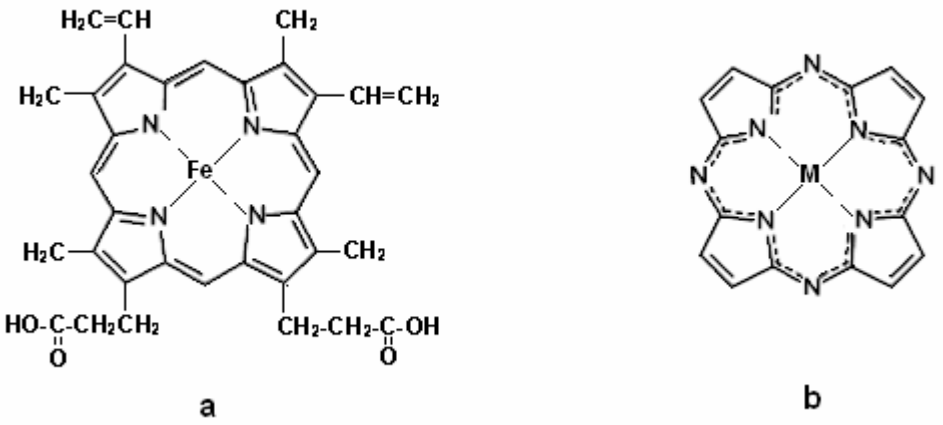

Figure 1.3 Hemoglobin (a) as a natural porphyrin and the simplest porphyrazine (b)

Recently, heteroatomic substitutions directly fusing to the macrocyclic periphery have brought an increasing attention to the porphyrazine studies [6-10]. Relative ease of their synthetic preparation, and also the strong correlation between the nature of the substituent and the electronic and optical properties of the macrocyclic ring system play roles on this recent interest. Comparing to the phthalocyanine analogues, direct fusion of heteroatomic substituents onto the porphyrazine β-positions results in an evident effect; on the other hand, there is no such accessible analogous derivatives for the porphyrins.

In comparison to the phthalocyanine counterparts, the porphyrazines also often display a vastly increased solubility in organic solvents. Thus, they maintain a unique position among the tetrapyrrolic macrocycles, and their straightforward synthesis coupled with their tuneable electronic and optical properties, renders them exciting candidates for a whole range of applications [11].

Porphyrazines are considerably less studied than phthalocyanines. There have been several positive properties of porphyrazines, specifically those closest to synthetic analogs of phthalocyanines and their high stability against oxidation favoring their use in wide practical application as dyes and pigments. Recently, porphyrazines have found several applications in new fields such as bleachable dyes in laser technique, discotic liquid crystals, components of electrochromic and electrophotographic materials, gas sensors, radiation protectors, catalysts of various processes (in particular, electrochemical), antimicrobial drugs, in luminescent diagnostics and photodynamic therapy of cancer tumors [12,13].

1.2.1 General Synthesis Methods

The porphyrazine ring has amphoteric properties, which in acidic media acts as a base due to μ-nitrogen atoms, while in basic media it results in acidic properties due to ionization of central imino groups (Fig. 1.4). The basic Porphine (PH_2) from which porphyrazine ring derived forms complexes with many metals of various groups of the Periodic system of elements. Various methods for the preparation of metal-porphyrazine complexes (MPA) from other porphyrazine derivatives or 1,2-dicyanoethenes are known [14-17]. These methods include (a) fusion of ethene-1,2-dicarbonitriles with metals or their salts, sometimes in the presence of urea; (b) boiling of solutions of ethene-l,2-dicarbonitriles with metals, their salts, or alkoxides (for example, magnesium alkoxide), often in the presence of a catalyst (for example, ammonium molybdate); (c) boiling of an (PH_2) solution with metal salts; and (d) boiling of solutions of labile metal complexes of porphyrazine (for example, magnesium complex) with metal salts.

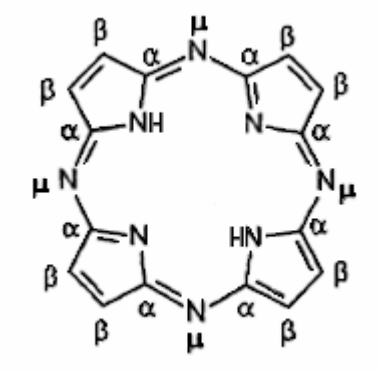

Figure 1.4 Positions for a porphyrazine molecule

One of the synthesis methods of porphyrazines is tetramerization of pyrrole derivatives by analogy with the known synthesis of porphyrins, namely: by reaction of 4-ethyl-3-methylpyrrole with bromine and ammonia or by treatment of 4-ethyl-3-methylpyrrole-2,5-diisocyanate with a mixture of pyridine and tetramethylammonium hydroxide. However, tetraethyltetramethyl-porphyrazine has been obtained only in low yields (Fig. 1.5) [18,19].

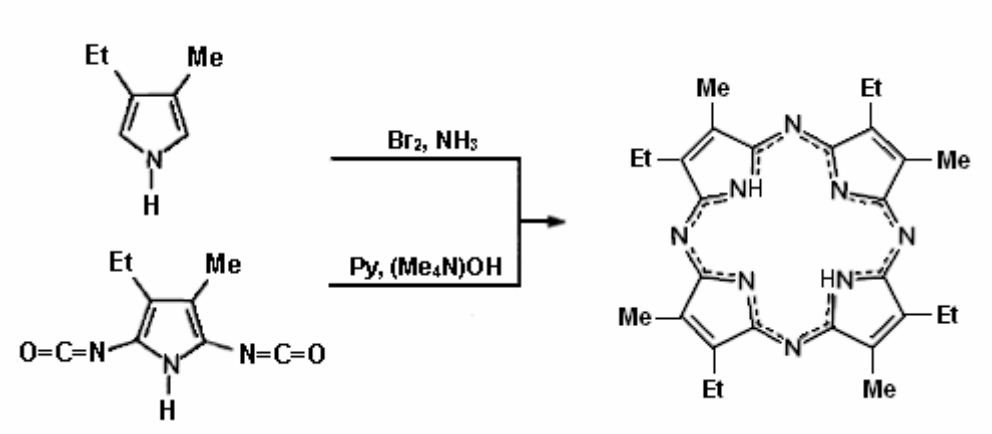

Figure 1.5 Synthesis of porphyrazine by tetramerization of pyrrole derivatives [18]

The existing methods for synthesizing porphyrazine are based on the tetramerization of derivatives of the corresponding 1,2-dicarboxylic acids, maleonitriles (Z-1,2-dicyanoethenes), or their adducts with ammonia, 2-amino-5-iminopyrrolenines. The cyclic system is initially closed to form dehydro-porphyrazine, which then is reduced to porphyrazine under the reaction conditions.

In 1952, Linstead reported a general approach to porphyrazine macrocyclization, using magnesium alkoxide and maleonitrile reagent to synthesize the unsubstituted porphyrazine (Fig.1.6) [11]. This is still the most widely used method for porphyrazine formation since then. Cyclotetramerization (Fig. 1.7) of the maleonitrile reagent(s) templated by a divalent magnesium ion results in the formation of porphyrazine products that contain a magnesium ion in the central cavity. Magnesium porphyrazines are easily demetallated under acidic conditions to form the free-base porphyrazine ligand, which subsequently can be complexed to a plethora of metallic centers.

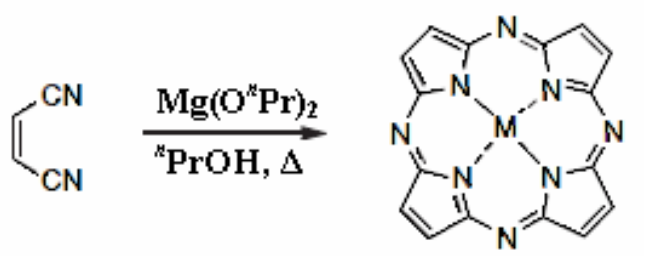

Figure 1.6 Cyclotetramerization of the maleonitrile reagent

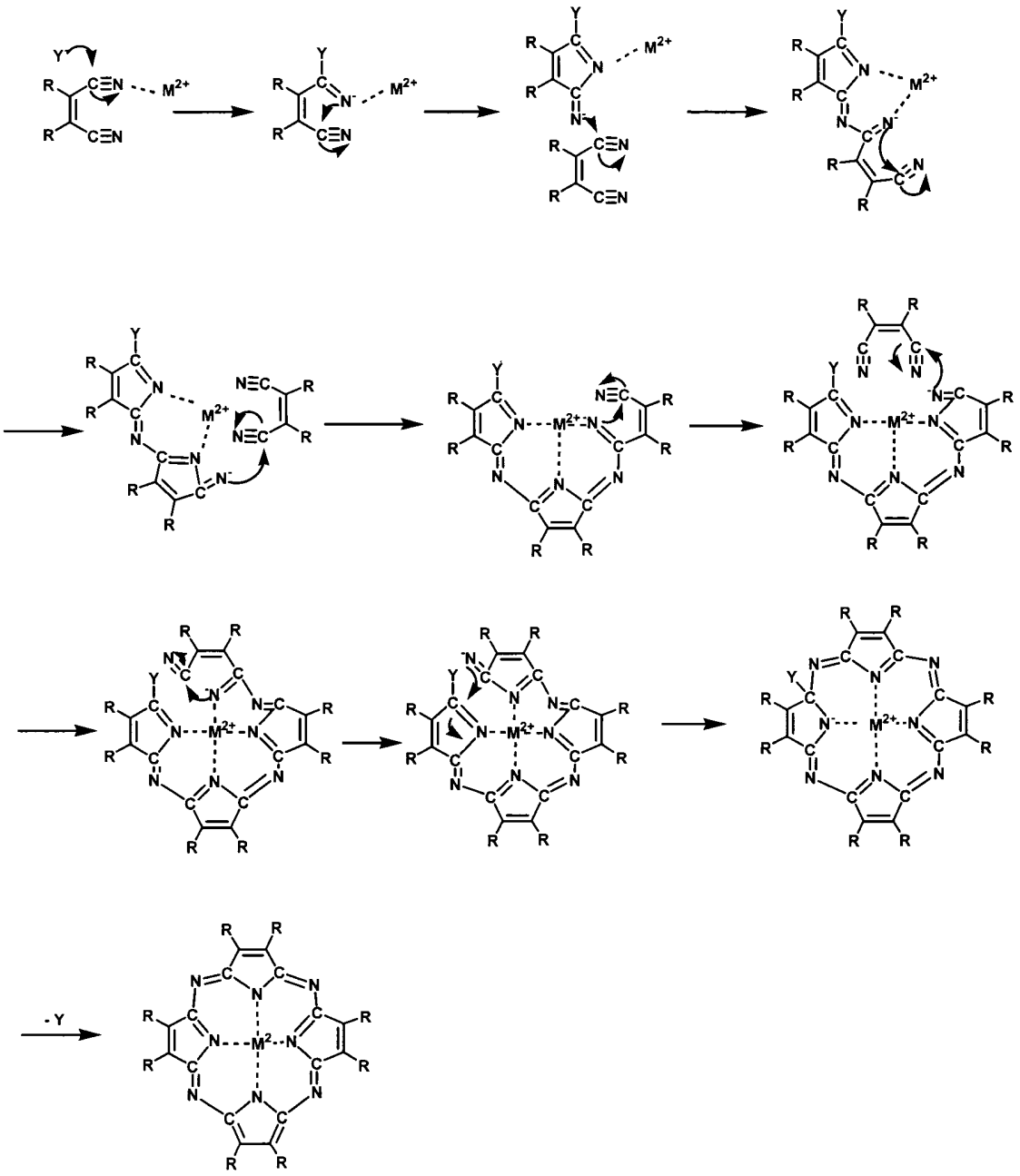

Figure 1.7 Possible mechanism for porphyrazine cyclization [20]
(Y: nucleophile, most likely an alkoxide)

According to the studies by Ercolani and coworkers, it has come out that the magnesium is not the only template available in the synthesis of the porphyrazine macrocycles [21]. They used NaOEt and LiOAm instead of magnesium alcoholate to synthesize annulated diazepine ring fused porphyrazines. Thus, they demonstrated that sodium(I) and lithium(I) could also act as templates to produce the sodium ($PzNa_2$) or lithium ($PzLi_2$) porphyrazines respectively, in good yields. Besides, the lability of these

counter cations was exploited by performing direct metal-exchange reactions (rather than by demetallation) to produce Mn^{II}, Co^{II}, Cu^{II}, and Zn^{II} complexes. However, it has been found that these methods less effective for the electron-rich aminomaleonitrile reagents although they are efficient for the diazepino maleonitrile starting materials [11].

Additionally, there has been reported another method by Chandrasekharam and coworkers, a one-pot synthesis of metalloporphyrazines from maleonitrile starting materials with hexamethyldisilazane (HMDS), catalytic amount of *p*-toluenesulfonic acid and a metal template (ZnX_2, MgX_2, CuX_2, NiX_2, etc.) [22]. They used this method to produce amino-, thio-, and phenyl group including pophyrazines, and by using accelerating effect of microwave irradiation on the tetramerization, they could overcome long reaction time (10-24 h) problem [23].

Recently, Hofmann and his coworkers have synthesized a highly polar unsymmetrical porphyrazine on a large scale, with minimal chromatographic purification by employing a novel-one pot, 3-step sequence (Fig. 1.8) [24]. According to the method, two maleonitrile precursors, one of which was present as a mixture of *E*- and *Z*-isomers, were transformed, via the corresponding pyrroline diimine, into the target porphyrazine and its *seco*-porphyrazine derivative, which is under exploration as a targeted photodynamic therapeutic agent.

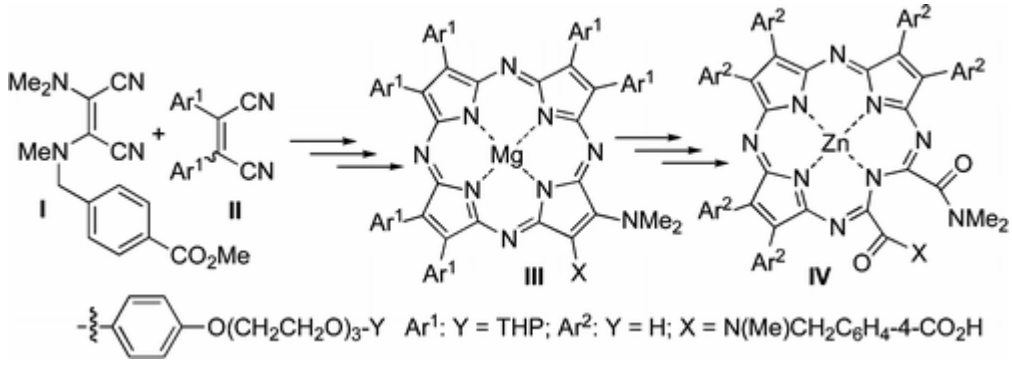

Figure 1.8 Highly polar unsymmetrical porphyrazines: Porphyrazine III has been synthesized on a large scale, with minimal chromatographic purification by employing a novel one-pot, 3-step sequence. Two dinitrile precursors I and II, the latter of which consisted of a mixture of geometric isomers, were transformed, via the corresponding pyrroline diimines, into a mixture of III and the octa-Ar1-porphyrazine. Isolated macrocycle III was subsequently transformed into IV, a water-soluble seco-porphyrazine suitable for the labeling of biological vectors [24].

1.2.2 Applications of Porphyrazines

1.2.2.1 Porphyrazines as Catalysts

The enhanced stability of porphyrazine derivatives toward the action of oxidants compared to phthalocyanines and porphyrins brings them into the class of very promising catalysts of various oxidation processes. The studies in this direction have emerged for the creation of efficient and stable catalysts within this class of compounds. For example, the introduction of 10^{-4}-10^{-5} mol L^{-1} of Co^{II} porphyrazine increases the reaction rate and the selectivity of styrene transformation in the liquid-phase oxidation of styrene by molecular oxygen in chlorobenzene at 120 °C [25]. The epoxidation is realized by activated oxygen due to the formation of its complex with the catalyst. Mn^{III} porphyrazine complexes are also efficient catalysts of olefin epoxidation by peracetic acid under mild conditions [26]. Further search for efficient catalysts of hydroxylation of saturated hydrocarbons like cytochrome P-450 was accomplished by porphyrazines.

The Porphyazines have found to be more suitable than the porphyrins and phthalocyanines [27]. For instance, the oxidation of cyclohexane by cumene hydroperoxide in presence of Co^{II} and Fe^{II} porphyrazines complexes gives a mixture of cyclohexanol and cyclohexanone with an overall yield of 60% [8]. In case of tetracyanotetrakis(o-trifluoromethylphenyl)-Co^{II} porphyrazine, the yield of cyclohexanol and cyclohexanone was 74 % and the catalyst is completely retained, while Co^{II} phthalocaynine completely decomposed under analogous conditions. Zn-poprhyrazine is an efficient sensitizer for the photochemical oxidation of 1,5-dihydroxynaphthalene by air oxygen to form 5-hydroxy-l,4-naphthoquinone (juglone), the known preservative for food industry [8].

One area of interest for the application of the metalloporphyrazines lies in their ability to act as catalysts for organic transformations. Perhaps in part, because of their similarity to the naturally occurring porphyrinic oxygenase enzymes, many reports have focused on their use as oxidation catalysts. For example, Deng and coworkers have explored the use of iron(II) thioporphyrazines in the oxidative degradation of organic pollutants, which mimic the structure of iron-containing cytochrome P450 enzymes [28,29]. In these studies, catalytic thioporphyrazines, in combination with hydrogen peroxide, were examined in the oxidative degradation of Rhodamine B. Related studies

by this group has examined the immobilization of such catalysts on anion-exchange resins [30,31]. Other studies of metal-catalyzed transformations using porphyrazine ligands include the catalytic antioxidant behaviour of manganese(II)/(III) Porphyrazines [32], and the use of oxygen-appended macrocycles as epoxidation catalysts [33].

1.2.2.2 Biomedical Agents

Phthalocyanine derivatives can be utilized as sensitizers in photodynamic therapy of cancer (PDT). Sensitizers for PDT require high photostability, high selectivity to tumors, no dark cytotoxity, strong absorption in the region between 600 and 800 nm where penetration of tissue is good, a long triplet lifetime, and satisfactory photosensitization of singlet oxygen. Phthalocyanine derivatives are known to satisfy the aforementioned conditions [34-39]. Nyokong et al. reported that phthalocyanine analogues, tetra-2, 3-pyridoporphyrazine and its quaternized compounds have excellent properties compared to zinc phthalocyanine-type photosensitizer [40]. The amphiphilic phthalocyanine derivatives were concluded the best compound for a new generation of photosensitizers for PDT [41].

The phthalocyanines are used as photosensitising agents which can be promoted to an electronically excited state by absorption of visible light wavelengths, thus promoting a sequence of photophysical, photochemical and photobiological events which result in the irreversible inactivation of a variety of biological systems [42]. The phthalocyanines are used to enhance the phototoxic action through their association with carriers such as liposomes and peptides which favour their accumulation in target cells. The chemical structure provides the antimicrobial phototoxic action of phthalocyanines [43].

1.2.2.3 Non-Linear Optics

In fact, following previous reports of cationic porphyrins as potential DNA-binding and cleavage agents [44], as well as sensitizers for PDT [45], is the first to report the synthesis of an octacationic pyridyl porphyrazine in 1999 [46]. These novel systems underwent standard metallation reactions were both freely soluble in water as the chloride salt, and showed strong binding to calf thymus DNA [47]. In continuation

of these studies, the synthesis of unsymmetrical pyridyl-substituted aminoporphyrazines was carried out. The resultant macrocycles displayed rich and varied redox chemistry and, therefore, show potential in the application to non-linear optics because of the presence of both donor and acceptor functionality [48]. Recently, Bordbar and co-workers have reported the synthesis of tetracationic cobalt porphyrazines, with pyridine rings directly fused to the periphery [49]. Open aperture Z-scan measurements have revealed that indium(III) porphyrazines are new nonlinear optical absorption (or reverse saturable absorption) materials at 532 nm. Optical limiting (OL) studies have further demonstrated that they are potential materials in sensors or human eye protections at the same wavelength. Due to their high photostability and good solubility in common organic solvents, these compounds could also be promising materials for fabrication of practical solid optical limiters [50]. The phthalocyanine and porphyrazine materials are photostable and highly soluble in common organic solvents and they show good process ability for solid optical limiter fabrication.

1.2.2.4 Chemical Sensors

In addition to the potential biomedical and non-linear optical applications of pyridyl-appended porphyrazines, it has been demonstrated that the synthesis of amino porphyrazines that bear pyridyl-based metal donor pockets [51]. Such systems show efficient binding of four equivalents of a variety of metal cations including heavy metals such as cadmium(II) and, therefore, have potential in sensor applications. To further investigate the potential of pyridyl-mediated metal binding, and also reported the synthesis of a bipyridyl-appended porphyrazine [48]. The dark conductivity changes which exposure to gases such as NO_2 and NH_3 cause to pthalocyanines in the form of thin films have also led to various chemical sensor studies [52-55]. Under certain conditions photoconductivity changes (determined by the same interdigitated microcircuit arrays used in the studies reported here), induced by the adsorption of gases, can exceed changes in dark conductivity, but the responses of the photoconductivity-based sensors are strongly dependent upon prior exposure to atmospheric O_2 [56]. The complete synthesis and characterization of a new family of peripherally functionalized porphyrazines with four, three, or two (in a trans conformation) bis[thioethoxy(ethoxy)ethanol] moieties appended at the pyrroles has

been shown to have applications as chemical sensors [57]. These “polyetherol” groups serve as weak exocyclic binding sites for a number of metal ions and also provide solubility of the porphyrazines in low molecular-weight alcohols and water. Modified porphyrazines exhibit distinct electronic spectral changes in the visible region (both absorbance and fluorescence) in response to treatment with Ag^{+}, Pb^{2+}, Cd^{2+}, Cs^{+}, and Ni^{2+} in solution. Such properties make these compounds intriguing candidates for incorporation into the transducer layers in optically based chemical sensors. The peripherally modified porphyrazines synthesized and spectroscopically investigated represent a unique class of selective metal-ion chelators that absorb/emit in the visible region. Solubility in polar media (alcohols and water) aids the quantification of the metal−macrocycle interactions in solution that finds application in chemical sensors.

CHAPTER 2

PORPHYRAZINES WITH ANNULATED S, N- AND Se, N-CONTAINING HETEROCYCLES

2.1 GENERAL INFORMATIONS

Two novel families of porphyrazines the tetrakis(thia/selenodiazole) porphyrazines, [TTDPzM] and [TSeDPzM] (Fig. 2.1), were reported by Ercolani and his co-workers in the years 1998 [58-61]. Since the peripheral pentaatomic heterocyclic rings of the TTDPz and TSeDPz skeletons are isoelectronic with the benzene rings present in the phthalocyanine analogues, these new macrocyclic species closely resemble the class of phthalocyanines, particularly [58]. These new macrocycles (called hereafter as "S- and "Se-porphyrazines") are isolated as stable solid materials and characterized by the presence of four heterocyclic five-membered rings, namely 1,2,5-thiadiazole and 1,2,5-selenodiazole (simplified hereafter as thia- and selenodiazole), annulated to the pyrrole rings of the porphyrazine core[1]. These S- and Se-containing porphyrazines structurally resemble to the phthalocyanine molecular framework and share with the phthalocyanine ring important properties like low solubility, stability, sublimability (S-compounds) and comparable chromophoric character, showing intense absorptions in the Soret and Q band regions [58]. However, due to the peripherally present strongly electron-withdrawing N–S–N and N–Se–N moieties, they show distinct electronic features, physicochemical behavior and reactivity. The electron deficiency of the thia/selenodiazole rings, contiguous to the porphyrazine core in these novel series of macrocycles as well as in their parent low-symmetry species, strongly influences the σ/π electronic distribution within the entire highly π-conjugated molecular system [1]. For these types of macrocycles, the UV/vis spectroscopy method is used due to learn the level of electron deficiency and comparison with the data on phthalocyanines adequately illustrates this aspect.

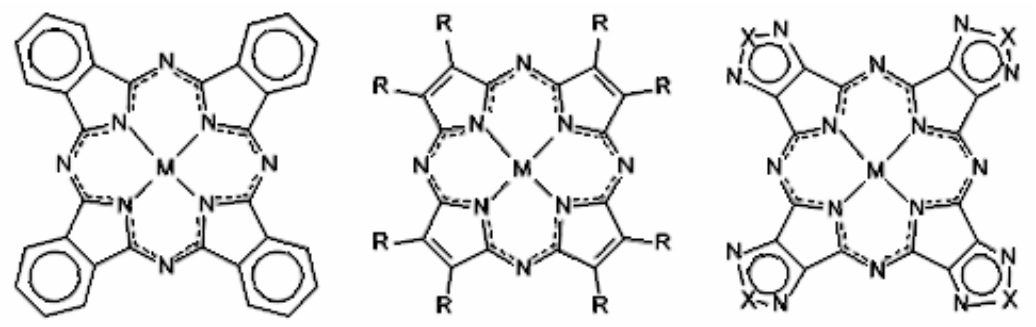

[PcM] **[R_8PzM]** **X=S - [TTDPzM]**
X=Se - [TSeDPzM]

Figure 2.1 Metallo phthalocyanine and porphyrazines with alkyl and annulated heterocycles

2.1.1 Synthetic Pathways

Due to the synthesis of these two novel families, S- and Se-porphyrazines, the dicyano compounds **1** and **2** (Fig. 2.2) are used as the key precursors, which can be easily obtained in a high yield by treatment of the inexpensive and commercially available diaminomaleodinitrile (DAMN) with $SOCl_2$ or SeO_2, respectively [58,59].

2.1.1.1 Symmetrical tetrakis(thia/selenodiazolo)porphyrazines

The preparation of [TTDPzMg(H_2O)] (**3**) or [TSeDPzMg(H_2O)] (**4**) has been reported as tetramerizations of **1** or **2** respectively in the presence of Mg^{II}-propylate or Mg^{II}-butylate in the corresponding alcohol under reflux (Linstead's method) [58,59]. The formulation of these two Mg^{II} complexes with one coordinated water molecule to the central metal atom has been established experimentally, in line with the such type of tetrapyrrolic systems, including the phthalocyanine Mg^{II} species [62,63]. CF_3COOH is the best solvent for demetalation of the both Mg^{II} complexes to form the free-base macrocycles **5** and **6**. Nevertheless short treatment with 94–98% H_2SO_4 is applicable for demetalation of the Se complex [TSeDPzMg(H_2O)] (**4**), but not for the sulfur analogue [TTDPzMg(H_2O)] (**3**), due to rapid hydroprotolytic destruction of the latter (in 96.6% H_2SO_4 $\tau_{1/2}$ = 21 and 1.3 min for **6** and **5**, respectively [64]).

Template macrocyclization is not an exclusive property of Mg^{II}. In fact, direct cyclotetramerization of dinitrile **1** has just been shown to occur easily with p metal salts [65]. Thus, reaction of **1** in hot quinoline with Al^{III} or Ga^{III} halides leads to the "S-porphyrazines" [TTDPzM(X)] (**9a**–**c**), whereas the In^{III} complex [TTDPzIn(OAc)] (**9d**)

is better obtained by complexation of [$TTDPzH_2$] with In^{III} acetate in acetic acid under reflux (Fig. 2.2).

As it is seen in the Table 2.1 symmetrical metal derivatives of S- and Se-porphyrazines (M=Mn^{II}, Fe^{II}, Co^{II}, Ni^{II}, Cu^{II}, Zn^{II}) could be prepared only by incorporating the metal centers into the freebases **5** and **6** with MX_2 salts in a coordinating solvent (pyridine, DMSO) [1].

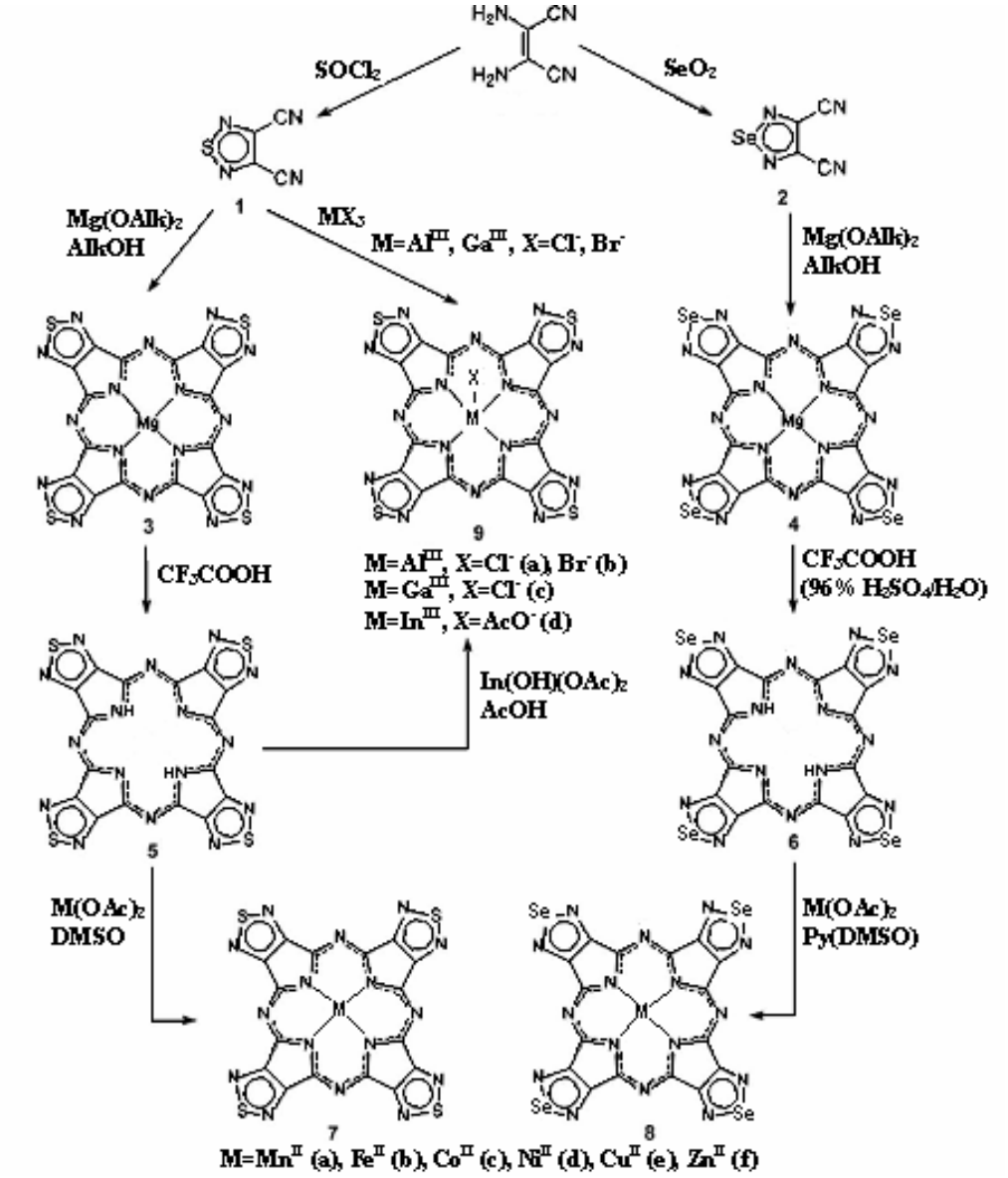

Figure 2.2 Template complexation of TTDPzM and TSeDPzM [1]

The main drawback of these two novel pophyrazine familes is solubility problem. Specific solvation occurring at the central metal atom or central NH groups in the free-base macrocycle provides them higher solubility in donor solvents such as pyridine, DMF and DMSO, but not in organic solvents [58]. Some solubility is also achieved in

acidic solvents (CF_3COOH, H_2SO_4) due to proton interaction with the *meso*- and heterocyclic N atoms. The presence of peripheral heterocycles also leads to a strong tendency of the solid samples to retain clathrated water and/or carboxylic acids. Indeed, all solid samples are usually obtained as highly solvated materials (see Table 2.1) and the number of solvent molecules (water, carboxylic acids) can vary from one preparation to another [1]. Tetrakis(thiadiazole)porphyrazines, unlike their Se-analogues, can be sublimed in a high vacuum [59,60] or under a slow flow of inert gas [66,67] giving materials or films with different crystallinity.

Table 2.1 Synthesis of tetrakis(thiadiazole)- and tetrakis(selenodiazole)porphyrazines [1]

M	No.	Synthetic procedures	Solvated form	Yield
TeTDPzM				
$2H^{I}$	5	3+CF_3COOH	[$TTDPzH_2$]	35
Mg^{II}	3	Dinitrile 1 +$Mg(OAlk)_2$	[$TTDPzMg(H_2O)$]·(H_2O)·(AcOH)	47
Mn^{II}	7a	5 +$Mn(OAc)_2$ in DMSO	[$TTDPzMn(DMSO)_2$]→[TTDPzMn]	70
Fe^{II}	7b	5 + $(NH_4)_2Fe(SO_4)_2$ in DMSO	[$TTDPzFe(DMSO)_2$]→[TTDPzFe]	85
Co^{II}	7c	5 + $Co(OAc)_2$ in DMSO	[TTDPzCo]·2(H_2O)	83
Ni^{II}	7d	5 + $Ni(OAc)_2$ in DMSO	[TTDPzNi]·2(H_2O)	70
Cu^{II}	7e	3 + $Cu(OAc)_2$ in CF_3COOH	[TTDPzCu]	44
		5 + $Cu(OAc)_2$ in pyridine	[TTDPzCu]	62
Zn^{II}	7f	5 + $Zn(OAc)_2$ in DMSO	[TTDPzZn]·2(H_2O)	90
Al^{III}	9a	Dinitrile 1 + $AlCl_3$ in quinoline	[TTDPzAlCl]·4(H_2O) (quinoline)	56
	9b	Dinitrile 1 + $AlBr_3$ in quinoline	[TTDPzAlBr]·4(H_2O) (quinoline)	39
Ga^{III}	9c	Dinitrile 1 + $GaCl_3$ in quinoline	[TTDPzGaCl]·2(H_2O) (quinoline)	35
In^{III}	9d	5 + $In(OH)(OAc)_2$ in AcOH	[TTDPzIn(OAc)]·2(H_2O)	55
TSeDPzM				
$2H^{I}$	6	4+CF_3COOH	[$TSeDPzH_2$]·3(H_2O)·(CF_3COOH)	65
		4 + 96% H_2SO_4/ice	[$TSeDPzH_2$]·3(H_2O)·(AcOH)	50
Mg^{II}	4	Dinitrile 2 +$Mg(OPr)_2$	[$TSeDPzMg(H_2O)$]·3(H_2O)·(AcOH)	70
$Mn^{I}I$	8a	6 +$Mn(OAc)_2$ in DMSO	[TSeDPzMn]·4(H_2O)·(AcOH)	67
		In pyridine	[TSeDPzMn(py)]·2(H_2O)·(AcOH)	61
Co^{II}	8c	6 + $Co(OAc)_2$ in DMSO	[TSeDPzCo]·5(H_2O)·(AcOH)	69
		In pyridine	[TSeDPzCo(py)]·3(H_2O)·(AcOH)	51
Ni^{II}	8d	6 + $Ni(OAc)_2$ in DMSO	[TSeDPzNi]·6(H_2O)·(AcOH)	72
		In pyridine	[TSeDPzNi(py)]·4(H_2O)·(AcOH)	60
Cu^{II}	8e	4 + $Cu(OAc)_2$ in CF_3COOH	[TSeDPzCu]·3(H_2O)·(AcOH)	47
Zn^{II}	8f	6 + $Zn(OAc)_2$ in DMSO	[TSeDPzZn]·4(H_2O)·(AcOH)	61
		In pyridine	[TSeDPzZn]·5(H_2O)·(AcOH)	48

2.1.1.2 Thia/Selenodiazoloporphyrazines with Low-Symmetry

The synthetic approach, in principle quite simple, leads to a mixture of two symmetrical porphyrazines (AAAA and BBBB) and four low-symmetry porphyrazines (AAAB, AABB, ABAB and ABBB). If the two dinitrile precursors, having equal reactivity, are taken in a 1:1 molar ratio, and their co-macrocyclization occurs in a two-step mechanism [1,78,79] first implying the formation of dimeric units followed by their coupling in the ultimate step, then the amounts of low-symmetry porphyrazines formed should be in the order AABB> AAAB, ABBB>ABAB [1,70].

Solubility problem of these novel families enforces chemists consider to study with porphyrazines carrying less than four annulated thiadiazole or selenodiazole rings [68-77]. Fig. 2.3 shows the full series of symmetrical and low-symmetry thia/selenodiazoloporphyrazines possibly formed by reaction of **1** or **2** in a template co-cyclotetramerization process with different precursors.

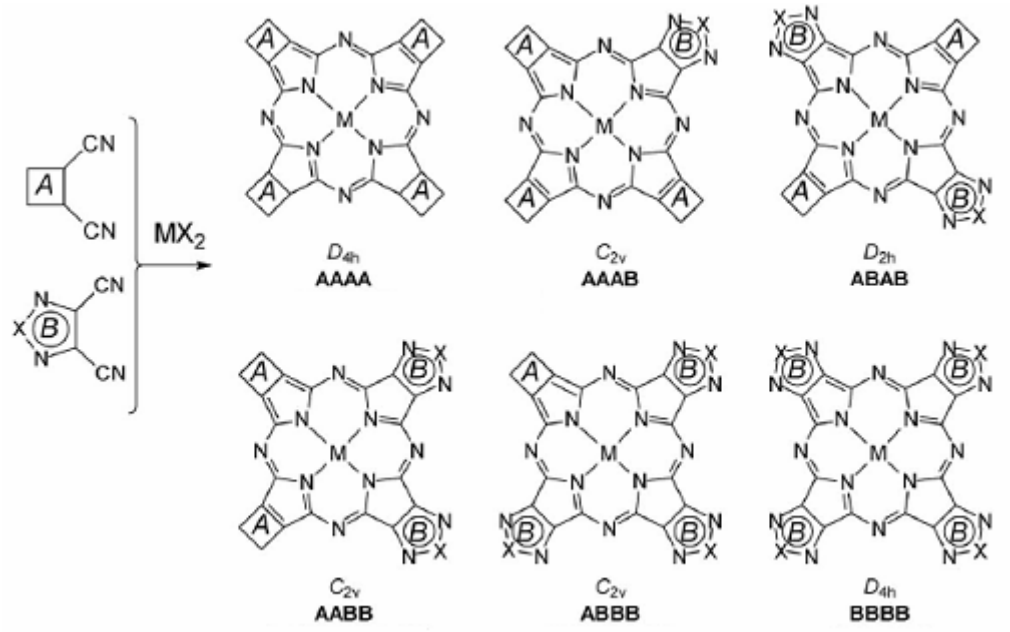

Figure 2.3 The full series of symmetrical and low-symmetry thia/selenodiazoloporphyrazines

2.1.1.3 Peripheral Modification of 1.2.5-Selenodiazolo Porphyrazines

One of the most relevant forms of reactivity shown by the Se-porphyrazines is that the annulated selenodiazole rings can undergo reductive ring opening under the action of H_2S with releasing of the Se atom and formation of vicinal diamino functionalities which are open to possible different kinds of derivatization [1,58], as shown in Fig. 2.4. The species formed, i.e. the octaaminoporphyrazine macrocycle,

which has been observed in solution but not isolated as a pure species in the solid state, can be directly converted, by reaction with an α-diketone (benzil), into a tetrapyrazinoporphyrazine system (specifically octaphenyl-tetrapyrazinoporphyrazine, $[(H_2N)_8PzM]$ (**10**), as a Mg^{II} complex) [58]. Attempts to directly form porphyrazines carrying vicinal NH_2 groups from diaminomaleodinitrile (Fig. 2.4) were unsuccessful [7]. It was first recognized by Ercolani and coworkers in 1999 [60] that the deselenation process could be applied to the symmetrical Mg^{II} and Cu^{II} complexes [TSeDPzMg] (**4**) and [TSeDPzCu] (**8e**) by bubbling H_2S into a pyridine (or DMF) solution. And they realized that obtained instable intermediate species could be straightforwardly used in situ for further transformations, as is exemplified in Fig. 2.4 for their conversion to pyrazinoporphyrazines $[(R_2Pyz)_4PzM]$ (**11**) by reaction with α-dialdehydes [60], or to an imidazole derivative $[(ImH)_4PzM]$ (**12**) by reaction with DMF in the presence of $POCl_3$ [7].

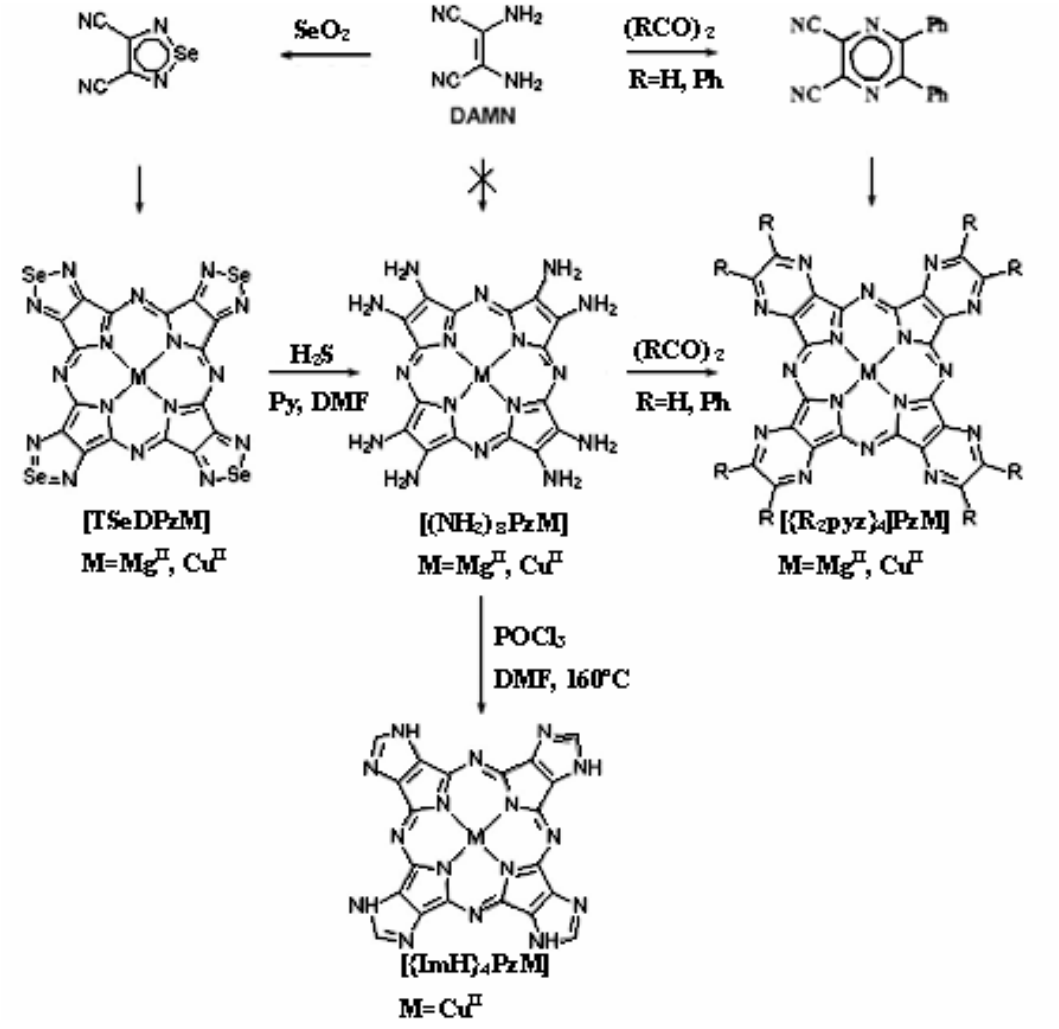

Figure 2.4 Deselenation process of symmetrical macrocycles and peripheral modifications [7]

The reductive opening of the peripheral rings in [TSeDPzMg] under the action of H_2S is accompanied by a color change from bluish-green to violet, indicating the formation of the octaamino derivative [$(NH_2)_8$PzMg], which ahows a UV-Vis spectrum with an unresolved Q-band, broadened due to aggregation and low-lying n→π* transitions (Fig 2.5). Following condensation with benzil, a narrow porphyrazine-like Q-band is reestablished, the maximum of which is hypsochromically shifted to the position expected for the complex [{Ph_2pyz}$_4$PzMg] [7,58].

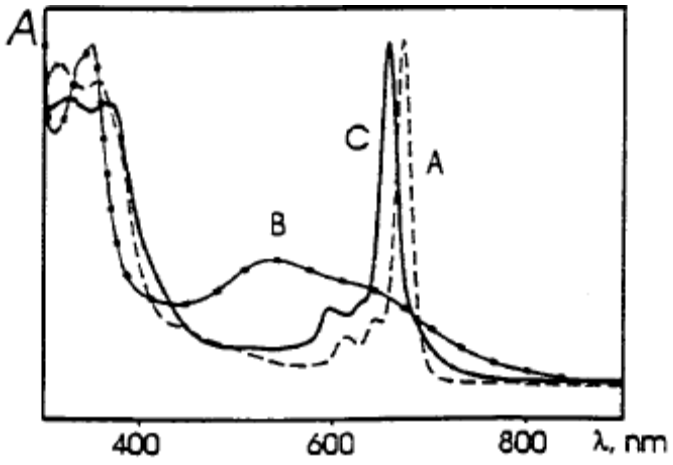

Figure 2.5 UV-vis spectra of pyridine solutions of (A) TSeDPzMg, (B) OAPzMg (after bubbling of H_2S) and (C) Ph_8TPyzPzMg (obtained by reaction of OAPzMg with benzil) [58]

The deselenation process can be also applied to the selenodiazole rings in low-symmetry porphyrazines. Release of selenium from mono(selenodiazole) porphyrazines affords the corresponding porphyrazines carrying one external vicinal diamino functionality first obtained for hexaphenylporphyrazine **13** [1,79]. By reaction of **14** obtained in situ with different electrophiles (Fig. 2.6), ring reclosure takes place and imidazo-, 1,2,3-triazolo-, 1,2,5-thiadiazolo- and pyrazinoporphyrazines, **15**–**18**, are formed [1,7,79].

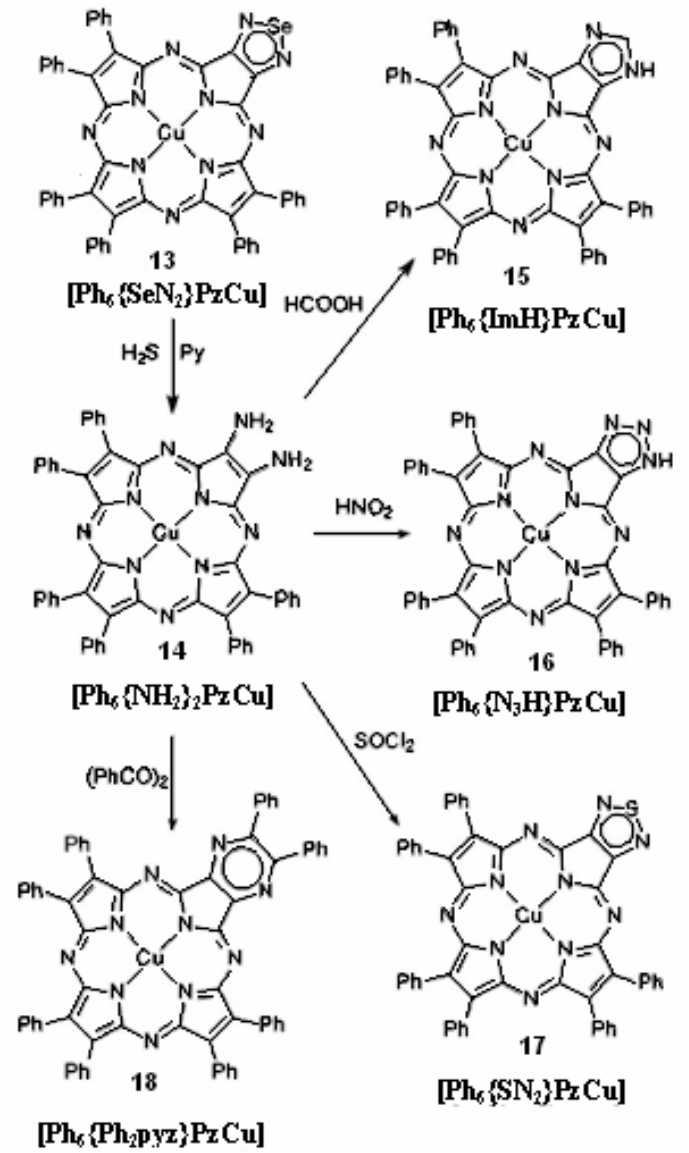

Figure 2.6 Deselenation process of low-symmetry macrocycles [1]

2.2 ELECTRONIC STRUCTURE

The analysis of the numerous structural data on relatively simple organic compounds containing the 1,2,5-thiadiazole ring [80,81] and results of their quantum chemical investigations [82-85] have shown that none of the structures **A**–**E** (Fig. 2.7) can individually explain the structural and chemical properties of these species. It was concluded [80,84] that the real aromatic structure is best depicted by the representation

F, mainly contributed by structures **A** and **D**, with minor participation of the others (**B**, **C**, and **E**) [1].

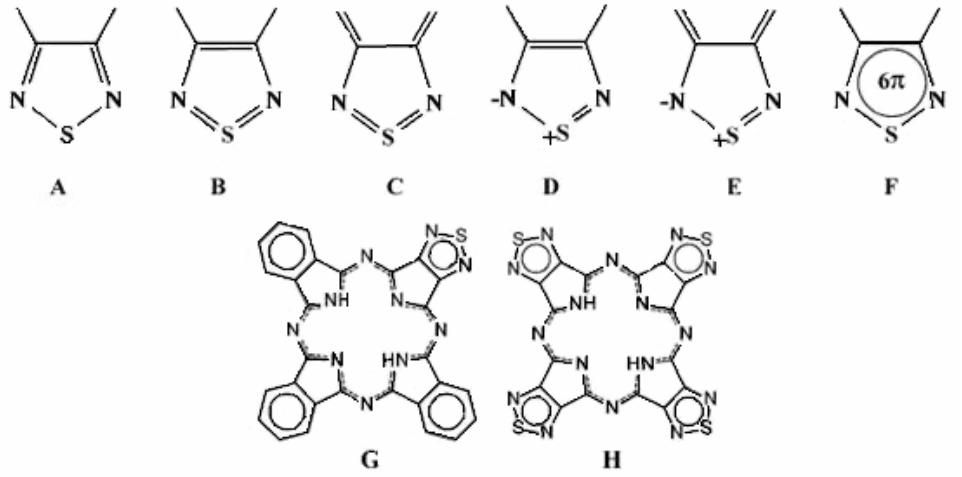

Figure 2.7 Classical resonance structures containing single and double bonds (A–E) and involving the sulfur atoms in the oxidation states +2 (A) and +4 (B and C) and in meso-ionic structures (D and E).

2.3 SPECTROSCOPIC PROPERTIES

Annulation of thia/selenodiazole rings to the porphyrazine core highly influences the electronic and vibrational states of the present “S- and “Se-porphyrazines”. In this section, under each subheadings, the only review article belonging to M.P. Donzello et al [1] was used to inform spectroscopic properties of these novel families of porphyrazines.

2.3.1 UV/visible spectra

The UV/visible solution spectra of the symmetrical freebases [$TTDPzH_2$] and [$TSeDPzH_2$], their metal derivatives and all related low-symmetry species have a spectroscopic pattern which is typical for porphyrazine-type macrocycles and consists of the presence of intense absorptions due to intraligand π-π* transitions in the Soret (300–400 nm) and Q band (600–800 nm) regions. The Soret band is usually broadened since it originates from the configuration interaction of several closely lying π-π* transitions and underlying n–π* transitions involving the N atoms of the porphyrazine macrocycle and annulated thia/selenodiazole rings. The Q absorption in porphyrazine originates from the pure π-π* transitions from the HOMO to LUMO and LUMO+ 1 energy levels in accordance with Gouterman model [1,86]. The shape and peak position

of the absorption bands are determined by the number and location of annulated thia/selenodiazole rings and by the presence and type of metal center.

2.3.1.1 Neutral solvents

The symmetrical free-bases [$TTDPzH_2$] and [$TSeDPzH_2$] and their metal derivatives, like their phthalocyanine analogues, are nearly insoluble in nondonor solvents (chlorobenzene, dichloromethane, etc.) and only qualitative spectra can be obtained. Table 2.2 summarizes the spectroscopic data for the free-bases [$TTDPzH_2$] and [$TSeDPzH_2$], their Mg^{II} complexes and related species. Tables 2.3 and 2.4 list the data for the TTDPz and TSeDPz metal derivatives [1].

Table 2.2 UV–visible solution spectra of free-base and Mg^{II} tetrakis(thia/selenodiazole) porphyrazines and related porphyrazines Porphyrazine Solvent. [58]

Porphyrazine	Solvent	λ_{max} (nm)(log ε)						Ref
		Free-base			*Mg^{II} complex*			
		Soret	Q_y	Q_x	Soret	Qvib	Q	
[PzH_2]	PhCl Py	333(4.70) 333(4.79)	545(4.60) 542(4.57)	617(4.75) 613(4.71)	332(4.70)	535(4.14)	587(5.07)	[105] [95]
[PcH_2]	ClNP[a] Py	350(4.74)	665(5.18) 659	698(5.21) 694	347(4.73)	611(4.08) 610(4.45)	680(4.93) 675(4.94)	[23] [23]
[$(pyz)_4PzH_2$]	ClNP DMSO		625 580sh	660 635		580sh	635	[93] [93]
[$TTDPzH_2$]	PhCl Py	333 375(4.53)	641 622sh	653 648(4.71)	330 371(4.51)	590sh 585(4.00)	647 642(4.85)	[59] [59]
[$TSeDPzH_2$]	Py	382(4.56)	650sh	682(4.65)	356(4.31)	618(3.77)	674(4.38)	[58]

[a] CINP, 1-chloronaphthalene.

Table 2.3 UV/visible spectroscopic data of the metal derivatives of tetrakis(thiadiazole)porphyrazine [59,60,65]

[TTDPzM]		λ (nm)							
M	**Solvent**	**Soret region**			**CT region**		**Q region**		
Zn^{II}	Py	336	367	369sh			588	619	645
	DMSO	329	353	398sh			585	609sh	638
	CF_3COOH	327					583	613sh	643
	H_2SO_4	323					603	632sh	664
Cu^{II}	PhCl	337					584	618	642
	Py	331	363hs		439		586	618	642
	CF_3COOH	275	325	395sh	457sh		575	609sh	631
	H_2SO_4	270	306sh	322			598sh	627sh	661
Ni^{II}	Py	311	327sh	365			578	605sh	631
	DMSO	305		358			571	603	627
	CF_3COOH	322		390sh			576sh	597sh	635
	H_2SO_4	317					601	627sh	660
Co^{II}	Py	341			445		585sh	605sh	639
	DMSO	331			458		580sh	605sh	632
	CF_3COOH	315					578sh	602sh	632
	H_2SO_4	314					593sh	631sh	656
Fe^{II}	Py	344		411	443	504	603sh	646sh	676
	CF_3COOH	320			472	577sh	599sh	627sh	643
	H_2SO_4	306			481		481	667sh	693
Mn^{II}	DMSO	309	352sh	375sh	466sh	498sh	599sh	623sh	653
	CF_3COOH	330			513		593sh	618sh	646
	H_2SO_4	316sh	384sh				601sh	642sh	662
$Al^{III}Cl$	Py	340	364sh	393sh			590	622	647
	DMSO	340					590	623	649
	CF_3COOH	329					583	620	
	H_2SO_4	330					600sh	649sh	660
$Ga^{III}Cl$	Py	337	367sh	400sh			585	617	645
	DMSO[a]	338					587	624	647
	CF_3COOH	329					615	640sh	645
	H_2SO_4	330					597sh	648sh	659
$In^{III}OAc$	Py	321	365sh	390sh			602		658
	DMSO	357sh					609	636sh	658
	CF_3COOH	328	371sh				594	629	646,652sh
	H_2SO_4	317	390sh				618sh		670

Table 2.4 UV/visible spectroscopic data of the metal derivatives of tetrakis(selenodiazole)porphyrazine [58,61].

[TSeDPzM]		λ (nm)								
M	**Solvent**	**Soret region**			**CT region**			**Q region**		
Zn^{II}	Py	313		360				626	652	681
	DMSO	320		353				626	659	680
	CF_3COOH		340					610	641	667
	H_2SO_4	256	332	361				607	645	699
Cu^{II}	Py	321sh		361				427sh	651sh	677
	H_2SO_4			355				611	652	705
	CF_3COOH	305								662
Ni^{II}	CINP		356		424			620	656	686
	Py			357				604	631	661
	DMSO		353					602	631	657
	CF_3COOH	311						610	640	669
	H_2SO_4		335	358				601	638	693
Co^{II}	CINP		358		438	469	497	620	655	687
	Py		334	352	396	441	473	606	645	673
	DMSO		331sh	347		476		609		670
	CF_3COOH	319						598	631	664
	H_2SO_4		344		430	499	604	541	667	700
Mn^{II}	DMSO	283,294	347		445				626	685
	CF_3COOH		305	339				537	613	668
	H_2SO_4		341				625	657	682	709

For [TTDPzM] and [TSeDPzM] as well as for the phthalocyanine and porphyrazine analogues, [PcM] and [PzM], due to the effective D_{4h} symmetry of their π-chromophore, the LUMO and LUMO+ 1 are degenerate and a single sharp Q band with vibronic satellites on the blue side is observed in neutral and basic solvents as is exemplified in Fig. 2.8 for the series of Mg^{II} complexes in pyridine solution. For the corresponding free bases, the symmetry is lowered to D_{2h}, the degeneracy of LUMO is lifted and a double-peaked Q band containing Q_x and Q_y components is observed as shown in the series of spectra recorded in chlorobenzene (Fig. 2.9). The Q band region in porphyrazines is generally highly sensitive to the type of substitution or annulation. When four thia/selenodiazole rings are fused to the central porphyrazine core, the macrocyclic 26π electron chromophore present in unsubstituted porphyrazine [PzH_2] and its metal complexes [PzM] is extended to the 42π-electron chromophoric system in [TTDPzM] and [TSeDPzM]. Such a π-extension results in a considerable bathochromic

shift of the Q band maxima, similarly to what is observed for the benzene or pyrazine annulation in formally π-isoelectronic phthalocyanines [PcM] and tetrapyrazinoporphyrazines [{Pyz}$_4$PzM]. As shown in Figs. 2.8 and 2.9, the Q band which is observed at 587 nm for [PzMg] and at 617 nm (Q_x) and 545 nm (Q_y) for [PzH_2] in the case of thiadiazole annulation is bathochromically shifted to 642 nm for [TTDPzMg(H_2O)] ($\Delta\lambda$(Q) = 55 nm (1460 cm^{-1})) and to 653 and 641 nm for [$TTDPzH_2$] ($\Delta\lambda$(Qx) = 36 nm (890 cm^{-1}) and $\Delta\lambda$(Qy) = 96 nm (2750 cm^{-1}). The value of the bathochromic shift is substantially smaller than in the case of benzene annulation in [PcMg] ($\Delta\lambda$(Q) = 88 nm (2220 cm^{-1})) and in [PcH_2] ($\Delta\lambda(Q_x)$ = 78 nm (1880 cm^{-1}) and $\Delta\lambda(Q_y)$ = 114 nm (3270 cm^{-1})). The observed effect of thiadiazole rings is similar to the effect of pyrazine rings in [(Pyz)$_4$PzMg] ($\Delta\lambda$(Q) = 48 nm (1290 cm^{-1}) and in [(Pyz)$_4$$PzH_2$] ($\Delta\lambda(Q_x)$ = 43 nm (1060 cm_{-1}) and $\Delta\lambda(Q_y)$ = 80 nm (2350 cm^{-1}) [1,87], (Table 2.2). This indicates that the thiadiazole ring as well as the pyrazine ring exhibit a π-deficient character in agreement with the observed redox behavior [1,65] and MO calculations [1,88,69]. The bathochromic effect of selenodiazole annulation in [TSeDPzMg(H_2O)] ($\Delta\lambda$(Q) = 87 nm (2200 cm^{-1})) is larger than that of thiadiazole rings and comparable with the effect of benzene annulation (Table 2.2; Fig. 2.8). This is explained by the difference in electronegativity of the Se and S atoms and less effective $4d_\pi$(Se)–$2p_z$(N) interaction than $3d_\pi$(S)–$2p_z$(N) interaction.

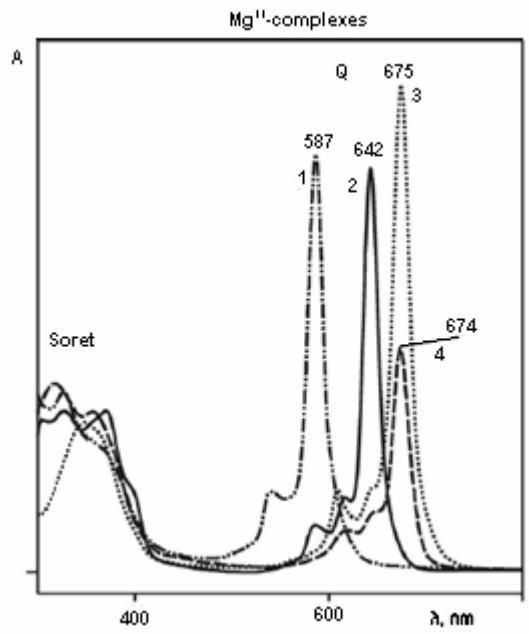

Figure 2.8 UV/vis spectra of [PzMg] (1), [TTDPzMg(H_2O)] (2), [PcMg] (3) and [TSeDPzMg(H_2O)] (4) in pyridine[1].

As regard to low-symmetry porphyrazines, the symmetry of the π-chromophore is lower than D_{4h} and a double Q band is observed both for the free-bases and metal complexes (Fig. 2.10), unless LUMO and LUMO+ 1 are occasionally degenerate (e.g. [S_2B_2PzMg].

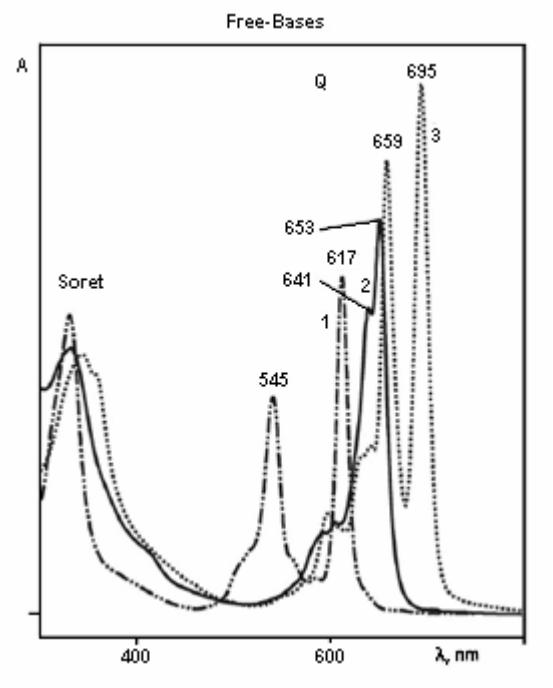

Figure 2.9 UV/vis spectra of [PzH_2] (1), [$TTDPzH_2$] (2) and [PcH_2] (3) in chlorobenzene [1].

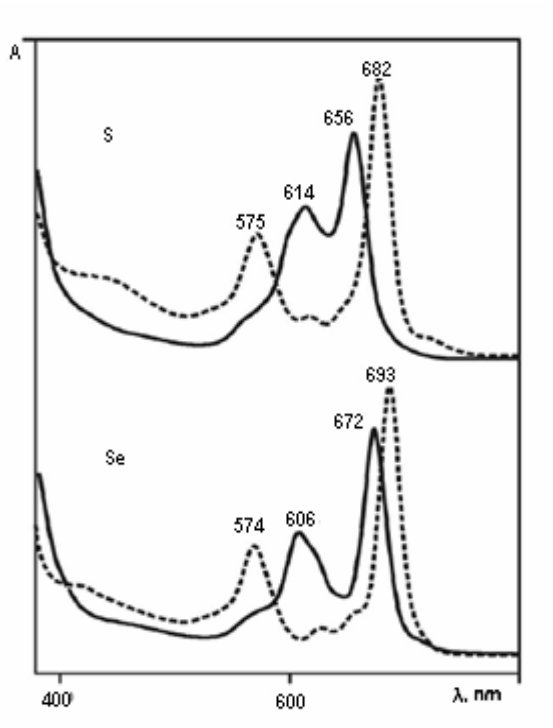

Figure 2.10 UV/vis spectra in CH_2Cl_2 of [Ph_6SPzH_2] and [Ph_6SePzH_2] (dashed lines) and [Ph_6SPzZn] and [$Ph_6SePzMg$] (solid lines)[1].

2.3.1.2 Basic Solvents

The basic solvents (pyridine, DMF, DMSO) have only moderate solvatochromic effect on the peak position of the Soret- and Q bands in the UV/vis spectra of the metal complexes [TTDPzM] and [TSeDPzM] (M =$Mg^{II}(H_2O)$, Mn^{II}, Co^{II}, Ni^{II}, Cu^{II}, Zn^{II}) [1,58,61] and [TTDPzMX] (M =Al^{III}, Ga^{III}, In^{III}) [65]. In the case of the free-bases, a peculiar aspect is that the spectra of [$TTDPzH_2$] and [$TSeDPzH_2$] in pyridine are similar to those of the related metal complexes since they show an unsplit Q band (see Fig. 2.11 for comparison of the spectra of [$TTDPzH_2$] (B) and its Mg^{II} (A) and Ni^{II} (F) complexes), whilst Q band splitting is observed in neutral and acidic solvents (Fig. 2.11 C–E) [1,58,59,64].

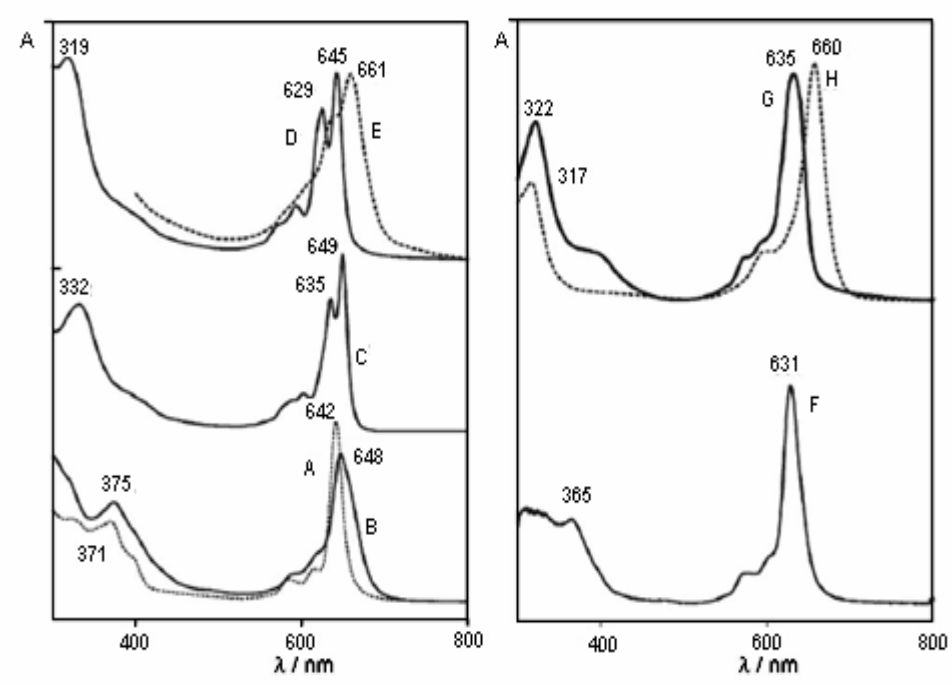

Figure 2.11 UV/vis spectra of [$TTDPzMg(H_2O)$] (*A*), [$TTDPzH_2$] (B–E) and [TTDPzNi] (F–H) in pyridine (A, B and F). CH_2Cl_2 (C), CF_3COOH (D and G) and in H_2SO_4 (E and H). Spectrum B shows the pyridinium salt $[TTDPz]^{2-}(H^+Py)_2$. Spectra of [$TTDPzMg(H_2O)$] in CF_3COOH and in H_2SO_4 are identical to the spectra D and E,5.[1]

This behavior is due to the combined effect of σ-acceptor and π-deficient properties of the thia/selenodiazole fragments, leading to a high acidity of the central NH groups with implied easy deprotonation and formation of the corresponding symmetrical dianions $[TTDPz]^{2-}$ and $[TSeDPz]^{2-}$ as pyridinium salts. A similar spectroscopic effect can be observed upon addition of a strong base, i.e. tetrabutylammonium hydroxide, to a solution of $[TTDPzH_2]$ in neutral solvents such as CH_2Cl_2 [1,64,71]. For unsubstituted free-base phthalocyanine and porphyrazine, the deprotonation process can be seen only upon heating or UV-irradiation of the pyridine solutions [1,90].

Formation of the deprotonated macrocycles as pyridinium salts immediately upon dissolution in pyridine is a clear indication of the high acidity character of the pyrrolic NH groups in porphyrazines. So, whereas no deprotonation is observed for unsubstituted $[PzH_2]$ nor for $[PcH_2]$, porphyrazines with strongly electron-withdrawing substituents (β-halogen, β-sulfophenyl, β-4-methylpyridiniumyl) or annulated electrondeficient heterocycles (tetra(pyrido)-, tetra(pyrazino)porphyrazines) easily form such salts in pyridine and other basic solvents [1,91].

2.3.1.3 Acidic Solvents

The presence in the molecular framework of thia/selenodiazoloporphyrazines of several basic centers – four *meso*- N atoms (Nmeso) bridging the pyrrole units, eight N atoms of thia/selenodiazole rings (Nhet) and in the free-bases two internal pyrrolenine nitrogens (Npyr) – endows these macrocycles with relatively high solubility in acidic media such as HCOOH, CF_3COOH, H_2SO_4, due to specific solvation and acid–base interaction processes. Since all basic centers belong to the conjugated π-chromophore, a strong solvatochromic effect determined by the acidity of the media is a characteristic feature of diazoloporphyrazines. Stable solutions are obtained in CF_3COOH for all investigated free-bases and related metal complexes, exception made for the Mg^{II} species, due to demetalation. Free-bases undergo hydroprotolytic destruction in aqueous concentrated H_2SO_4 but are more stable in non-aqueous H_2SO_4. $[TTDPzH_2]$ is by 10 times less stable than the Se-analogue, the rate constants of their destruction in 96.6% aqueous H_2SO_4 at 25 °C being 910×10^5 and 56×10^5 s^{-1}, respectively [1,64].

For $[TTDPzH_2]$ and $[TSeDPzH_2]$ and their metal complexes only a slight hypsochromic shift of the Q band (up to 200 cm^{-1}) or its broadening is observed even

in strong carboxylic acids such as HCOOH and CF_3COOH (Hammet acidity functionH_0 is −2.22 [1,75] and −3.03 [1,76], respectively). The Soret band envelope becomes more sharp. These spectroscopic changes suggest acid solvation or partial protonation occurring at the N atoms of annulated thia/selenodiazole rings. For the unmetalated macrocycles, the splitting of the Q band becomes more well-defined, this demonstrating that no protonation of internal pyrrolenine N atoms is taking place in these media. In H_2SO_4 for [$TTDPzH_2$] and [$TSeDPzH_2$] and their metal complexes, a bathochromic shift of the Q band is observed (15–30 nm, 500–800 cm^{-1}) which is indicative of protonation of one of the *meso*-N atoms.

2.3.2 Vibrational spectra

2.3.2.1 IR Spectra

The IR spectra of [$TTDPzH_2$], its Se-analogue [$TSeDPzH_2$] and their metal complexes were examined and discussed [1,58,61]. The main IR modes were assigned on the basis of the comparison with the data available for 1,2,5-thia- and 1,2,5-selenodiazoles [1,92,93] and other tetrapyrrolic macrocycles [1,94]. Fig. 2.12 reports the IR spectra of [$TTDPzH_2$], [$TSeDPzH_2$] and their Ni^{II} complexes as representative species for the metal derivatives. For [$TTDPzH_2$] and [$TSeDPzH_2$] the NH stretching vibrations, ν(NH), appear at 3290 and 3280 cm^{-1} and the NH out of-plane deformations γ(NH) at 753 cm^{-1}. For [$TTDPzH_2$], the assignments for both modes was made [1,59] by deuteration and for [$TTDPzD_2$] ν(ND) and γ(ND) were found at 2465 and 585 cm^{-1}, respectively. The in-plane NH deformations, δ(NH), are strongly coupled with the vibrations of the pyrrole ring and their assignment is not straightforward. In the region of the inplane deformation modes (1000–1600 cm^{-1}), the IR spectra of the free-bases are different from the spectra of the corresponding metal complexes because of the presence in the former species of weak-to-medium bands at 1565 and 1535 cm^{-1}, strong bands at 1215 and 1210 cm^{-1} and medium-strong bands at 1014 and 1030 cm^{-1}, for [$TTDPzH_2$] and [$TSeDPzH_2$], respectively (Fig. 2.12). Initially, the δ(NH) mode in [$TTDPzH_2$] has been associated [1,59] with the band at 1565 cm^{-1} on the basis of the assignment made for the 1539 cm^{-1} band in the case of [PcH_2] [1,95]. However, in the case of porphyrins [1,94] and unsubstituted porphyrazine [1,96,97] the deuteration experiments and calculations of the potential energy distribution have shown that the

local δ(NH) mode highly contributes to the band in the 1210–1260 cm^{-1} region. The recent theoretical study [1,98] reinterpreted the assignment of the in-plane NH vibrations in the IR spectra of [PcH_2] and suggested that the δ(NH) mode corresponds to the 1250 cm^{-1} band. Taking these results into account, it can be concluded that also for [$TTDPzH_2$] and [$TSeDPzH_2$] δ(NH) vibration have the highest contribution in the band near 1210–1215 cm^{-1}.

The vibrations of the central porphyrazine core are strongly coupled with those of annulated heterocycles. As a result, the TTDPz and TSeDPz macrocycles have a unique IR spectroscopic pattern which is quite different from those of their phthalocyanine and other porphyrazine analogues. Some pertinent assignments were suggested [1,61]. The stretching vibrations of the *meso*-N atom bridge, ν(CNmeso), give weak-medium IR bands in the 1500–1550 cm^{-1} region. The skeletal vibrations of pyrrole rings, ν(Pyr), are strongly mixed with the ν(C=N) vibrations of the annulated thia/selenodiazole rings and give the most intense IR band at 1240–1270 cm^{-1}. The in-plane deformations of the pyrrolenine rings, δ(Pyr), give a strong IR band at 1080–1140 cm^{-1} and a weak-medium band at 1050–1060 cm^{-1}. For free-bases, an additional strong band of the in-plane pyrrole deformations δ(PyrH) is present at 1010–1030 cm^{-1}. The out-of-plane deformations of pyrrole rings γ(Pyr) appear at 660–670 cm^{-1} for the free-bases and are shifted to higher energy to 680–690 cm^{-1} for the metal complexes.

Some local modes of the annulated heterocyclic rings can be also assigned by comparison of the IR spectra of thia/selenodiazoloporphrazines [1,58-61] with those of the 1,2,5- thia- and 1,2,5-selenodiazoles [1,92,93]. Thus, the stretching vibrations of the SN and SeN bonds which are strong in 1,2,5-thia- and 1,2,5-selenodiazoles (ν(SN) 806 and 780 cm^{-1} and ν(SeN) at 728 and 589 cm^{-1} [1,92,93]) give bands of weak-medium intensity for TTDPz (ν(SN) at 810–830 and 760–770 cm^{-1}) and TSeDPz macrocycles (ν(SeN) at 700–725 and 640–650 cm^{-1}). The strong in-plane deformations of the annulated heterocycle appear near 850 cm^{-1} in the free-bases and near 890 cm^{-1} in metal complexes, whilst they are observed at 895 and 880 cm^{-1} in 1,2,5-thia- and 1,2,5-selenodiazoles [1,92,93]. The out-of-plane deformations of the heterocycles give weak bands at 615–625 and 480–495 cm^{-1} for S- and Se porphyrazines, respectively. The ring torsion vibrations of the annulated heterocycles appear as strong bands at 515–510 and 450–465 cm^{-1} for TTDPz and TSeDPz, respectively. Being only slightly shifted from their position in 1,2,5-thia- and 1,2,5-selenodiazoles (520 and 438 cm^{-1}), they provide the most clear indication of the presence of the annulated thia- or selenodiazole

rings in the porphyrazine macrocycle and their intensity correlates with the number of heterocycles present in each species [1,77].

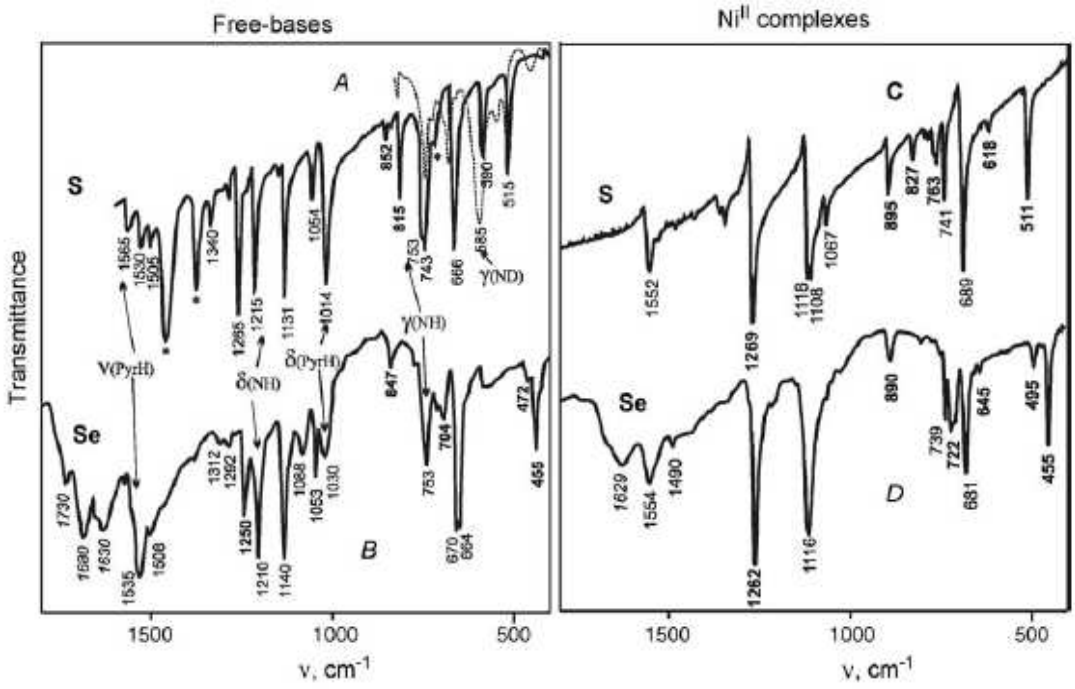

Figure 2.12 IR spectra of [TTDPzH$_2$]: (A, the dashed line is for deuterated material), [TSeDPzH$_2$] (B) and their Ni^{II} complexes (C and D) in nujol (A) and KBr (B–D). Position of peaks associated with annulated 1,2,5-thia/selenodiazole rings are given in bold-type, and those in italics are related to solvent molecules [1].

2.3.2.2 Raman Spectra

The FT-Raman spectra were reported [1,61] for the Ni^{II} complexes [TTDPzNi] and [TSeDPzNi] (Fig. 2.13). Although excitation wavelength λ_{ex} = 1064 nm is far from the position of the Q band maxima, the vibrations of the annulated heterocycles have low intensity and only the vibrations of the bonds forming the central porphyrazine π-chromophore are strongly enhanced. Whilst the stretching vibrations of the *meso*-N atom bridged moiety, *ν*(CNmeso), appear as weak-medium bands at 1500–1550 cm^{-1} in the IR spectrum, they give the strongest band near 1570 cm^{-1} in the FT-Raman spectrum. Another strong RR band which is observed at ca. 1180 cm^{-1} belongs to pyrrole in-plane deformations *δ*(Pyr). Noteworthy, these strong bands show no dependence from the chalcogen atom (S or Se) in the annulated ring.

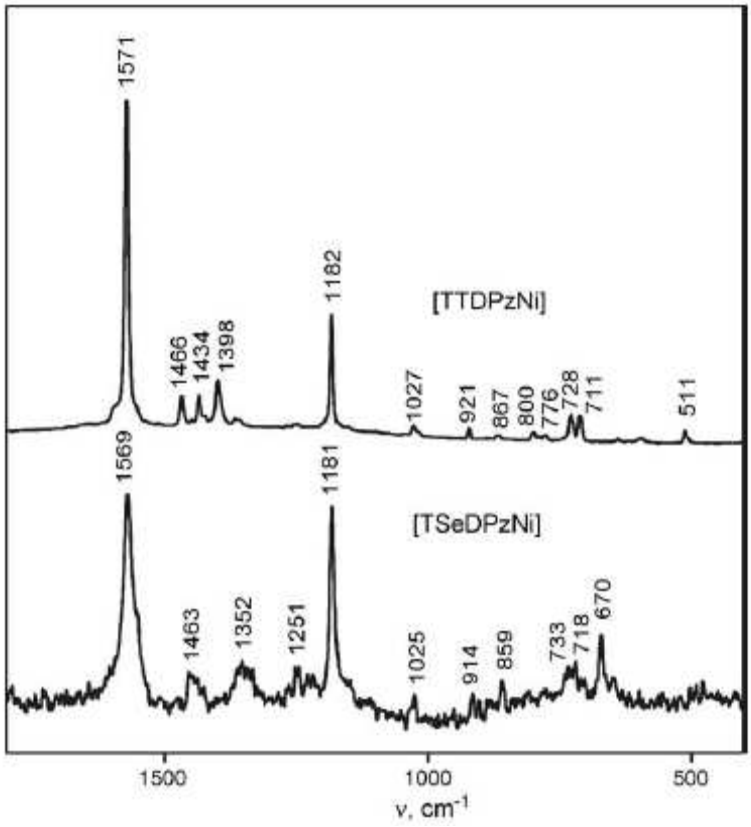

Figure 2.13 FT-Raman spectra of [TTDPzNi] and [TSeDPzNi] obtained at λ_{ex} = 1064 nm [61]

CHAPTER 3

EXPERIMENTAL PART

3.1 CHEMICALS

The following chemicals were used in the synthesis: Solvents (propyl alcohol, chloroform, dichloromethane, CH_3COOH, CF_3COOH, DMSO, DMF, pyridine, ethyl alcohol, 96% H_2SO_4) and reagents (diaminomaleodinitrile, SeO_2, Mg turnings, $VOSO_4.5H_2O$), Na_2CO_3, *p*-toluenesulfonic acid, cyclohexadione were purchased from Alfa Aesar, Aldrich and Merck and used as received.

3.2 INSTRUMENTATION

3.2.1 Fourier Transform Infrared (FTIR)

IR spectra of solid samples were recorded by Perkin Elmer FT-IR System, Spectrum BX, in the region 400-4000 cm^{-1}.

3.2.2 UV Visible Spectroscopy

UV-visible spectra were recorded by UNICAM between the 300-800 nm in the related solvents.

3.2.3 Electron Paramagnetic Resonance (EPR)

EPR spectra were recorded with a Bruker EMX X-band spectrometer (9.8 GHz) with about 63.5 mW microwave power and 100 kHz magnetic field modulation with 2 G of amplitude.

3.3 EXPERIMENTAL PROCEDURE

3.3.1 Synthesis of 3,4-Dicyano-1,2,5-selenodiazole (1)

This precursor was synthesized according to the literature [58]: Diaminomaleodinitrile (2.16 g, 20 mmol) and SeO_2 (2.22 g, 20 mmol) were dissolved in CH_2Cl_2 (20 ml) and the mixture was stirred for 30 min (exothermic reaction), refluxed for a further 30 min. After cooling and filtration, the solvent was evaporated under reduced pressure, leaving a white–yellow crystalline material with 92% yield. The melting point of **1** (91^oC) and its IR values ((in KBr, cm^{-1}): ν = 2240s, 1295vs, 773s, 880w, 728s, 589s, 438m, 418s) correspond to those reported in the literature [58]. Anal. calc. for the formula C_4N_4Se: C, 26.25; H, 0.00; N, 30.61. Found: C, 26.30; H, 0.00; N, 30.66.

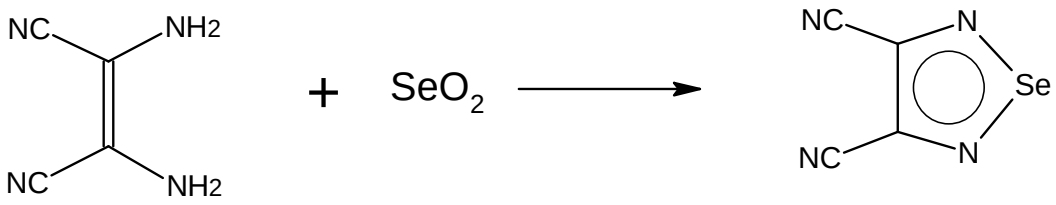

1

Figure 3.1 Synthesis of 3,4-Dicyano-1,2,5-selenodiazole ligand

3.3.2 Synthesis of Tetrakis(selenodiazole)porphyrazinato Magnesium, TSeDPzMg (2)

TSeDPzMg was produced corresponding to the literature [58] according to the Linstead macrocyclization. Magnesium metal (1 g, 0.041 mol) was suspended, with stirring, in propyl alcohol (25ml) in the presence of a small amount of I_2. After refluxing for 8 h, which ensures complete conversion of Mg into its corresponding propylate, ligand **1** (2.4 g, 13 mmol) was added, and the mixture was refluxed for further 8 h. During the reaction, the grey colored mixture changed to dark bluish green. At the end of the reaction, propanol was evaporated under reduced pressure, and CH_2Cl_2 was repeatedly added to the solid blue ground material to dissolve excess unreacted **1**. Acetic acid (50% in water) was then added to the solid material to dissolve unreacted magnesium propylate, and the mixture was stirred at room temperature for 1–

2 h. After filtration, the blue solid material obtained was washed with water to neutrality, then with methanol, and brought to constant weight under vacuum (yield 65%). Spectroscopic characterization results correspond to the literature values[58]: IR, ν_{max}/cm^{-1}: 1528s, 1236s, 1084s, 1042m, 716m, 676s, 640w, 480w, 455s. UV–Vis (in DMSO) λ_{max} (nm) (log ε): 356 (0.757), 668 (1.032). Calc. for $C_{16}N_{16}Se_4Mg$: 756.42, Found: MALDI-MS (m/z):754.52 $[M^+]$.

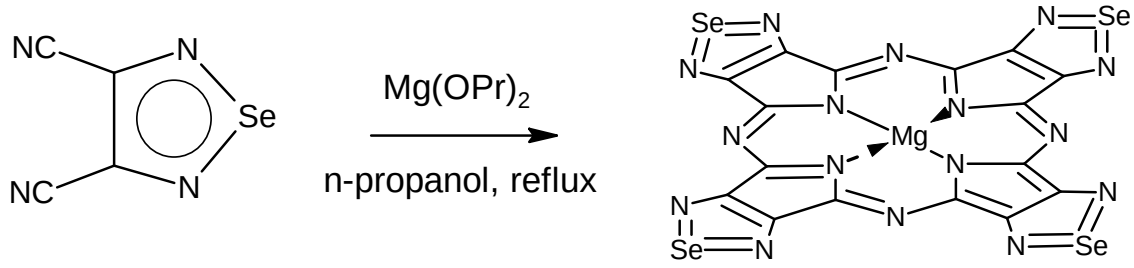

Figure 3.2 Synthesis of TSeDPzMg

3.3.3 Preparation of Metal-free Tetrakis(selenodiazole)porphyrazine (3)

TSeDPzMg complex (0.20 g, 0.23 mmol) was dissolved in CF_3COOH (7 ml) and refluxed for 24 h. After distillation of the solvent, the solid residue was washed with water until neutrality, and then with methanol. Finally, the $TeSeDPzH_2$ **(3)** was brought to constant weight under vacuum (yield ca. 65%). IR: ν_{max}/cm^{-1}: 3265w ν(N–H), 2920m (C–H, acetic acid), 1529vs δ(N–H)), 1380s and 1290w (C=N selenodiazole ring), 1250m (C=C), 1130s (C=N pyrrole). UV–Vis (DMSO) λ_{max} (nm) (log ε): 348 (4.06), 668 (3.74).

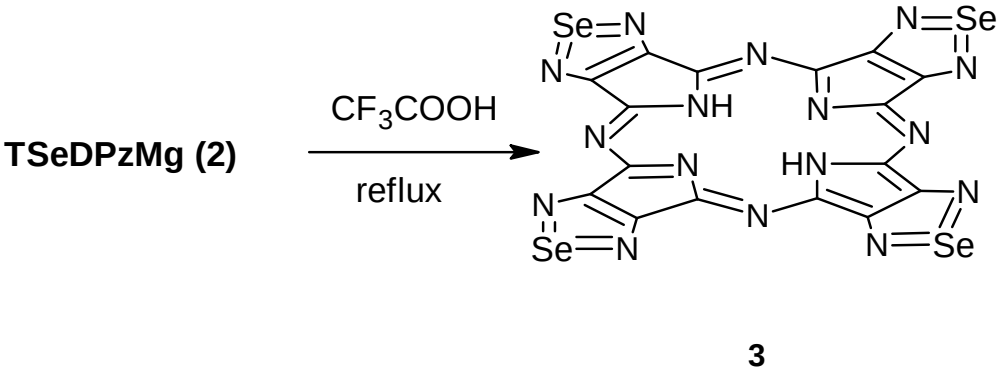

Figure 3.3 Demetallation of TSeDPz

3.3.4 Synthesis of Vanadyl Tetrakis(selenodiazole)porphyrazine (4)

A mixture of $TSeDPzH_2$ (0.13 g, ca. 0.17 mmol) and $VOSO_4.5H_2O$ (0.20 g, 0.8 mmol) was refluxed for about 20 h in 20 ml of DMSO. After cooling to room temperature, the metalloporphyrazine was precipitated by addition of methanol and the solid compound was isolated by centrifugation. The complex was brought to constant weight under vacuum (yield ca. 68%). IR: ν_{max}/cm^{-1}: 1380s and 1290w (C=N selenodiazole ring), 1248m (C=C), 1128s (C=N pyrrole), 990m (V=O). UV–Vis (in pyridine) λ_{max} (nm) (log ε): 364 (3.66), 692 (3.44) and (in DMSO); 630 (2.84) and 685 (3.22). Found (MALDI-MS); 799.925 [M^+].

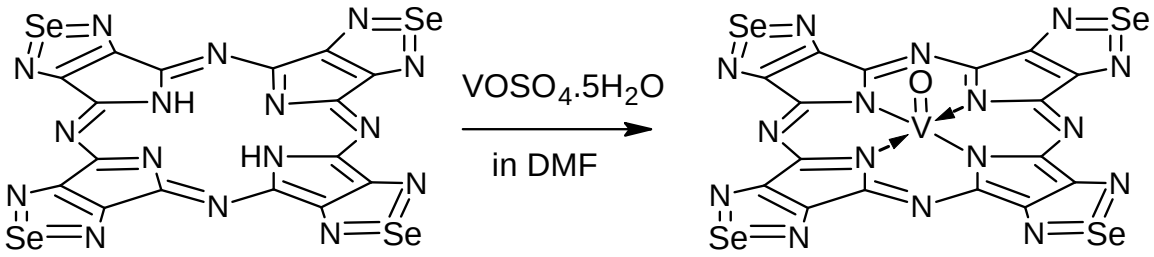

3 **4**

Figure 3.4 Synthesis of TSeDPzVO

3.3.5 Synthesis of Tetrakis(cyclohexyl pyrazino)porphyrazine (5a)

TeSeDPz (50 mg, 0.057 mmol) was suspended in pyridine (20 ml), and gaseous H_2S was bubbled through the suspension. After the color changing from bluish-green to violet in about 5 minute, the solvent was evaporated under reduced pressure and the solid material was washed several times with $CHCl_3$. At this point the bulk material from the by-products (Se, SeS, etc.) was not purified. The solid (ca 300mg) was suspended in absolute ethanol (25ml) and, after addition of 1,2-cyclohexadione (158mg, 1,4mmol) and catalytic amounts of p-toluenesulfonic acid, the reaction mixture was refluxed for 8h. After cooling, the solid material was separated by centrifugation, then washed with ethanol and brought to constant weight in a vacuum desiccator. The solid was treated with pyridine with several portions and after removing the solvent and followed by washing with ethanol, the dark green of tetrakis(pyrazino)porphyrazine was obtained (yield: 45%). IR: ν_{max}/cm^{-1}: 2985m (C-H),

1630w (C=C), 1500w (ν(CNmeso)), 1238s (ν(pyr)), 1142s (ν(CN)), 1090m (δ(pyr)). UV–Vis (in DMSO) λmax (nm) (log ε): 352 (0.857), 636 (0.698). Calc. for $C_{40}N_{16}H_{32}Mg$: 760.42, Found: MALDI-MS (m/z) 761.52 [M^+]. ^{1}H-NMR (ppm, in DMSO-d_6): 2.28(-CH_2^a, pyz) and 1.23(-CH_2^b, pyz).

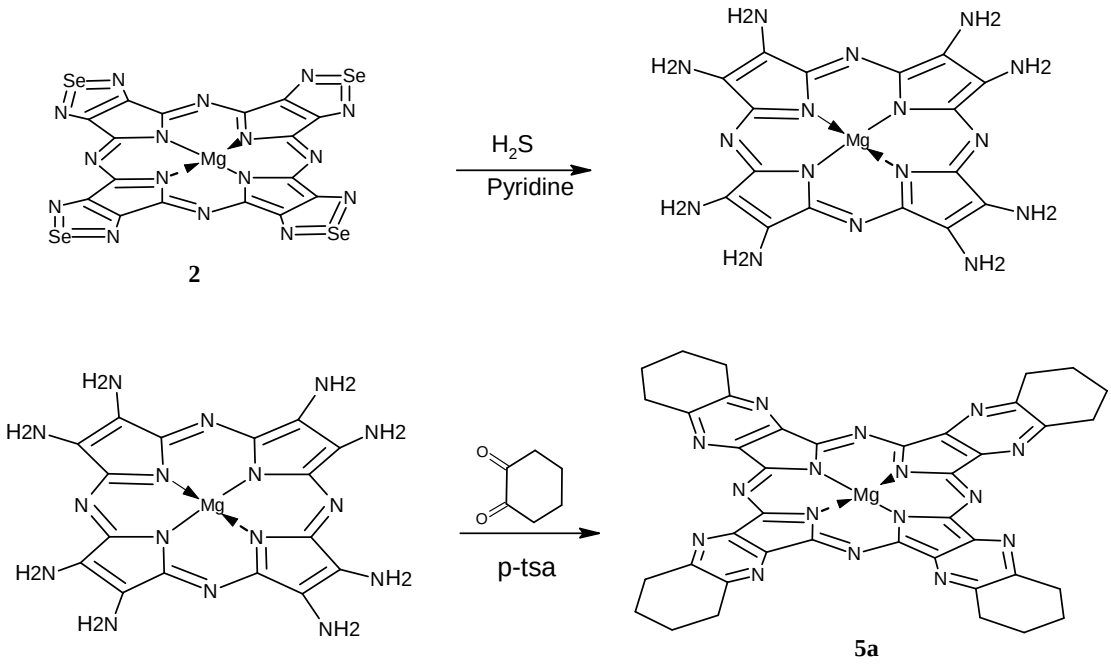

Figure 3.5 Synthesis of TCPyzPz by ring closure of octaamino porphyrazine with 1,2-cyclohexadione

3.3.6 Synthesis of 2,3-dicyano-5,6-cyclohexapyrazine (6)

Diaminomaleonitrile (250 mg, 2.31 mmol) and 1,2-cyclohexadione (63 mg, 5.62 mmol) were refluxed for 2 h in absolute ethanol (20 ml) in the presence of catalytic amount of p-toluenesulfonic acid. After evaporation of the solvent under reduced pressure, the ligand was taken into organic phase from viscose solid material by treating with diethyl ether. When the solvent was removed under reduced pressure, the ligand was obtained with 75% yield. IR: ν_{max}/cm^{-1}: 2945m (C-H), 2200m (C≡N), 1614m (C=C, in pyrazine), 1376s, 1206m. Calc. for $C_{10}N_4H_8$: 184.12, Found: MALDI-MS (m/z): 183.12. ^{1}H- NMR (400MHz, DMSO-d_6): δ/ppm: 3.05 (2H, t) and 1.92 (2H, t). ^{13}C-NMR (400MHz, DMSO-d_6): δ/ppm: 114.22 (C≡N), 129.89 (C=C), 158.29 (C=N), 21.00 (C-C) and 31.75 (C-C). Anal. calc. for $C_{10}N_4H_8$: C, 65.21; H, 4.38; N, 30.41. Found: C, 65.19; H, 4.35; N, 30.38.

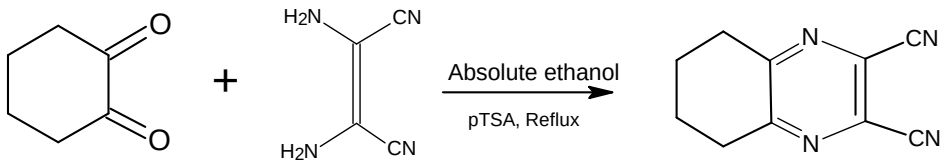

6

Figure 3.6 Synthesis of 2,3-dicyano-5,6-cyclohexapyrazine ligand

3.3.7 Synthesis of Tetrakis(cyclohexyl pyrazino)porphyrazine (5b) by Direct Tetramerization of 2,3-dicyano-5,6-cyclohexapyrazine

Magnesium metal (93 mg, 3.88 mmol) and propyl alcohol (15 ml) mixture was refluxed to obtain a suspension of magnesium propylate. After 8 h, ligand **6** (100 mg, 0.641 mmol) was added and reaction mixture was refluxed for further 6 h. After cooling to room temperature, the mixture was filtered and the solvent was evaporated. The solid material was washed with Na_2CO_3 several times, water till neutrality and ethanol, then dried under vacuum. 60 % yield IR: ν_{max}/cm^{-1}: 2934m (C-H), 1630w (C=C), 1532w (ν(CNmeso)), 1236m (ν(Pyr)), 1148m (ν(CN)), 1148m and 1046w (δ(Pyr)). UV–Vis (in DMSO) λ_{max} (nm) (log ε): 352 (0.875), 636 (0.995). Calc. for $C_{40}N_{16}H_{32}Mg$: 760.42, Found: MALDI-MS (m/z):761.52 [M^+]. ^{1}H-NMR (ppm, in DMSO-d_6): 2.29(-CH_2^a, pyz) and 1.24(-CH_2^b, pyz). Anal. calc. for TCPyzPzMg **(5b)**, $C_{40}N_{16}H_{32}Mg$: C, 63.12; H, 4.24; N, 29.44. Found: C, 63.14; H, 4.27; N, 29.41.

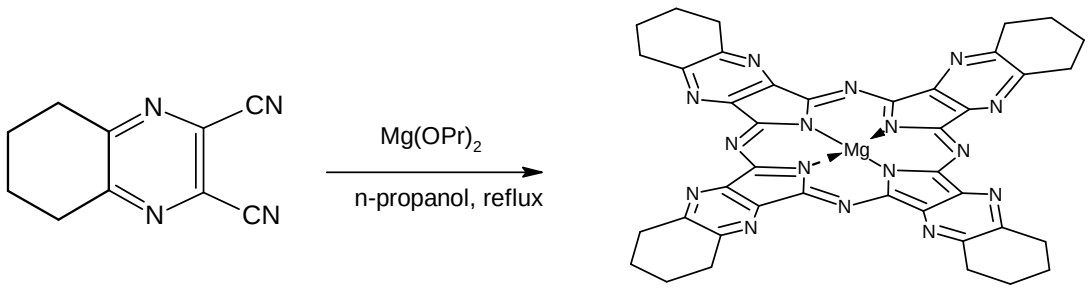

6 **5b**

Figure 3.7 Tetrakis(cyclohexyl pyrazino)porphyrazine (5b) by Direct Tetramerization of 2,3-dicyano-5,6-cyclohexapyrazine

CHAPTER 4

RESULTS AND DISCUSSIONS

4.1 3,4-Dicyano-1,2,5-selenodiazole (1)

3,4-dicyano-1,2,5 selenodiazole **(1)** is the precursor of the Se-porphyrazines (SePz) which was synthesized as white–yellow crystalline of the reaction between diaminomaleodinitrile and SeO_2 in CH_2Cl_2 in a good yield (92%). The found melting point of **1** (around 91°C) corresponds to the literature value (92^{o}C) [58]. In the IR spectrum the sharp peaks around 2240 cm^{-1} and 731-601 cm^{-1} indicate the stretching of cyano groups (νC≡N) and 1,2,5 selenodiazoles (νSe-N), respectively. All those peaks are consistent with of those reported in the literature [58] (See App. A).

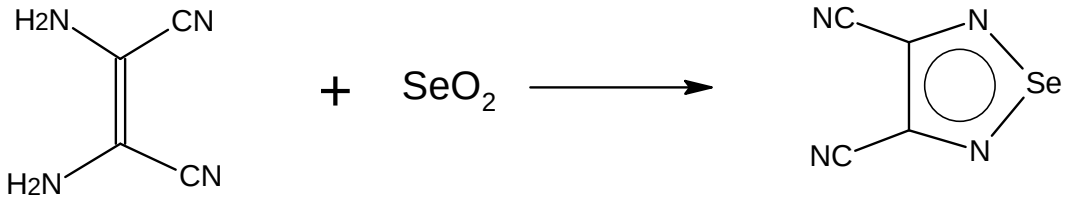

1

Figure 4.1 Synthesis of 3,4-dicyano-1,2,5 selenodiazole

4.2 Tetrakis(selenodiazole)porphyrazinato Magnesium (2) and Metal-free Tetrakis(selenodiazole)porphyrazin (3)

After the preparation of 3,4-dicyano-1,2,5 selenodiazole, symmetrical tetrakis (selenodiazole)porphyrazine, TSeDPz, was prepared by template macrocyclization in

the presence of Mg-propylate in propanol under reflux with 60–70% yield, as reported previously [58].

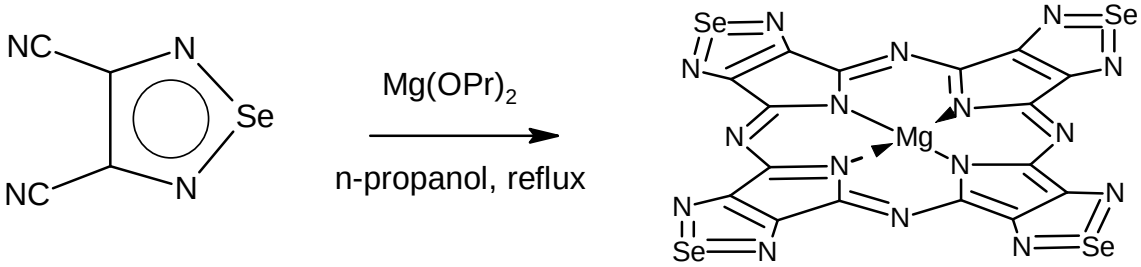

1 **2**

Figure 4.2 Synthesis of TSeDPzMg (2)

According to the elemental analysis and IR spectral data [58, 61], [TSeDPzMg]**(2)** $(H_2O)x(CH_3COOH)$ (x = 1–6) water molecules are weakly bound and can be easily eliminated by heating (>100 ^{0}C) under vacuum. The most relevant feature is the presence of an intense mode found at 455 cm^{-1} TSeDPz macrocycles. This mode has probably to be assigned to the skeleton vibration of the heterocyclic ring with a large contribution of Se—N bonds. The vibrations of the central porphyrazine core are strongly coupled with those of annulated heterocycles. As a result, TSeDPz macrocycles have a unique IR spectroscopic pattern which is quite different from those of their phthalocyanine and other porphyrazine analogues. The stretching vibrations of the meso-N atom bridge, $\nu(CN_{meso})$, give weak-medium IR bands in the 1528 cm^{-1} region. The skeletal vibrations of pyrrole rings, ν(Pyr), are strongly mixed with the ν(C= N) vibrations of the annulated selenodiazole rings and give the most intense IR band at 1236 cm^{-1}. The in-plane deformations of the pyrrolenine rings, δ(Pyr), give a strong IR band at 1084 cm^{-1} and a weak-medium band at 1042 cm^{-1}. The out-of-plane deformations of pyrrole rings γ(Pyr) appear at 676 cm^{-1}. Thus, the stretching vibrations of the SeN bonds which are strong in 1,2,5-selenodiazoles ν(SeN) at 728 and 589 cm^{-1} give bands of weak-medium intensity TSeDPz macrocycles (ν(SeN) at 716 and 640 cm^{-1}). The strong in-plane deformations of the annulated heterocycle appear near 867 cm^{-1} in the complexes, whilst they are observed at 880 cm^{-1} in 1,2,5-selenodiazole. The out-of-plane deformations of the heterocycles give weak bands at 480–495 cm^{-1} for Se-

porphyrazine, TSeDPzMg. The ring torsion vibrations of the annulated heterocycles appear as strong bands at 450–465 cm^{-1} for TSeDPzMg [58]. Being only slightly shifted from their position in 1,2,5- selenodiazoles (438 cm^{-1}), they provide the most clear indication of the presence of the annulated selenodiazole rings in the porphyrazine macrocycle and their intensity correlates with the number of heterocycles present in each species.

Acetic acid is more strongly retained, even under vacuum at 200 ^{0}C. Tetrakis(selenodiazole)porphyrazines, TSeDPz, are very poorly soluble in common organic solvents, such as hydrocarbons, ethanol, and chloroform, but they have higher solubility in donor solvents (pyridine, DMSO, DMF) [61].

The UV/visible solution spectra of the symmetrical freebase [$TSeDPzH_2$] and their metal derivative [TSeDPz] consist of the presence of intense absorptions due to intraligand π-π* transitions in the Soret (300–400 nm) and Q band (600–800 nm) regions. The Soret band is usually broadened since it originates from the configuration interaction of several closely lying π – π * transitions and underlying n– π * transitions involving the pyrrole- N atoms of the porphyrazine macrocycle and annulated selenodiazole rings. The Q absorption in porphyrazines originates from the pure π – π * transitions from the HOMO to LUMO and LUMO+ 1 energy levels in accordance with Gouterman model [61]. The shape and peak position of the absorption bands are determined by the number and location of annulated selenodiazole rings and by the presence and type of metal center. Moreover, strong solvatochromic effects are observed as it will be shown by the data in neutral, basic and acidic solvents. The Soret bands (300–400 nm) are usually broadened due to π–π* and n–π* transitions involving the N atoms of the porphyrazine macrocyle and peripheral annulated rings. The Q band absorptions are π–π* transitions from HOMO–LUMO energy levels having D_{4h} molecular symmetry [1]. As in Fig 4.3, the Q band absorptions of TSeDPz in pyridine, gave very intense and low aggregated peaks around 668 nm.

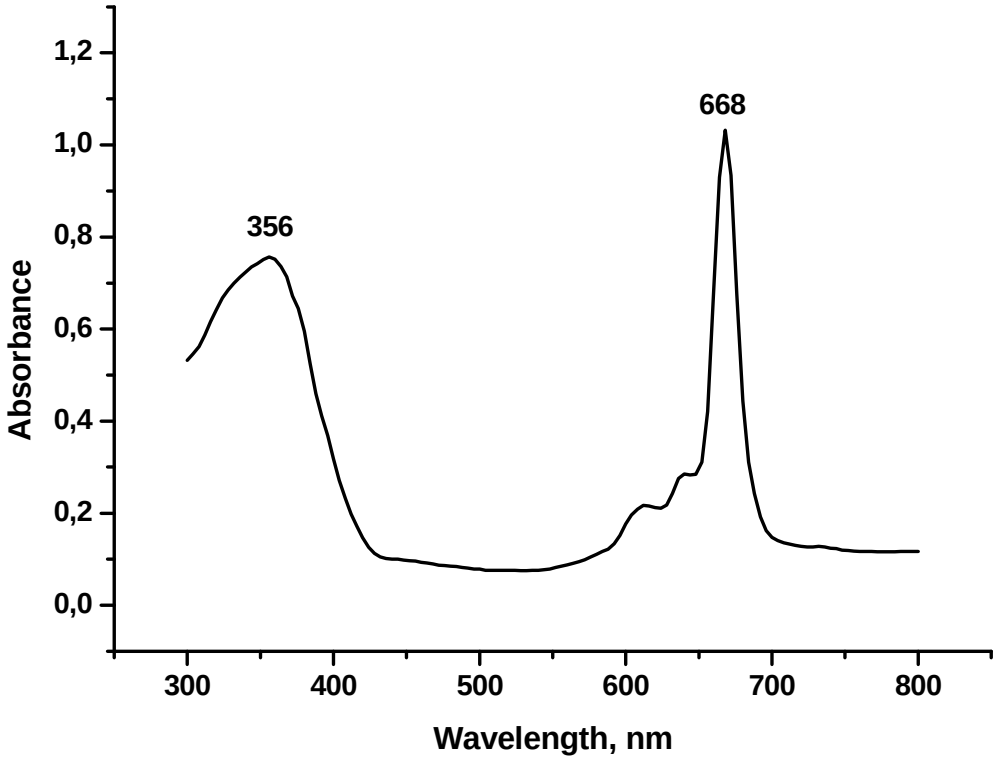

Figure 4.3 UV-visible spectrum of TSeDPzMg **(2)** in pyridine

Demetalation of Mg^{II} complex to the free-base porphyrazine, $TSeDPzH_2$, has been achieved in CF_3COOH under reflux. The central N–H groups of the molecule appear in the IR spectrum around 3265w (ν(NH)) and 1529vs (δ(NH)) and an additional strong band of the in-plane pyrrole deformations δ(PyrH) is present at 1010–1030 cm^{-1} support the formation of the freebase porphyrazine molecule.

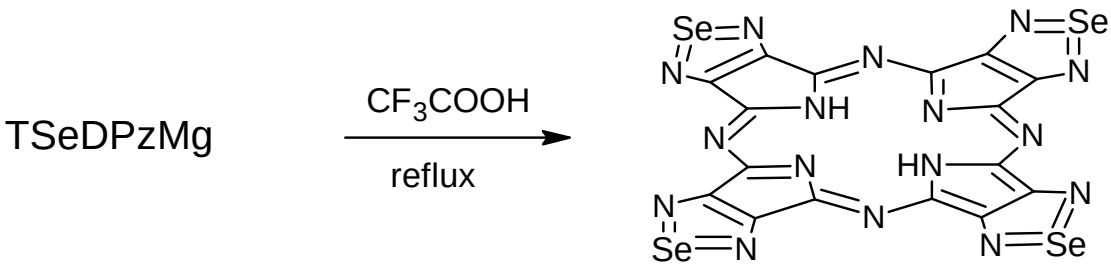

3

Figure 4.4 Synthesis of $TSeDPzH_2$ **(3)**

The UV–vis absorption spectrum of the free-base porphyrazine, $TSeDPzH_2$, in pyridine is similar to that of related metal complexes, TSeDPz, showing unsplitting Q band absorption around 668 nm (Q_x) and a shoulder at 632 nm(Q_y) (Fig. 4.5). The σ-bond distribution also needs to be considered in this context, especially for the effects on the acid– base properties of the macrocycle as a whole. One can expect that the peripheral selenodiazole rings in the TSeDPz skeleton are acting as σ-electron acceptors. As a result, the acidity of the central N-H bonds should increase. In keeping with this, $TSeDPzH_2$ immediately forms, upon dissolution in pyridine, the 'pyridinium salt'. In fact, $TSeDPzH_2$ in pyridine shows no splitting of the Q-band, as expected for the presence of the $[TSeDPz]^{2-}$ dianion (D_{4h} symmetry) [1].

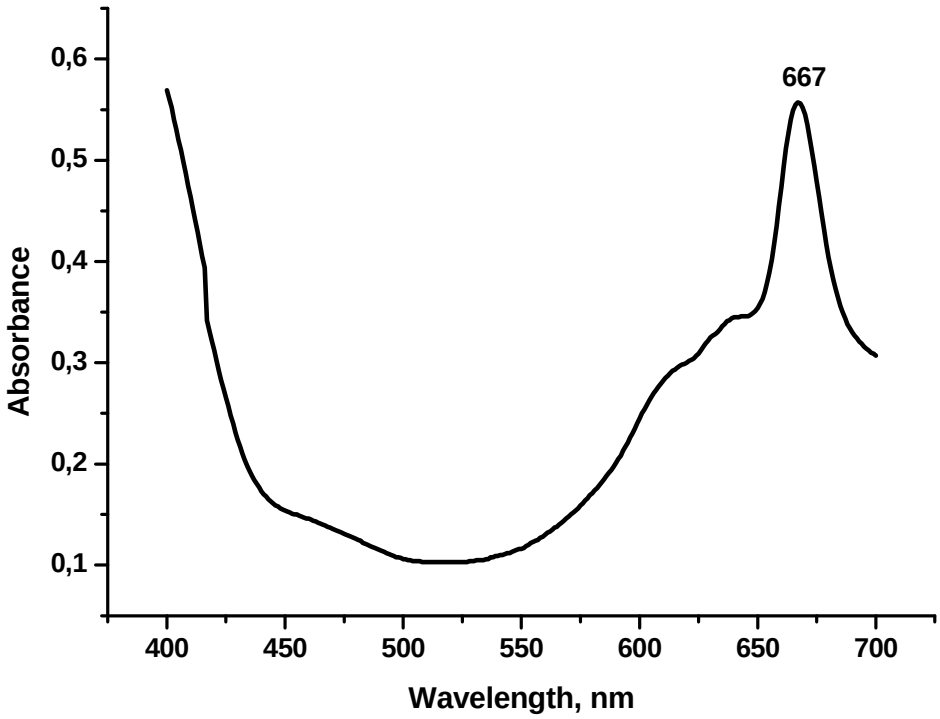

Figure 4.5 UV-visible spectrum of $TSeDPzH_2$ **(3)** in pyridine

4.3 Vanadyl Tetrakis(selenodiazole)porphyrazine (4)

We prepared the vanadyl complex, TSeDPzVO, from the reaction between $VOSO_4.5H_2O$ and **3** in DMSO under reflux.

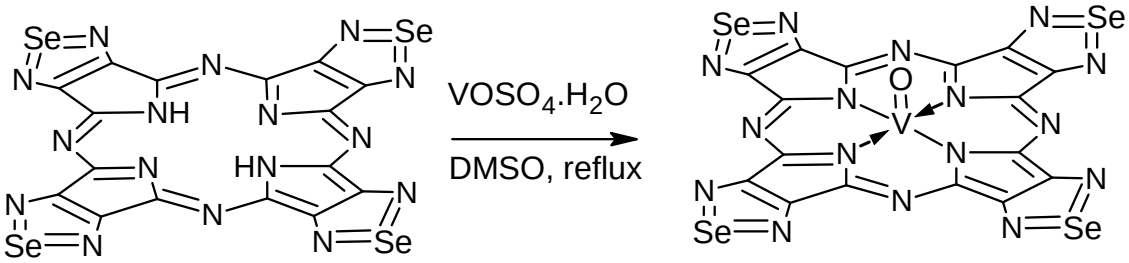

3 **4**

Figure 4.6 Synthesis of TSeDPzVO **(4)**

The absence of N–H peaks in the FT-IR spectrum and the presence of a V=O peak around 990 cm^{-1} are evidence for the formation of TSeDPzVO.

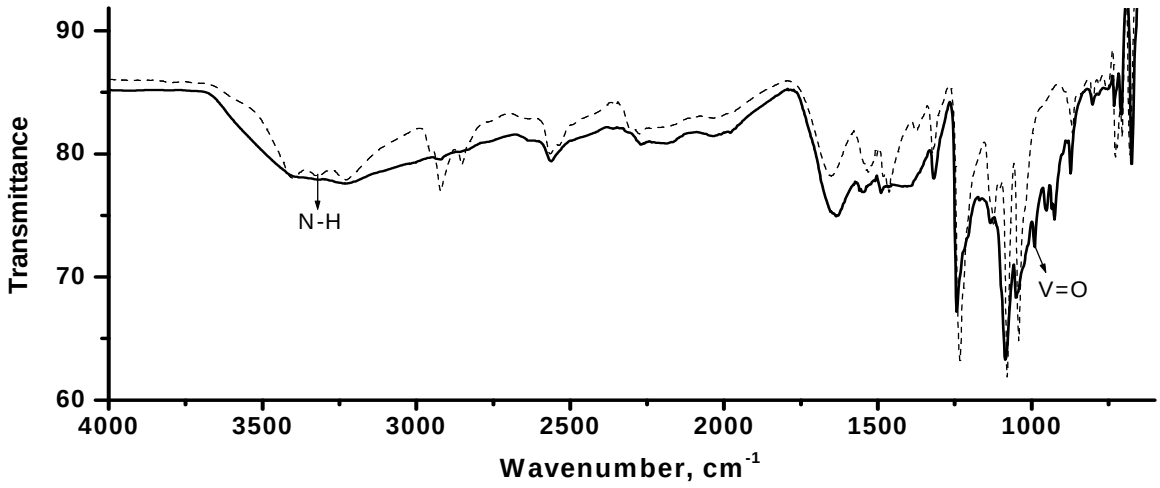

Figure 4.7 FT-IR spectra of $TSeDPzH_2$ (-------) and TSeDPzVO (——)

After the metalation process, the loss of the acetic acid could be followed in the IR and MALDI-MS spectra where the TSeDPzVO molecular ion peak [M^+] is clearly seen at 799.925 m/z given in the Appendix J

The absorption spectrum of TSeDPzVO in DMSO shows a peak around 685 nm (Fig. 4.6), which can be attributed to Q band absorption due to changing of the symmetry to C_{4v} when the VO^{2+} ion is inserted into the macrocyclic cavity. The Q band absorption of TSeDPzVO in pyridine appears as a sharp and very intense single peak which indicates axial ligation of the pyridine at the vacant site of vanadium center with similar symmetry that of the Mg^{II} complex.

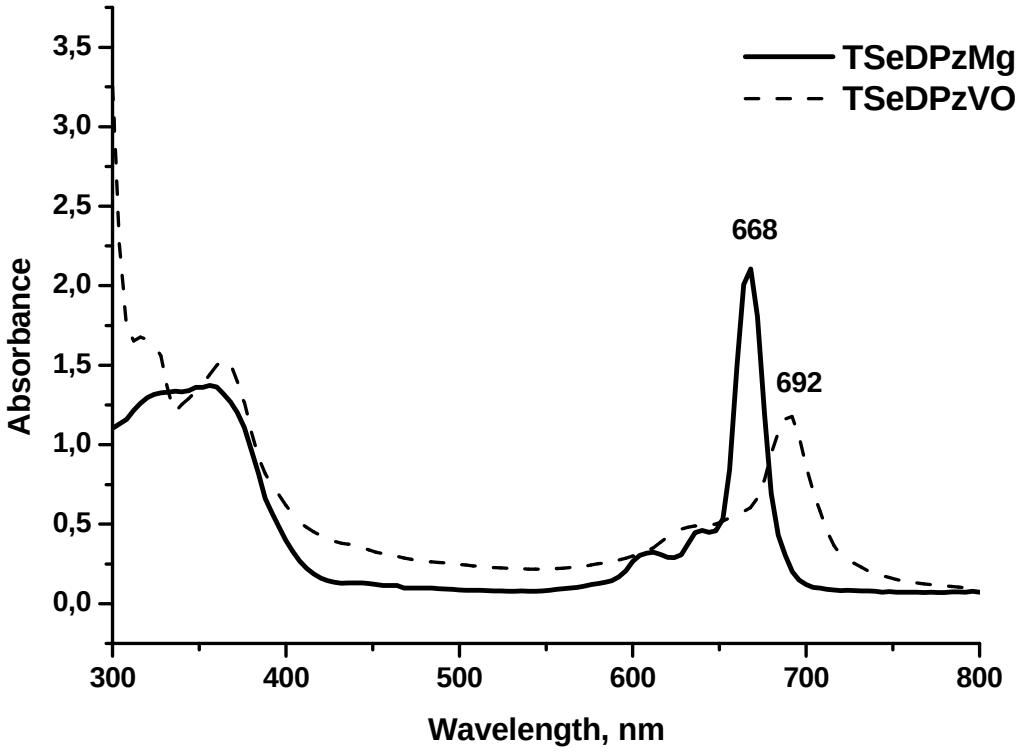

Figure 4.8 UV-visible spectra of TSeDPz (—) and TSeDPzVO (– – –) in pyridine.

4.3.1 EPR Measurement

The powder EPR spectrum of TSeDPzVO at room temperature is shown in (Fig.4.7), along with its computer simulation using the SimFonia program with the experimental values as input data. The spectrum shows parallel and perpendicular lines with hyperfine splitting. These are consistent with hyperfine patterns, which consist of two groups of eight lines characteristic of interaction of 51V nucleus (S = 1/2 and I = 7/2, 99.8% abundant) [101-104] with the single unpaired electron of the V^{4+} ion in $3d^1$ configuration. The values of $g_{//}$ and $g_{\perp}$ with hyperfine splitting constants ($A_{//}$ and $A_{\perp}$) were extracted from the spectrum as follows; $g_{//}$ = 1.976 and $g_{\perp}$ = 2.001 with g_{av} =

1.993, where g_{av} = 1/3($g_{//}$ + 2$g_{\perp}$); $A_{//}$ = 171 G and $A_{\perp}$ = 60 G with A_{av} = 97 G, where A_{av} = 1/3($A_{//}$ + 2$A_{\perp}$). The g values are in the order of $g_e > g_{\perp} > g_{//}$ (free electron g value, g_e = 2.0023). Small variations in the value of g and A indicate sensitivity of the VO^{2+} ion to different ligand field environments. More covalent bonding gives higher g values and lower hyperfine splittings [105-110].

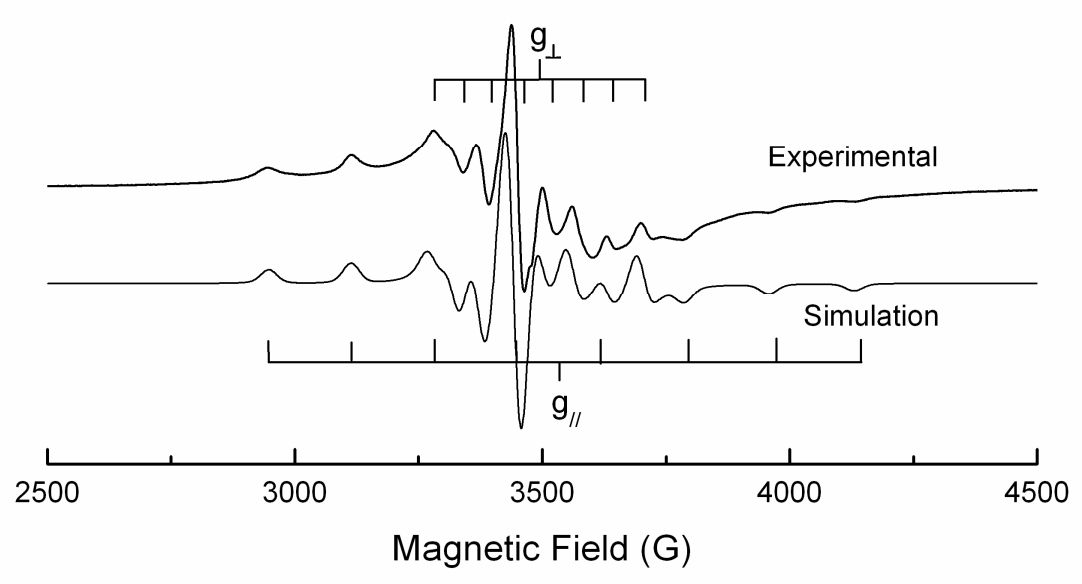

Figure 4.9 The powder EPR spectrum of TSeDPzVO at room temperature and its computer simulation.

The VO^{2+} ion has a strong tendency to form a very short V–O bond, which results in one very large principal value of the ^{5l}V hyperfine splitting constant, $A_{//}$; the other principal value $A_{\perp}$ (= A_{xx}, A_{yy}) is normally about three times smaller. $A_{//}$ (= A_{zz}) is approximately aligned along the V–O bond direction, which defines the O atom involved in the V–O bond. The observed inequality $g_{//} < g_{\perp}$ is the characteristic of a VO^{2+} moiety, because in a tetragonally compressed octahedron the b_2 (d_{xy}) level is lowest [111].

The EPR data can be interpreted in terms of molecular orbitals by using g and A parameters. The values of $A_{//}$ and $A_{\perp}$ for the VO^{2+} ion can be written as [105]:

$$A_{//} = -PK - \tfrac{4}{7}\beta_2^2 P - (g_e - g_{//})P - \tfrac{3}{7}(g_e - g_{\perp})P \quad (1)$$

$$A_{\perp} = -PK + \tfrac{2}{7}\beta_2^2 P - \tfrac{11}{14}(g_e - g_{\perp})P \quad (2)$$

where P is the direct dipole–dipole interaction constant of the magnetic moment of the electron with the magnetic moment of the vanadium nucleus (taken as 13.6 mT) [112], K is the Fermi contact term and indicates the d-orbital population for unpaired electron, β_2 is the in plane π-bonding coefficient of VO^{2+} with the ligands. Using the $A_{//}$, $A_{\perp}$ (taken as negative) and $g_{//}$, $g_{\perp}$values given in above for VO^{2+}, we obtained K= 0.70 and $\beta_2^2 = 0.93$. The largest value of β_2^2 is 1 and deviation from this value is a measure of the bonding of the d_{xy} orbital of VO^{2+} with the p-orbitals of ligands. The lowering of β_2^2 arises from delocalization of the electron onto the ligand with the increase in covalent bonding. In conclusion, a porphyrazine having four annulated selenodiazole rings $TSeDPzH_2$ and its vanadyl (VO^{2+}) complex TSeDPzVO have been prepared and characterized. The g parameters and hyperfine splittings indicate the presence of one paramagnetic axially symmetric VO^{2+} moiety coordinated by the pyrrolic N atoms support the C_{4v} axial symmetry for the structure of the compound. The values obtained in this study are in agreement with the literature values for VO^{2+} complexes of porphyrinic macrocycles [101-104,111,113-115].

4.4 Tetrakis(cyclohexyl pyrazino)porphyrazine (5)

4.4.1 Method a: *Conversion of TeSeDPz to tetrakis(cyclohexyl pyrazino) porphyrazine through octaaminoporphyrazine, (5a)*

Conversion of TeSeDPz to TCPyzPz (5a) through octaaminoporphyrazine was accomplished by using H_2S. The rings form of 1,2,5- selenodiazole are opened by the action of H_2S, the octa-aminoporphyrazine intermediate forms with release of the Se atoms. Some disadvantages of these symmetrically substituted macrocycles are the poor solubility of the TSeDPz and low yield and less stability of the octa-aminoporphyrazine. The reductive deselenation of TSeDPz using the conditions reported by Ercolani and co-workers to elaborate Pz-$(NH_2)_8$ (H_2S, pyridine) in the presence of α-diketones (1,2-cyclohexadione) gave the ring closure of the amino groups to form tetrakis(pyrazino)porphyrazines (Fig. 4.10).

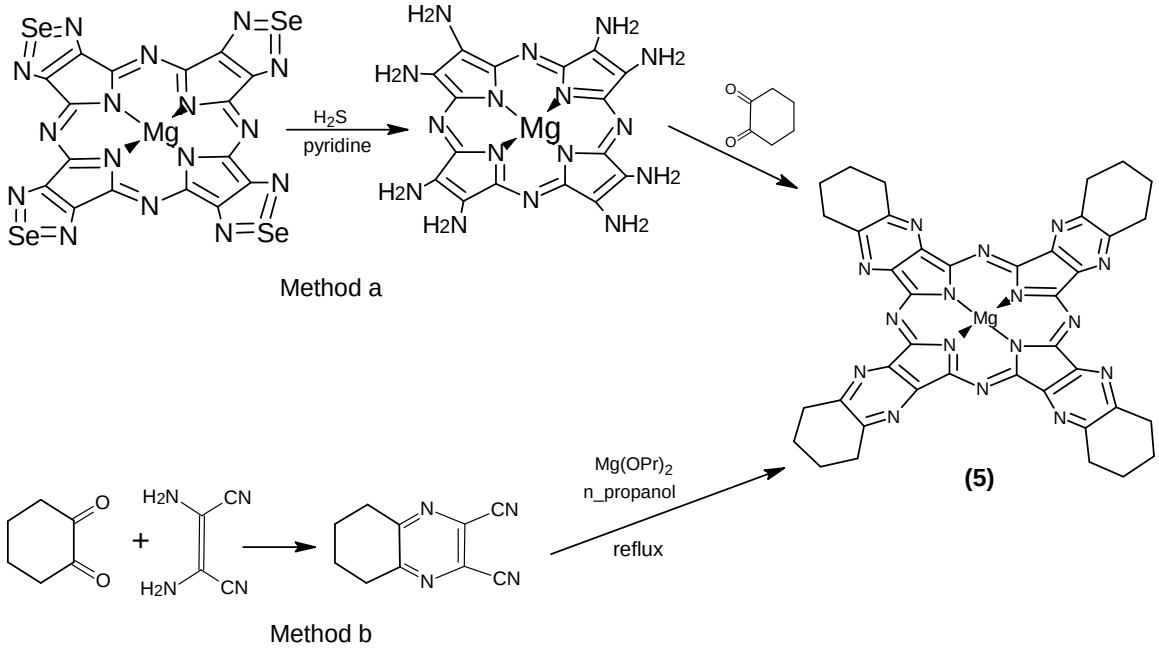

Figure 4.10 Schematic representation of preparation of tetrakis(cyclohexyl pyrazino) porphyrazine by **Method a** and **Method b**

4.4.2 Method b: *Synthesis of tetrakis(cyclohexyl pyrazino)porphyrazine by cyclotetramerization of 2,3-dicyano-5,6-cyclohexapyrazine, (5b)*

First, 2,3-dicyano-5,6-cyclohexapyrazine ligand was prepared from the reflux of diaminomaleonitrile (DAMN) and 1,2-cyclohexadione in absolute ethanol in the presence of catalytic amount of p-toluene sulfonic acid (p-TSA) in reasonable yield (80 %). In the mass spectrum the peak at 183.1166 m/z which is appropriate to the expected value was seen. In the ^{1}H-NMR spectrum of the ligand, two different peaks of CH_2 groups in the cyclohexyl part appeared at 3.05 ppm(t) and 1.92 ppm(t). And also in the ^{13}C-NMR spectrum, peaks were seen at 114.22 ppm, 129.89 ppm, 158.29 ppm, 21 ppm and 31.75 ppm.

The symmetrical tetrakis(cyclohexyl pyrazino)porphyrazine, was prepared by template macrocyclization of the 2,3-dicyano-5,6-cyclohexapyrazine ligand in the presence of Mg-propylate in propanol under reflux with 60–70% yield (Fig. 4.10)

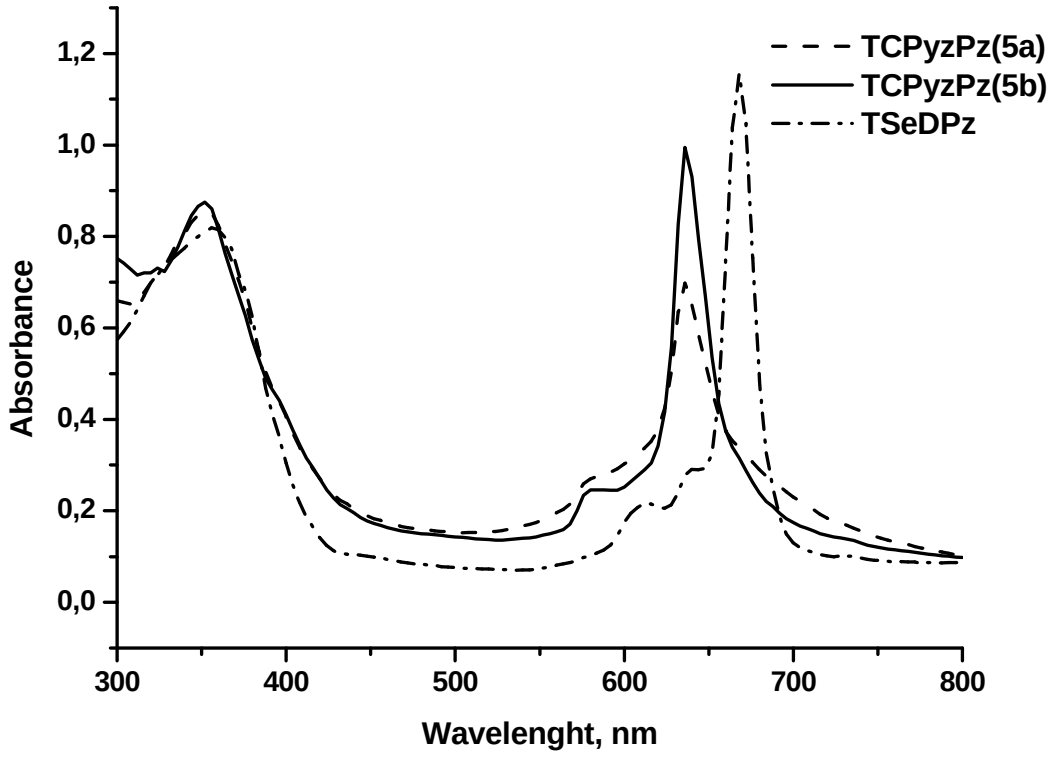

Figure 4.11 UV-visible spectra of TSeDPz (-···-), TCPyzPz(5a)(- - - -) and TCPyzPz(5b) (——) in DMSO

According to the ^{1}H-NMR (2.28 ppm, 1.23 ppm, and 2.29 ppm, 1.25 ppm for CH_2 groups in the cyclohexyl parts of **5a** and **5b** respectively), IR spectra and Mass spectrum analysis the proposed structures of the molecule are meaningfull (See App. M and U for IR spectra, App. O and X for MASS spectra, and App. P and Y for ^{1}H-NMR spectra of both products). The porphyrazine core is again identical with TSeDPz **(2)**. The C-H stretching vibrations are strong IR band at around 2934 cm^{-1} both in **5a** and **5b** correspond to the presence of the cyclohexyl groups on the peripheral positions of the porphyrazine core. For the compounds of **5a** and **5b,** the stretching vibrations of the meso-N atom bridge, $\nu(CN_{meso})$, and C=C are with weak-medium peaks in the 1530 cm^{-1} region and 1630-1637 cm^{-1}, respectively. The skeletal vibrations of pyrrole rings, ν(Pyr), of both **5a** and **5b** are strongly mixed with the ν(C= N) vibrations of the annulated selenodiazole rings and give the most intense IR band at 1235 cm^{-1} and 1236 cm^{-1}, respectively. The disappearance of the the stretching vibrations of the SeN bonds

which are strong in 1,2,5-selenodiazoles ν(SeN) at 716 and 640 cm^{-1} shows the deselenation of the **2.** The in-plane deformations of the pyrrole rings, δ(Pyr), give a strong IR band at 1084 cm^{-1} and a weak-medium band at 1042 cm^{-1}. The peaks around 1142-1147 cm^{-1} indicates the resonating C-N groups belong to six membered rings which was not observed in the spectrum of TSeDPz **(2)**. The mass spectrum of the **5a** and **5b** are both at $[M^+]$:763 m/z and consistent with molecular ion peaks. In the UV-visible spectra of cyclohexyl-pyrazino porhyrazines in DMSO the Q band absorptions for **5a** and **5b** are at 636 nm in which both are consistent with metal porphyrazines (Fig. 4.11). The hypsochromic shift of the cyclohexyl-pyrazino porhyrazines about 24 nm may be due to the π-expansion of the octaaminoporphyrazine ring by six membered pyrazine substitutions to the peripheries which the corresponding is in longer wavelength in TSeDPz.

CHAPTER 5

CONCLUSION

Porphyrins, phthalocyanines, and porphyrazines molecules have been extensively investigated in the field of basic research and as materials for practical applications such as materials science, molecular electronics, and sensor development. Porphyrazines in general, however, have so far been comparatively much less studied. Hence great possibility is presently offered for the synthesis and investigation of new classes of such macrocycles. In the recent, new porphyrazine macrocycles can be that directed to the synthesis of new phthalocyanine like macrocycles carrying heterocyclic rings directly annulated to the porphyrazine core, opening a route to new forms of investigation and promising potential practical applications. The fused heterocyclic groups on the peripheral positions, such as five membered selenodiazole (TSeDPz) provide a different electronic distribution for the porphyrazine macrocyclic core. The annulated 1,2,5-selenodiazole rings in the porphyrazine macrocycle, which can easily undergo different transformations, open up a new synthetic approach to octaaminoporphyrazines.

In this study, we have prepared the tetrakis(selenodiazole)porphyrazinato magnesium TSeDPzMg molecule from the tetramerization of 3,4-dicyano-1,2,5 selenodiazole ligand in propanol. After the demetallation of TSeDPzMg in the presence of trifluoroaceticacid, the metal free porphyrazine, $TSeDPzH_2$, has been prepared in resonable yield. The vanadyl complex has been prepared by the treatment of $TSeDPzH_2$ with $VOSO_4.5H_2O$ in DMSO. The All spectroscopic data and ESR measuments confirm the proposed vanadyl complex.

The tetrakis(cyclohexyl pyrazino)porphyrazine in which the porphyrazine molecule is annulated with six membered rings on the pepriferies was prepared by two different methods.

In the first method, we first used H_2S in pyridine to open the annulated 1,2,5-selenodiazole rings in the porphyrazine macrocycle, in which the deselenation processes at the annulated selenodiazole rings in symmetrical and low-symmetry macrocycles and the formation of vicinal diamino functionalities have allowed the pyrazino groups formation by in situ addition of 1,2 cyclohexadione porphyrazine macrocycles by ring reclosure.

In the second method, 2,3-dicyano-5,6-cyclohexapyrazine ligand has been prepared and macrocylized in propanol and gave the pyrazino porphyrazine molecule in good yield. All spectroscopic data (ATR, UV, MALDI Mass and ^{1}H-NMR) confirms the structure of the molecule.

In conclusion, we prepared the six membered heterocyclic pyrazino groups fused porphyrazaine molecules with two different methods. Also, vanadyl tetrakis(selenodiazole)porphyrazine has been sythesized and its paramagnetic properties were investigated by ESR measurements. In addition, the optical and physicochemical properties of those macrocyclic compounds can be adjusted through the right choice of coupling diketones. The poor solubilities in many organic solvents is always an obstructive problems for these compounds. To overcome these obstacles the fused heterocylic groups should have very rich and diverse but more adjustable physicochemical properties.

REFERENCES

[1] M. P. Donzello, C. Ercolani, P. A. Stuzhin, *Coordination Chemistry Reviews* 2006, 250, 1530–1561

[2] B. G. Mbatha, PhD. Thesis in University of Johannesburg, 2006.

[3] H. Ali and J .E. van Lier *Chem. Rev*. 1999, 99, 2379.

[4] M. J. Crossley, P. J. Sintic, R. Walton and J. R. Reimers *Org. Biomol. Chem.* 2003, 1, 2777.

[5] R. R. Allison, G. H. Downie, R. Cuenca, X. Hu, C. J. H. Childs, C. H. Sibata *Photodiagnosis and photodynamic therapy* 2004, 1, 27.

[6] S. L. Michel, S. Baum,A. G. M. Barrett, B. M. Hoffman, *in Progress in Inorganic Chemistry (Ed. K. D. Karlin) J.Wiley & Sons: NewYork, NY,* 2001, 50, 473.

[7] P. A. Stuzhin, C. Ercolani, *in The Porphyrin Handbook (Eds K. M. Kadish, K. M. Smith, R. Guilard) Academic Press: NewYork, NY,* 2003, 15, 263.

[8] V. N. Kopranenkov, E. A. Lukyanets, *Russ. Chem. Bull.* 1995, 44, 2216.

[9] M. S. Rodriguez-Morgade, P. A. Stuzhin, *J. Porphyrins Phthalocyanines* 2004, 8, 1129.

[10] A. G. Montalban, S. Baum, B. M. Hoffman, A. G. M. Barrett, *J. Chem. Soc., Dalton Trans.* 2003, 2093.

[11] M. J. Fuchter, C. Zhong, H.Zong, B. M. Hoffman, and A. G. M. Barrett, *Aust. J. Chem*. 2008, 61, 235–255.

[12] F. H. Moser and A. L. Thomas, *The Phthalocyanines, CRC Press, Boca Raton (Fla.),* 1983, 1, 2.

[13] C. C. Leznoff and A. B. P. Lever, *Phthalocyanines: Properties and Applications, VCH Publ., New York, San Francisco, London,* 1989, 1993, 1-3.

[14] Fischer and F. Endermann, *Ann. Chem.*, 1937, 531, 245.

[15] Brit. Pat. 686395, *Chem. Abstr.*, 1953, 47, 7223.

[16] K. Andersen, M. Anderson, O. P. Anderson, S. Baum, T. F. Baumann, L. S. Beall, W. E. Broderick, A. S. Cook, D. M. Eichhorn, D. Goldberg, H. Hope, W. Jarrell, S. J. Lange, Q. J. McCubbin, N. S. Mani, T. Miller, A. Garrido Montalban, M. S. Rodrigez-Morgade, S. Lee, H. Nie, M. M. Olmstead,M. Sabat, J.W. Sibert, C. Stern,A. J. P. White,D. B. G.Williams,D. J.Williams, A. G. M. Barrett, B. M. Hoffman, *J. Heterocycl. Chem*. 1998, 35, 1013.

[17] M. Zhao, PhD. Thesis in Northwestern University, 2004

[18] R. P. Linstead and M. Whalley, *J. Chem. Soc*. 1952, 4839.

[19] M. E. Baguley, H. France, R.P. Linstead, and M. Whalley, *J. Chem. Soc.* 1955, 3521.

[20] G. E. Ficken and R. P. Linstead, *J. Chem. Soc.* 1952, 484.

[21] M. P. Donzello, D. Dini, G. D'Arcangelo, C. Ercolani, R. Zhan, Z. Ou, P. A. Stuzhin, K. M. Kadish, *J. Am. Chem. Soc*. 2003, 125, 14190.

[22] L. Giribabu, M. Chandrasekharam, S. M. Mohan, C. S. Rao, M. L. Kantam, M. R. Reddy, P.Y. Reddy, T.Toru, *Synlett* 2006, 1604.

[23] M. Chandrasekharam, C. S. Rao, P. S. Surya, M. L. Kantam, M. R. Reddy, P. Y. Reddy, T. Toru, *Tetrahedron Lett.* 2007, 48, 2627.

[24] X. Guinchard, M. J. Fuchter, A. Ruggiero, B. J. Duckworth, A. G. M. Barrett, B. M. Hoffman, *Org. Lett.* 2007, 9, 5291.

[25] E. Yu. Svetkina, T. V. Filippova, E.A. Blyumberg, and V. N. Kopranenkov, *Kinet. KataL* 1984, 25, 1101

[26] S. Banfi, F. Montanari, S. Quici, S. v. Barkanova, O. L. Kaliya, V. N. Kopranenkov, and E. A. Luk'yanets, *Tetrahedron Lett*. 1995, 36, 2317

[27] O. L. Kaliya and E. A. Luk'yanets, *in Fundamental Research in Homogeneous Catalysis, Ed. A. E. Shilov, Gordon and Breach Sci. Publ., New York, London* 1986, 1, 335.

[28] J. Sun, Y. Sun, K. Deng, H. Hou, D. Wang, *Chem. Lett.* 2007, 36, 586.

[29] K. Deng, F. Huang, D. Wang, Z. Peng, Y. Zhou, *Chem. Lett.* 2004, 33, 34.

[30] M. Lui, D. Z. Han, K. Deng, D. Y. Wang, Chin. *J. Catal.* 2004, 25, 834.

[31] Y. P. Lei, J. Sun, C. J. Yang, K. Deng, D. Y. Wang, *J. Porphyrins Phthalocyanines* 2005, 9, 537.

[32] I. Spasojevic, I. Batinic-Haberle, *Inorg. Chim. Acta* 2001, 317, 230.

[33] S. Hachiya, A. S. Cook, D. B. G. Williams, A. G. Montalban, A. G. M. Barrett, B. M. Hoffman, *Tetrahedron* 2000, 56, 6565.

[34] R. Hirohashi, K. Sakamoto, and E. Ohno-Okumura, *Phthalocyanines as Functional Dyes*, *ICP, Tokyo, Japan*, 2004.

[35] I. Okura, *Photosensitization of Porphyrins and Phthalocyanines*, *Kodansya, Tokyo, Japan*, 2000.

[36] G. Jory, *Photochemistry and Photobiology* 1990, 52, 439–443.

[37] J. Moan, *Journal of Photochemistry and Photobiology B: Biology* 1990, 5(3-4), 521–524.

[38] M. J. Cook, I. Chambrier, S. J. Cracknell, D. A. Mayes, and D. A. Russell, *Photochemistry and Photobiology*, 1995, 62(3), 542–545.

[39] K. Tabata, K. Fukushima, K. Oda, and I. Okura, *Journal of Porphyrins and Phthalocyanines*, 2000, 4(3), 278–284.

[40] I. Seotsanya-mokhosi, N. Kuznetsova, and J. T. Nyokong, *Journal of Photochemistry and Photobiology A: Chemistry* 2001, 140(3), 215–222.

[41] K. Sakamoto, T. Kato, E. Ohno-Okumura, M. Watanabe, and M. J. Cook, *Dyes and Pigments* 2005, 64(1), 63–71.

[42] J. D. Miller, E. D. Baron, H. Scull, A. Hsia, J. C. Berlin, T. McCormick, V. Colussi, M. E. Kenney, K. D. Cooper, and N. L. Oleinick, *Toxicol. Appl. Pharmacol*. 2007, 224, 290-299.

[43] S. L. Haywood-Small, D. I. Vernon, J. Griffiths, J. Schofield, and S. B. Brown, *Biochem. Biophys. Res. Commun*. 2006, 339, 569-576

[44] J. T. Groves, T. P. Farell, *J. Am. Chem. Soc*. 1989, 111, 4998.

[45] A.Villanueva, L. Caggiari, G. Jori, C. Milanesi, *J. Photochem. Photobiol. B: Biol*. 1994, 23, 49.

[46] M. E. Anderson, A. G. M. Barrett, B. M. Hoffman, *Inorg. Chem*. 1999, 38, 6143.

[47] M. E. Anderson, R. L. Letsinger, A. G. M. Barrett, B. M. Hoffman, *J. Inorg. Biochem.* 2000, 80, 257.

[48] M. J. Fuchter, L. S. Beall, S. Baum, A. G. Montalban, E. G. Sakellariou, N. S. Mani,T. Miller,A. J. P.White, D. J.Williams, A. G. M. Barrett, B. M. Hoffman, *Tetrahedron* 2005, 61, 6115.

[49] A. K. Bordbar, M. Davari, E. Safaei, V. Mirkhani, *J. Porphyrins Phthalocyanines* 2007, 11, 139.

[50] S. Vagin, G. Y. Yang, M. K. Y. Lee, and M. Hanack, *Optics Communications* 2003, 228, 119-125

[51] L. S. Beall, N. S. Mani, A. J. P. White, D. J. Williams, A. G. M. Barrett, B. M. Hoffman, *J. Org. Chem*. 1998, 63, 5806.

[52] H. Mockert, D. Schmeisser, W. Gbpel, *Sensors Acctuators* 1989, 29, 159.

[53] B. Bott, T. A. Jones, *Sensors Actuators* 1984, 5, 43.

[54] A. J. Rim, S. J.Martin, T. E. Zipperian, *Sensors Actuators* 1985, 8, 319.

[55] A. W. Snow, W. R. Barger, M. Klusty, *Langmuir* 1986, 2, 513.

[56] J. W. Pankow, C. Arbour, J. P. Dodelet, G. E. Collins, and N. R. Armstrong. *Journal of Physical Chemistry* 1993, 97, 8485-8494

[57] L. A. Ehrlich, P. J. Skrdla, W. K. Jarrell, J. W. Sibert, N. R. Armstrong, S. S. Saavedra, A. G. M. Barrett, and B. M. Hoffman, *Inorganic Chemistry* 2000, 39, 3963-3969

[58] E.M. Bauer, C. Ercolani, P. Galli, I.A. Popkova, P.A. Stuzhin, *J. Porphyrins Phthalocyanines* 1999, 3, 371.

[59] P.A. Stuzhin, E.M. Bauer, C. Ercolani, *Inorg. Chem.* 1998, 37, 1533.

[60] E.M. Bauer, D. Cardarilli, C. Ercolani, P.A. Stuzhin, U. Russo, *Inorg. Chem.* 1999, 38, 6414.

[61] S. Angeloni, E.M. Bauer, C. Ercolani, I.A. Popkova, P.A. Stuzhin, *J. Porphyrins Phthalocyanines* 2001, 5, 881.

[62] M.S. Fischer, D.H. Templeton, A. Zalkin, M. Calvin, *J. Am. Chem. Soc*. 1971, 93, 2622.

[63] S. Matzumoto, A. Endo, J. Mizuguchi, Z. Krystallogr, *Inorg. Chim. Acta* 2000, 215, 182.

[64] P.A. Stuzin, E.A. Pozdysheva, O.V. Mal'chugina, I.A. Popkova, C. Ercolani, Chem. *Heterocycl. Comp.* 2005, 41, 246

[65] M.P. Donzello, R. Agostinetto, S.S. Ivanova, M. Fujimori, Y. Suzuki, H. Yoshikawa, J. Shen, K. Awaga, C. Ercolani, K.M. Kadish, P.A. Stuzhin, *Inorg. Chem.* 2005, 44, 8539.

[66] M. Fujimori, Y. Suzuki, H. Yoshikawa, K. Awaga, *Angew. Chem.* 2003, 115, 6043.

[67] Y. Suzuki, M. Fujimori, H. Yoshikawa, K. Awaga, *Chem. Eur. J.* 2004, 10, 5158.

[68] S.W. Oliver, T.D. Smith, *J. Chem. Soc. Perkin Trans. II* 1987, 1579.

[69] K.J.M. Nolan, M. Hu, C.C. Leznoff, *Synlett* 1997, 593.

[70] E.V. Kudrik, E.M. Bauer, C. Ercolani, P.A. Stuzhin, A. Chiesi-Villa, C. Rizzoli, *Mend. Comm.* 2001, 45.

[71] M.P. Donzello, C. Ercolani, A.A. Gaberkorn, E.V. Kudrik, M. Meneghetti, G. Marcolongo, C. Rizzoli, P.A. Stuzhin, *Chem. Eur. J.* 2003, 9, 4009.

[72] A.A. Gaberkorn, M.-P. Donzello, P.A. Stuzhin, *Russ. J. Org. Chem.* 2006, 42(6), 929.

[73] A.A. Gaberkorn, I.A. Popkova, P.A. Stuzhin, C. Ercolani, *Russ. J. Gen. Chem.* 2006, 76, 1494.

[74] S.M. Baum, A.A. Trabanco, A.G. Montalban, A.S. Micallef, C. Zhong, H.G. Meunier, K. Suhling, D. Phillips, A.J.P. White, D.J. Williams, A.G.M. Barrett, B.M. Hoffman, *J. Org. Chem.* 2003, 68, 1665.

[75] M. Zhao, C. Stern, A.G.M. Barrett, B.M. Hoffman, *Angew. Chem. Int. Ed.* 2003, 42, 462.

[76] M. Zhao, C. Zhong, C. Stern, A.G.M. Barrett, B.M. Hoffman, *Inorg. Chem.* 2004, 43, 3377.

[77] A.A. Gaberkorn, Y.B. Ivanova, O.V. Molodkina, M.-P. Donzello, I. Pimkov, C. Ercolani, V.B. Sheinin, P.A. Stuzhin, *J. Porphyrins Phthalocyanines* 2004, 8, 846.

[78] M. Zhao, C. Zhong, C. Stern, A.G.M. Barrett, B.M. Hoffman, *J. Am. Chem. Soc.* 2005, 127, 9769.

[79] C. Ercolani, E.V. Kudrik, S. Moraschi, I.A. Popkova, P.A. Stuzhin, *First International Conference on Porphyrins and Phthalocyanines*, Dijon, France, 2000, 575.

[80] A. Gieren, H. Betz, T. Huebner, V. Lamm, R. Neidlein, D. Droste, Z. *Naturforsch.* 1984, B39, 485.

[81] L.M. Weinstock, I. Shinkai, in: A.R. Katrizky (Ed.), *Comprehensive Heterocyclic Chemistry. The Structure, Reactions, Synthesis and Uses of Heterocyclic Compounds*, *Pergamon Press, Oxford*, 1984, 6, 513–543.

[82] A.M. Gyul'maev, I.V. Stankevich, Z.V. Todres, *Khim. Geterotsikl. Soedin.* 1973, 1473.

[83] M.H. Palmer, R.H. Findlay, J.N.A. Ridyard, A. Barrie, P. Swift, *J. Mol. Struct.* 1977, 39, 189.

[84] A. Bhattacharyya, A.A. Bhattacharyya, *Indian J. Chem.* 1983, 22B, 802.

[85] T. Strassner, J. Fabian, *J. Phys. Org. Chem.* 1997, 10, 33.

[86] M. Gouterman, G. Wagnier, L.C. Snyder, *J. Mol. Spectr.* 1963, 11, 108.

[87] M.G. Gal'pern, E.A. Lukyanets, *Zh. Obshch. Khim*. 1969, 39, 2536.

[88] P.A. Stuzhin, C. Ercolani, *in: Symposium Lecture ICPP3, J. Porphyrins Phthalocyanines* 2004, 8, 495.

[89] P.A. Stuzhin, *Diss. Dr. Chem. Sci. Ivanovo* 2004, 383.

[90] M. Whalley, *J. Chem. Soc*. 1961, 866.

[91] P.A. Stuzhin, *J. Porphyrins Phthalocyanines* 2003, 7, 813.

[92] E. Benedetti, V. Bertini, *Spectrochim. Acta* 1968, 24, 57.

[93] A.A. El-Azhary, *Acta Chem. Scand*. 1995, 49, 11.

[94] K.N. Solovyov, L.L. Gladkov, A.A. Starukhin, S.F. Shkirman, *Spektroskopija Porfirinov: Kolebatel'nye Sostojanija [Spectroscopyof Porphyrins: Vibrational States], Nauka i Tekhnika, Minsk*, 1985, 416.

[95] M.P. Sammes, *J. Chem. Soc.*, Perkin Trans. 1972, 2, 160.

[96] L.L. Gladkov, S.F. Shkirman, V.K. Konstantinova, K.N. Solov'ev, *Zh. Prikl. Spektr*. 2000, 67, 551.

[97] K.V. Berezin, V.V. Nechaev, *Zh. Prikl. Spektr*. 2003, 70, 182.

[98] X. Zhang, Y. Zhang, J. Jiang, *Vibr. Spectr*. 2003, 33, 153.

[99] R.P. Linstead, M. Whalley, *M. J. Chem. Soc*. 1952, 4839.

[100] A.B.P. Lever, *Adv. Inorg. Chem. Radiochem*. 1965, 7, 27.

[101] R. Öztürk, S. Güner, B. Aktaş, A. Gül, *Supramol Chem* 2005, 17, 233.

[102] R. Öztürk, S. Güner, B. Aktaş, A. Gül, *Synth React Inorg Met-Org Chem* 2001, 31, 1623

[103] R. Öztürk, A. Gül *Tetrahedron Lett*, 2004, 45, 947.

[104] P.M. Espinosa, A. Campero, R. Salcedo, *Inorg Chem* 2001, 40, 4543.

[105] T.F. Yen, L.J. Boucher, E.C. Tynan, *Electron spin resonance of metal complexes. Plenum press, New York,*1969

[106] Y. Yerli, F. Köksal, A. Karadağ, *Solid State Sciences,* 2003, 5, 1319.

[107] M. Narayana, S.G. Satyanarayana, G.S. Sastry, *Mol. Phys.,* 1976, 31, 203.

[108] K.S. Mısra, J. Sun, U. Orhun, *Phys. Stat. Sol. B.* 1990, 162, 585

[109] S.V.J. Lakshaman, Sunder, *J. Solid State Commun.* 1983, 45, 141.

[110] K.V.S. Rao, M.D. Sastry, P. Venkateswarlu, *J. Chem. Phys.* 1968, 49, 4984.

[111] Umesh BG, Satish MA, Anil DN, Vidyanad KR, Vinayak BM, *J. Mol. Struct. Theochem.* 2001, 572, 61.

[112] McGarvey BR, *J. Phys. Chem.* 1967, 71, 51.

[113] Y. Yerli, A. Zerentürk, K. Özdoğan, *Spectrochim. Acta A.* 2007, 68, 147.

[114] S. Kasthurirengan, S. Soundararajan, *J. Magn. Reson.* 1975, 19, 357

[115] P.I. Premovic, T. Allard, N.D. Nikolic, I.R. Tonsaa, M.S. Pavlovic`, *Fuel* 2000, 79, 813.

APPENDIX A

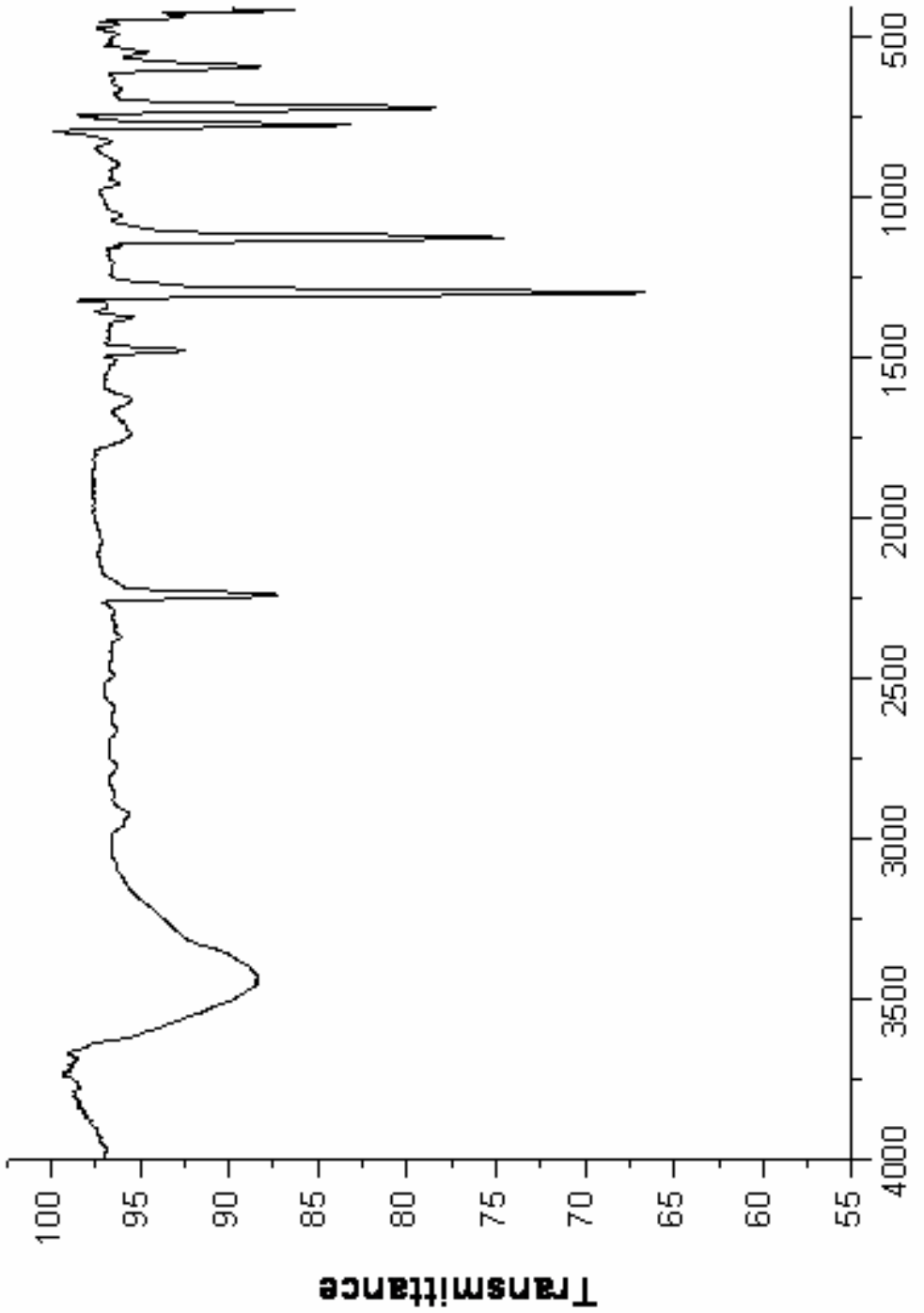

IR Spectrum of 3,4-Dicyano-1,2,5-selenodiazole (1)

APPENDIX B

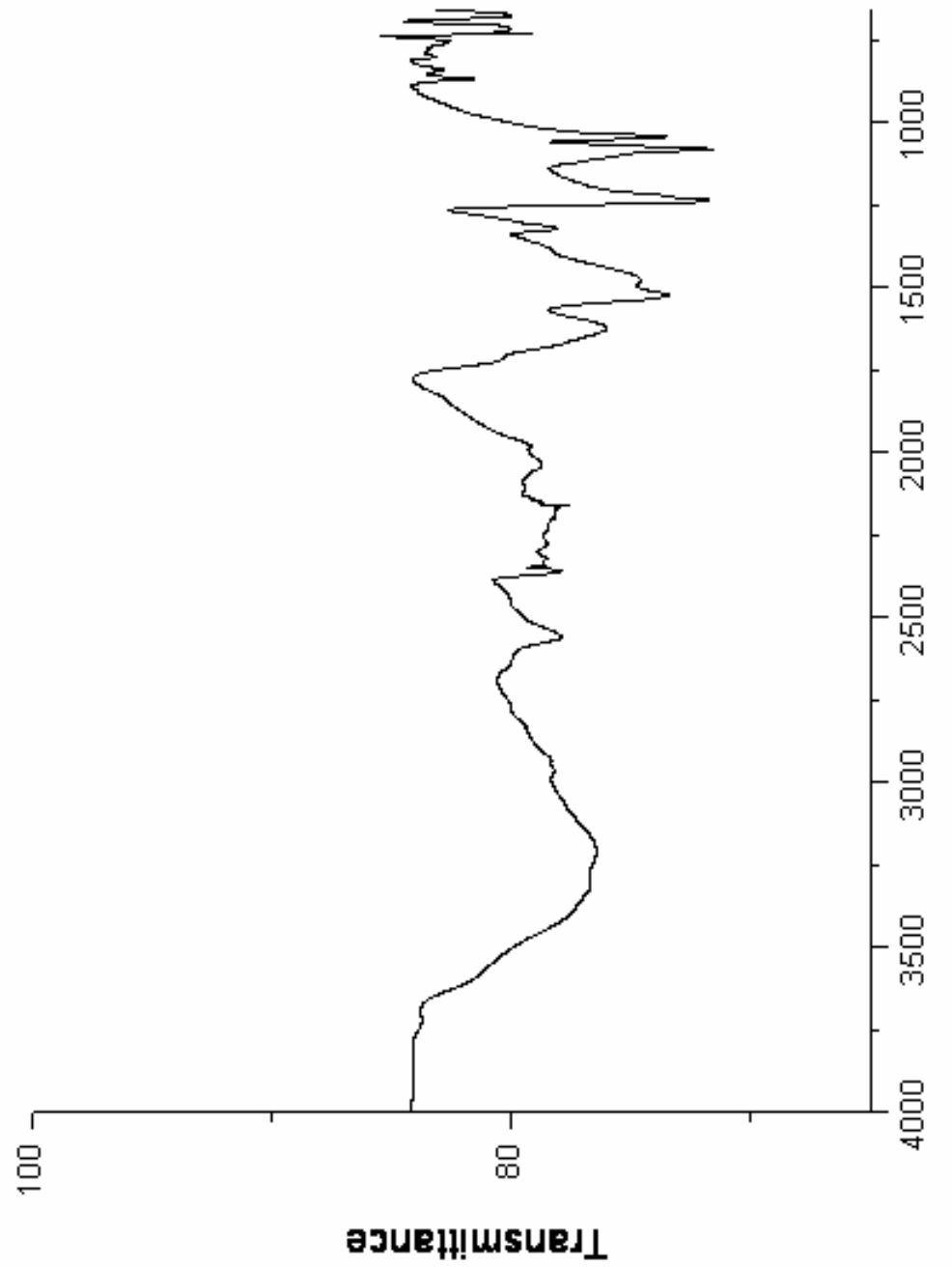

IR Spectrum of TSeDPzMg (2)

APPENDIX C

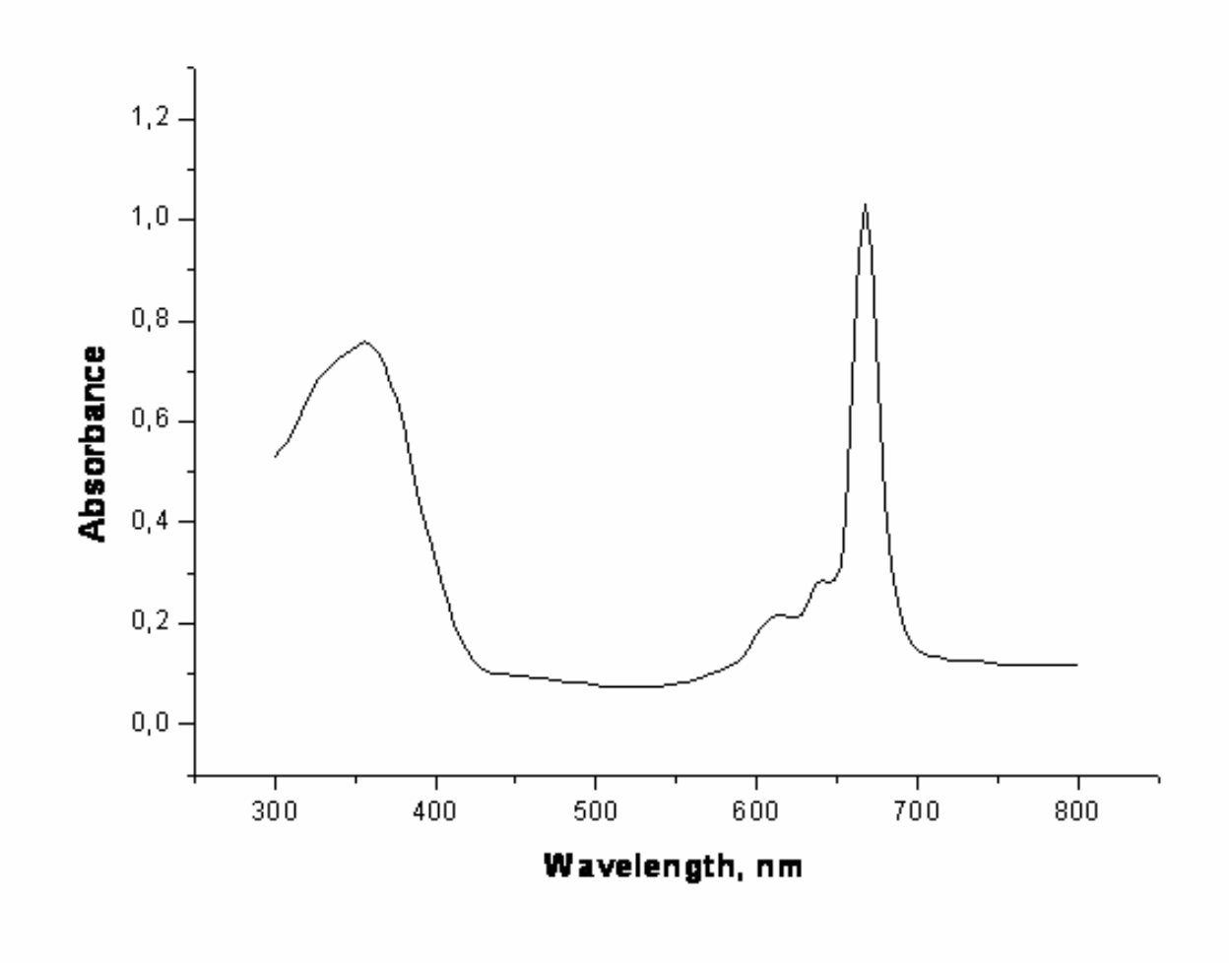

UV-VISIBLE Spectrum of TSeDPzMg (2) in DMSO

APPENDIX D

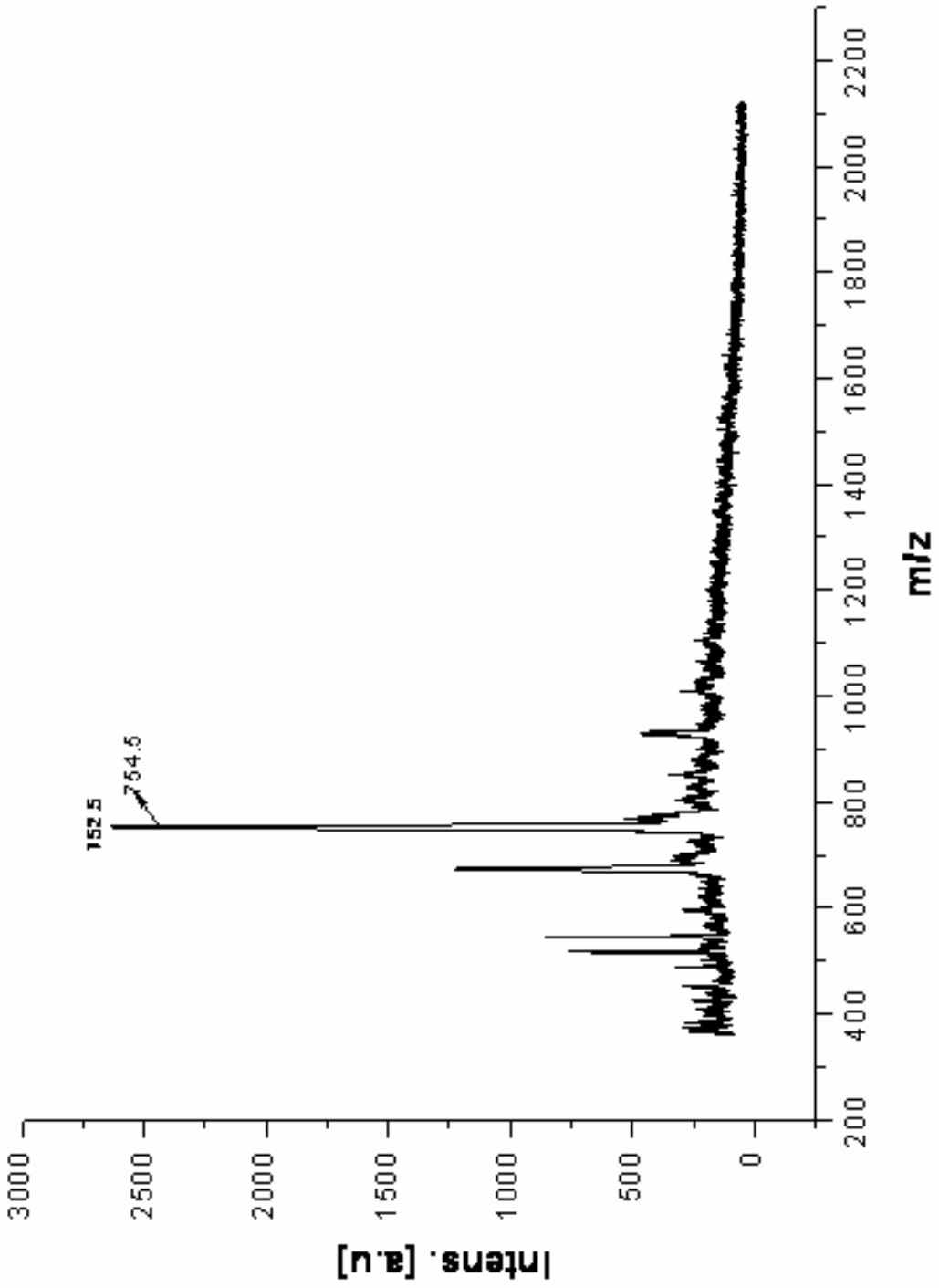

MALDI-MS Spectrum of TSeDPzMg (2)

APPENDIX E

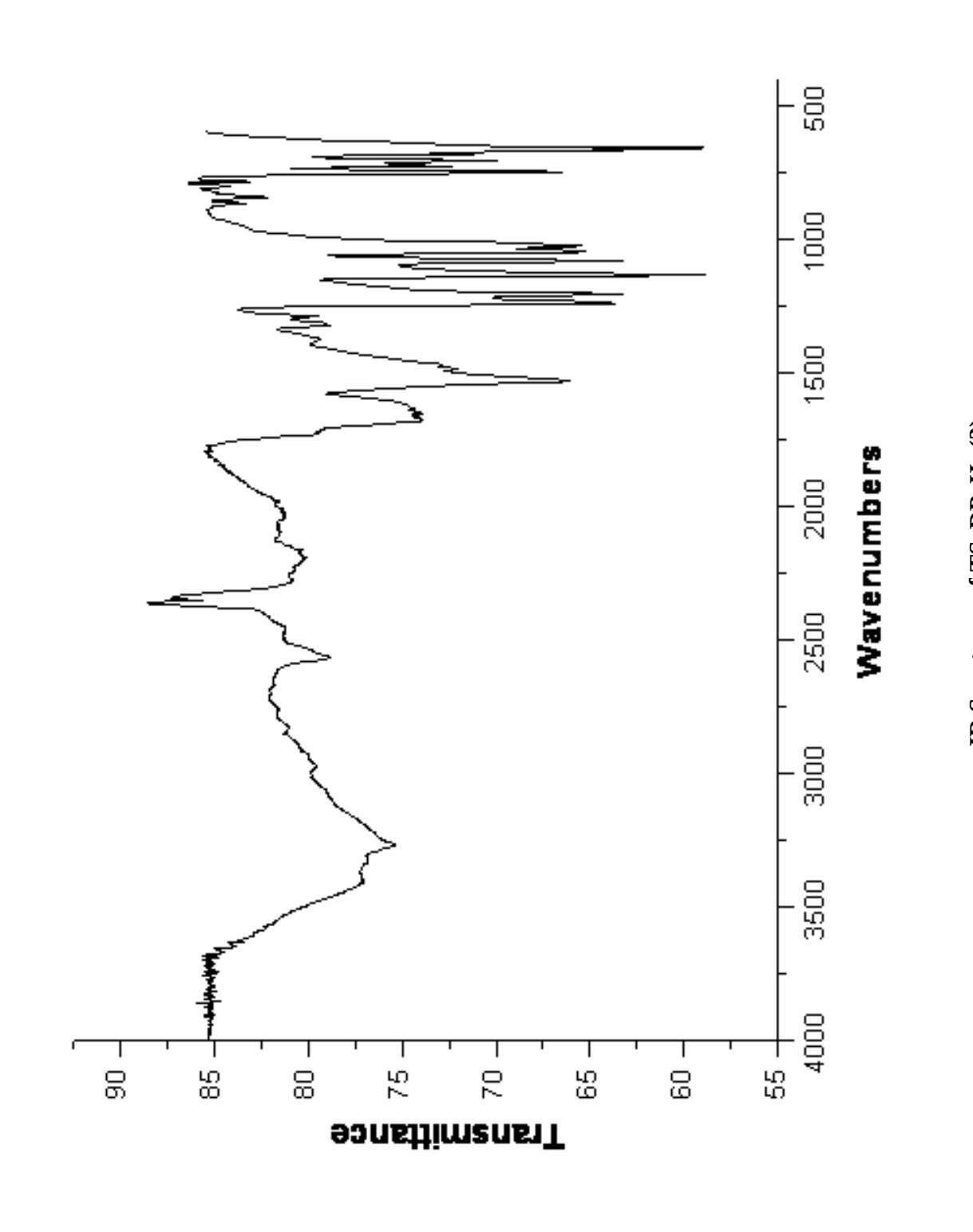

IR Spectrum of TSeDPzH$_2$ (3)

APPENDIX F

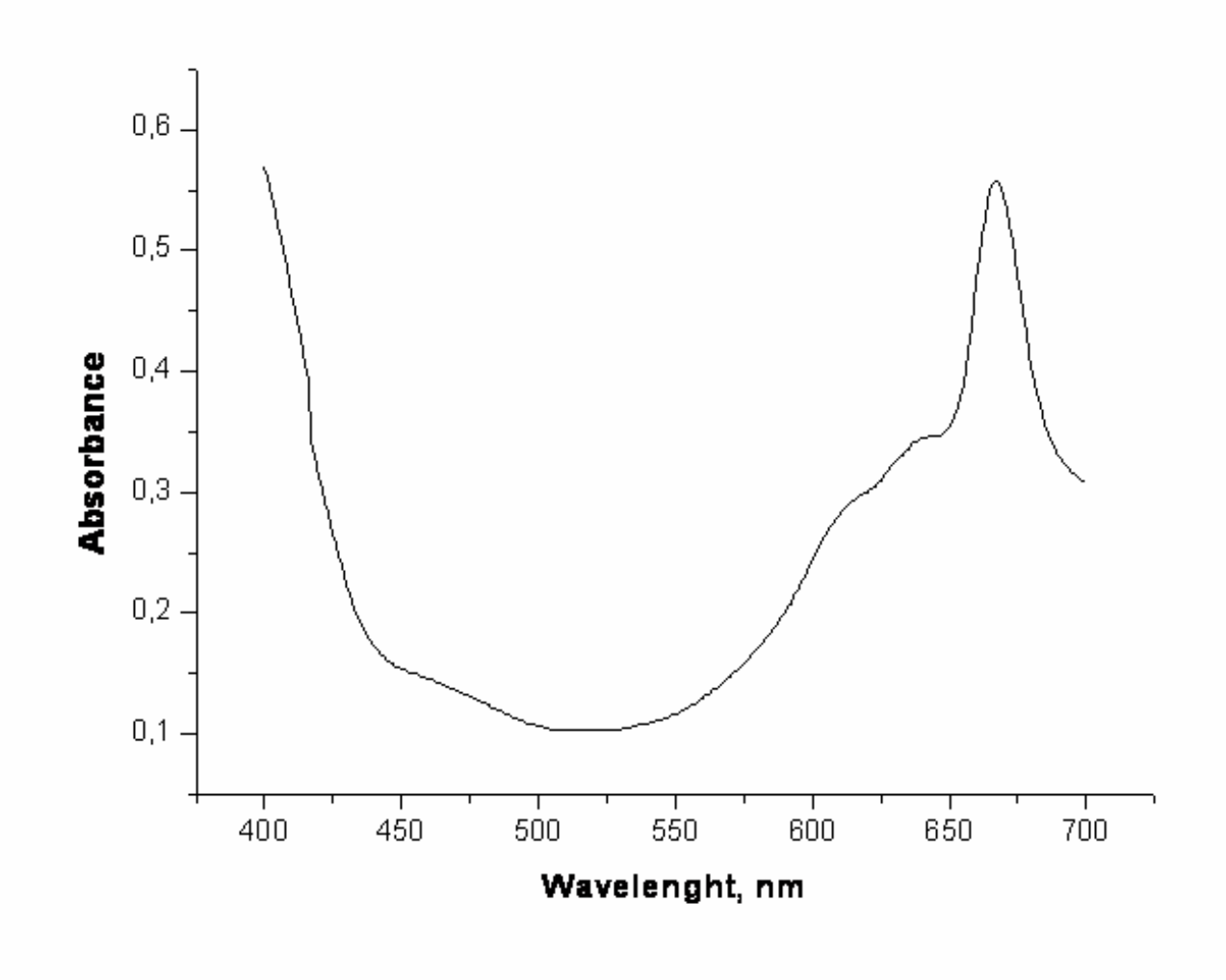

UV-VISIBLE Spectrum of $TSeDPzH_2$ (3) in DMSO

APPENDIX G

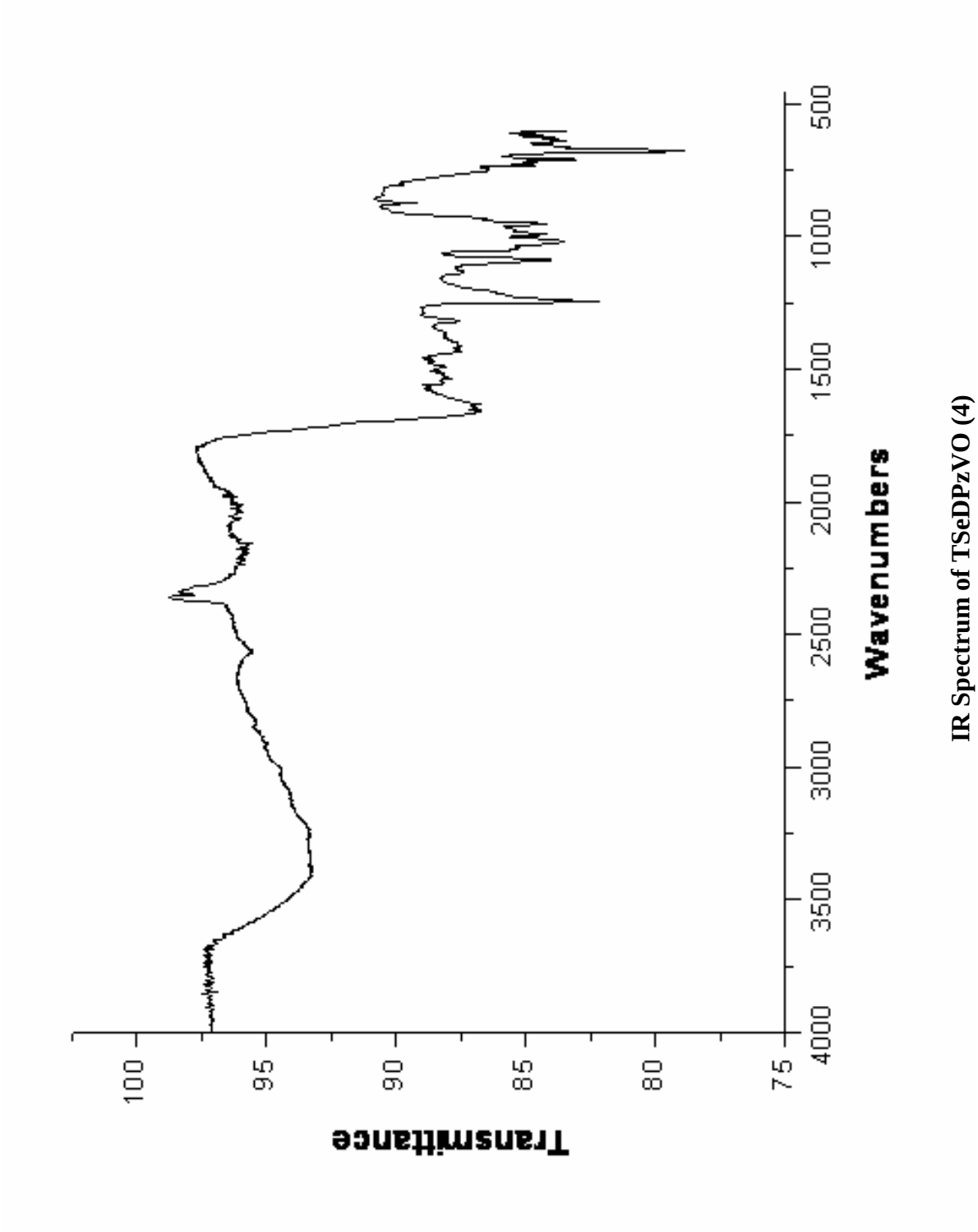

IR Spectrum of TSeDPzVO (4)

APPENDIX H

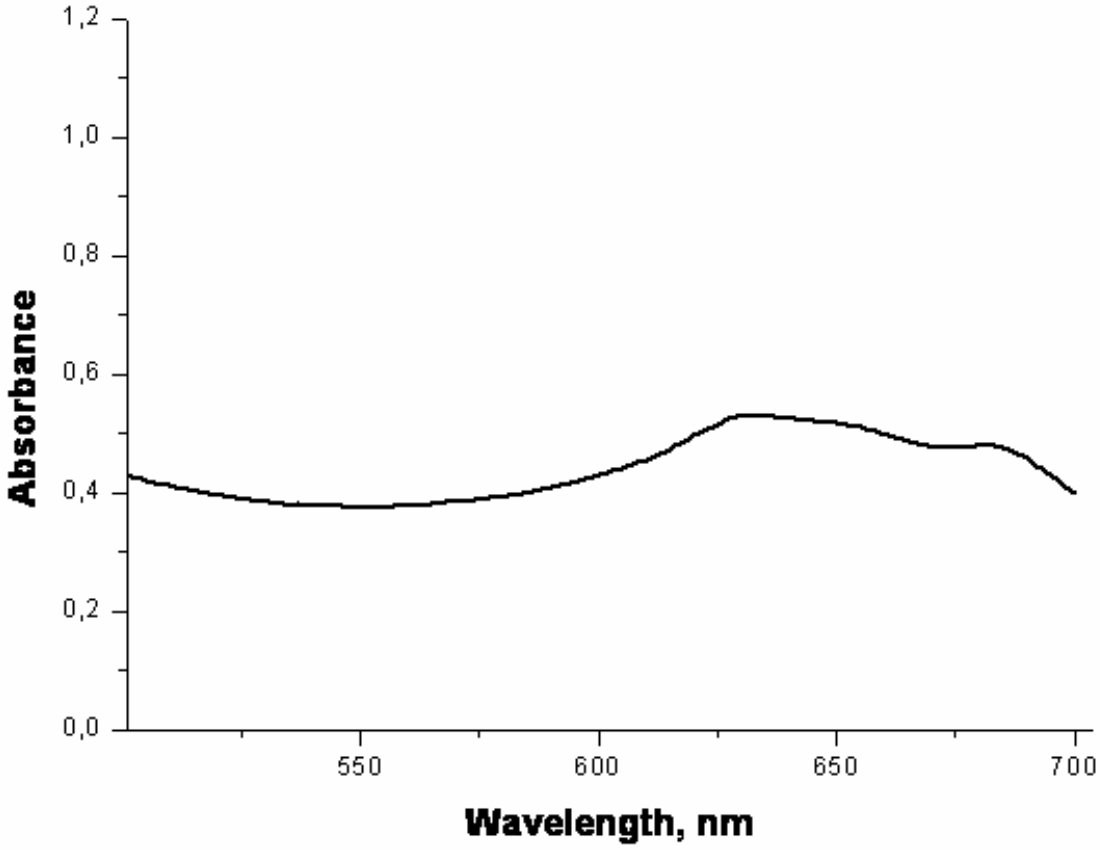

UV-VISIBLE Spectrum of TSeDPzVO (4) in DMSO

APPENDIX I

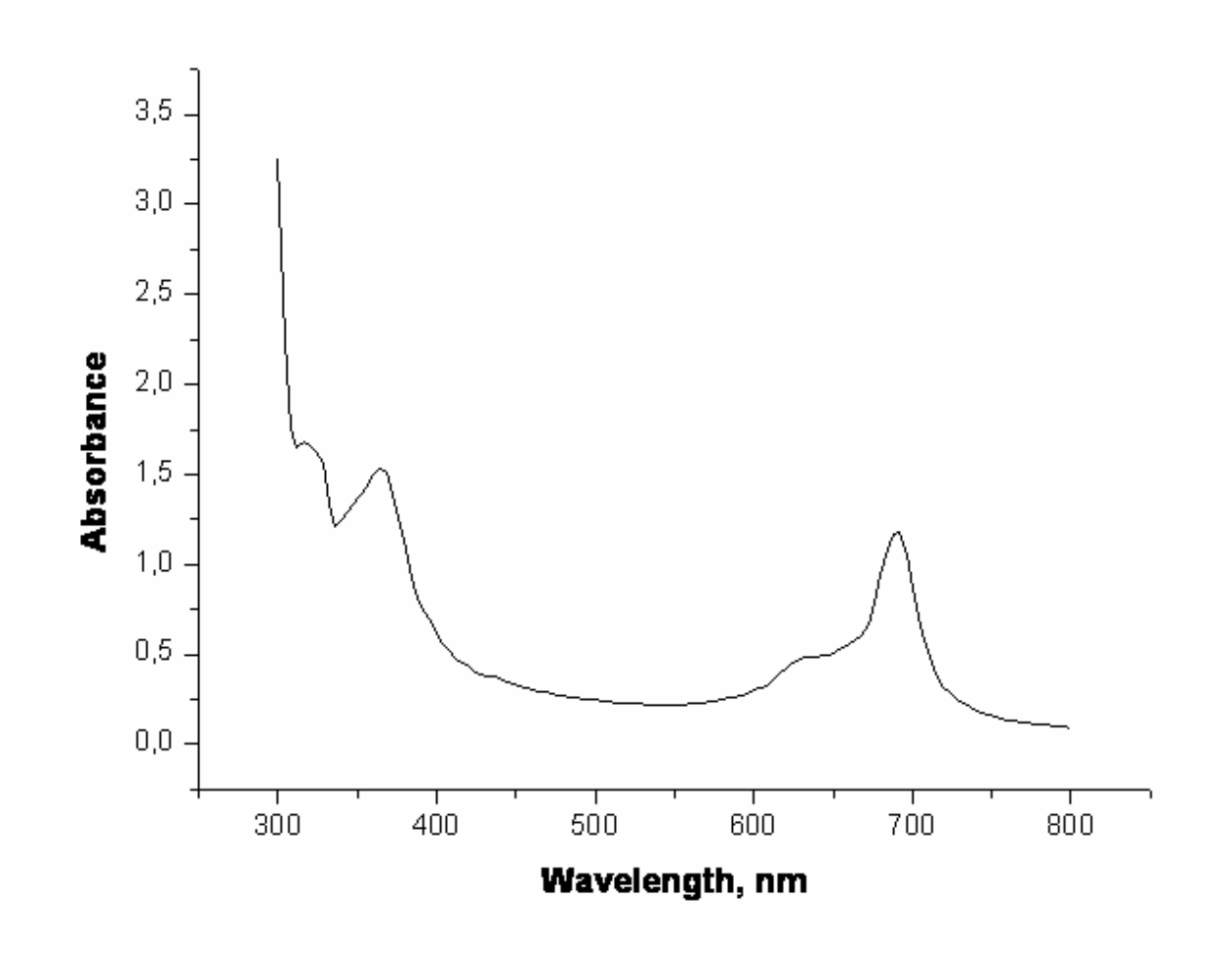

UV-VISIBLE Spectrum of TSeDPzVO (4) in Pyridine

APPENDIX J

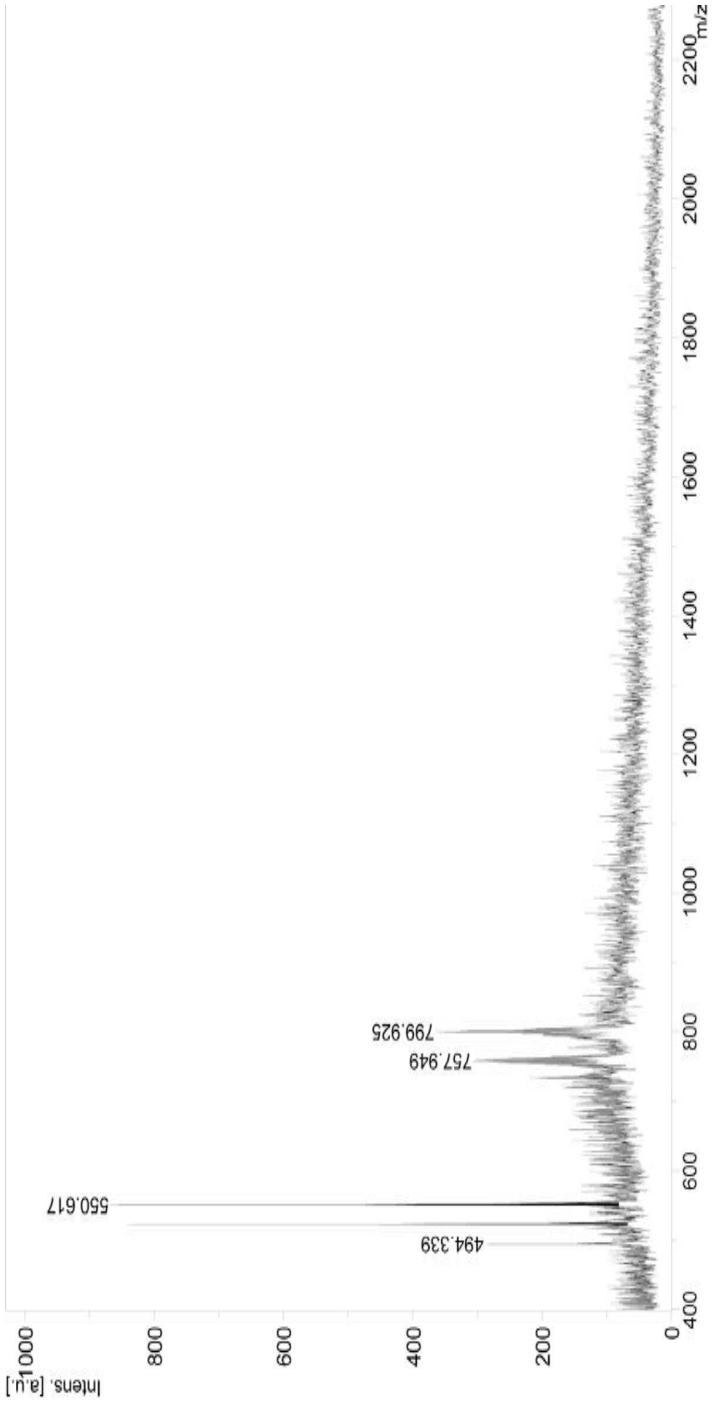

MALDI-MS Spectrum of TSeDPzVO (4)

APPENDIX K

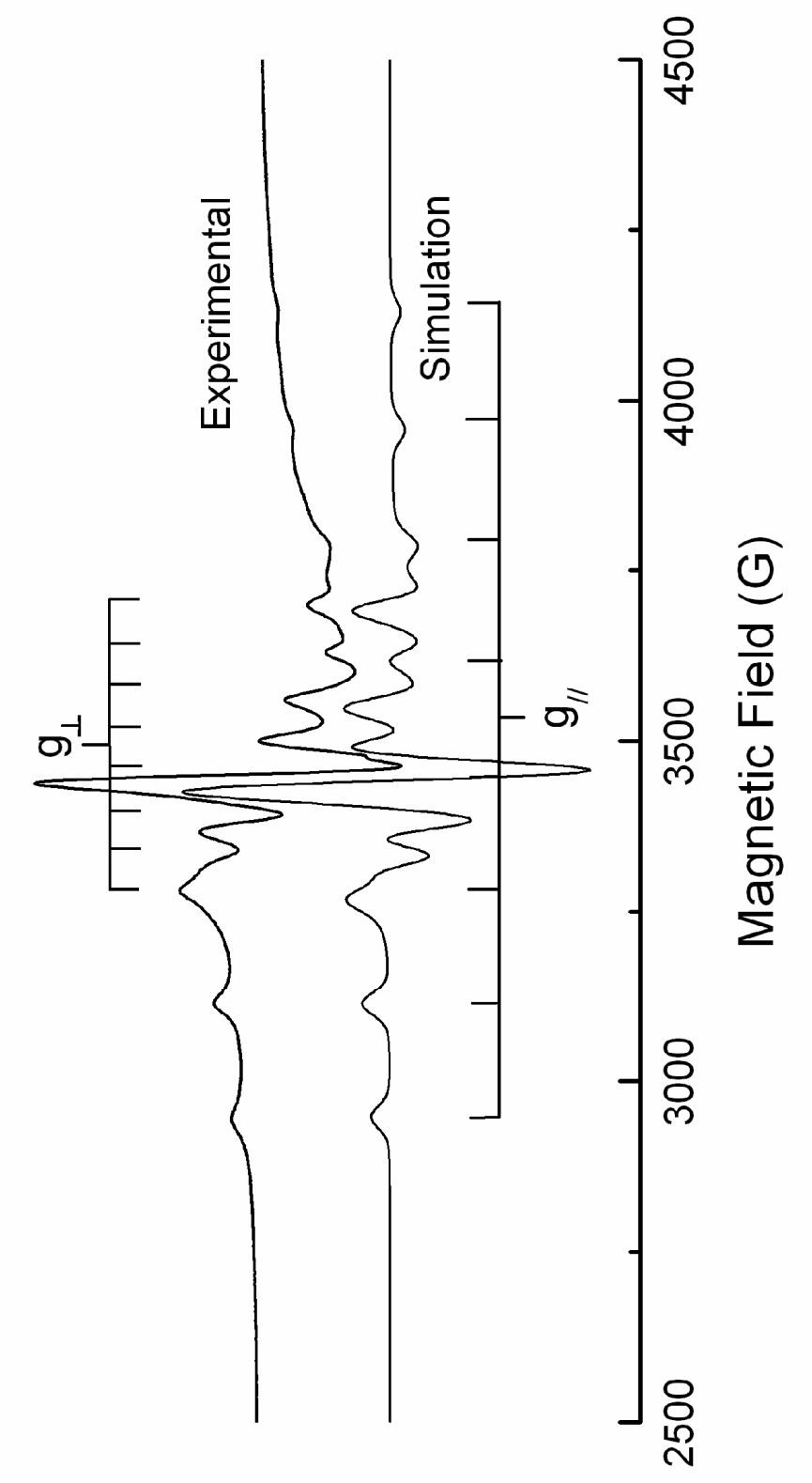

EPR Spectrum of TSeDPzVO (4)

APPENDIX L

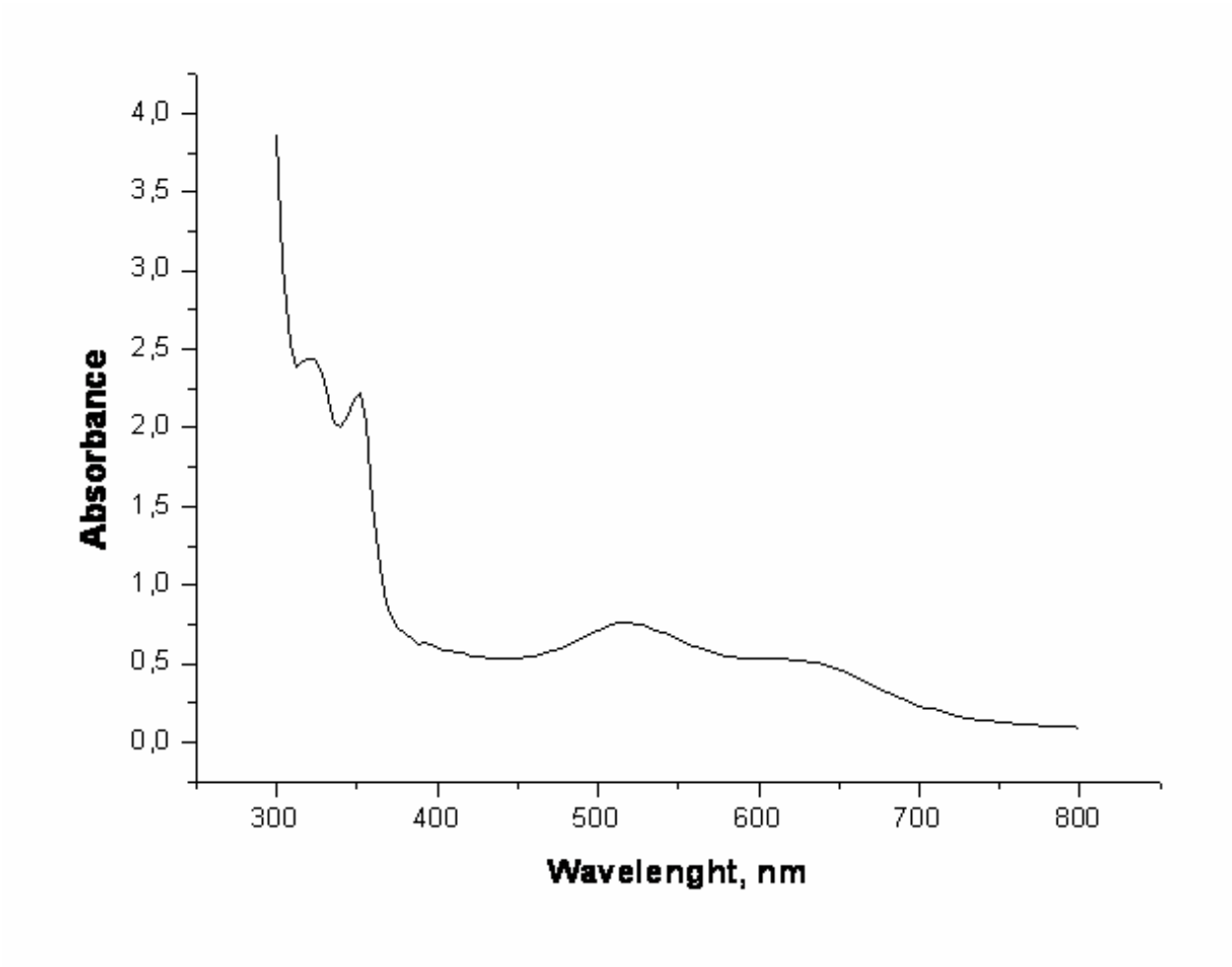

UV-VISIBLE Spectrum of $TSeDPzNH_2$ in Pyridine

APPENDIX M

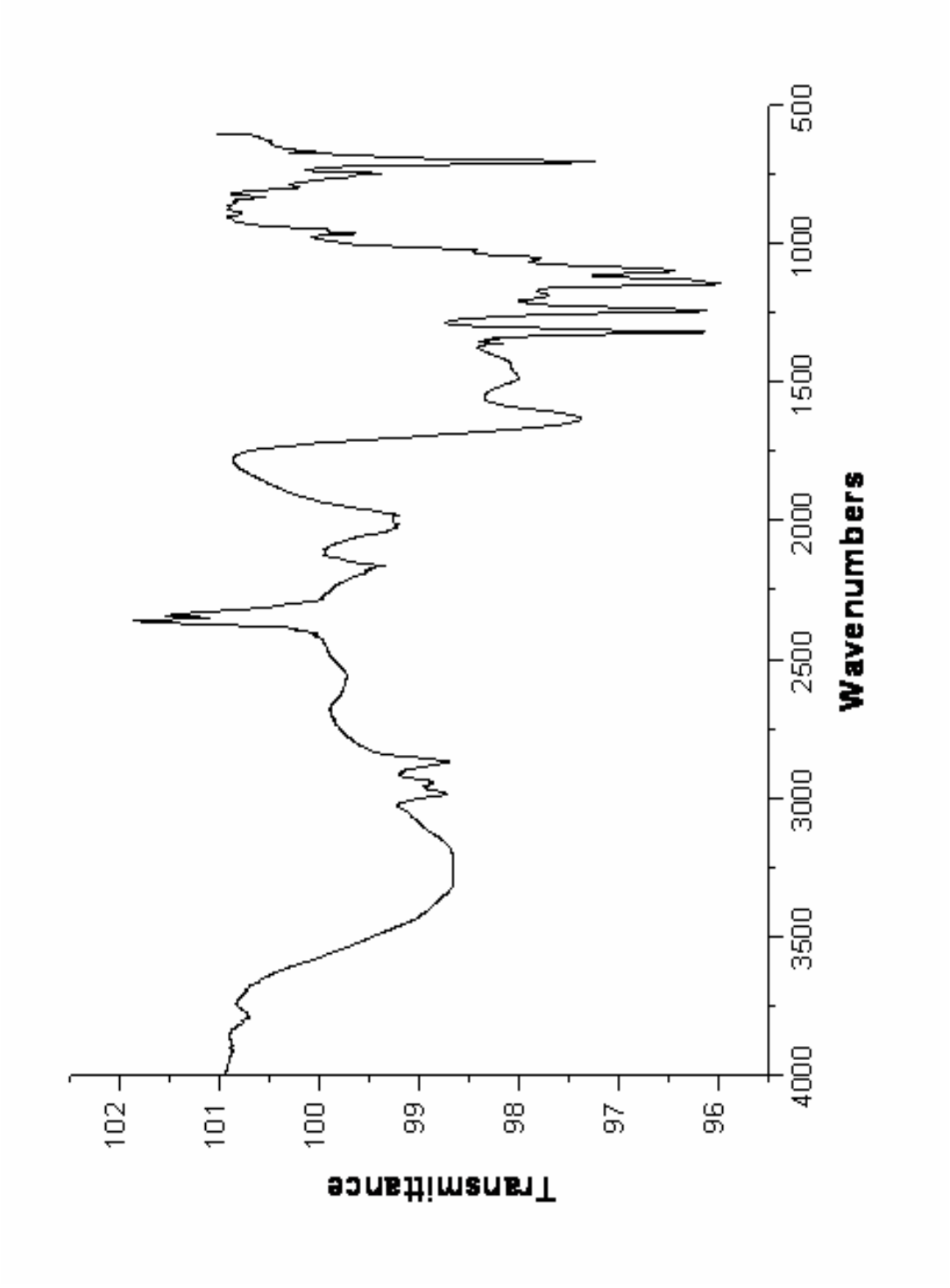

IR Spectrum of TCPyzPz (5a)

APPENDIX N

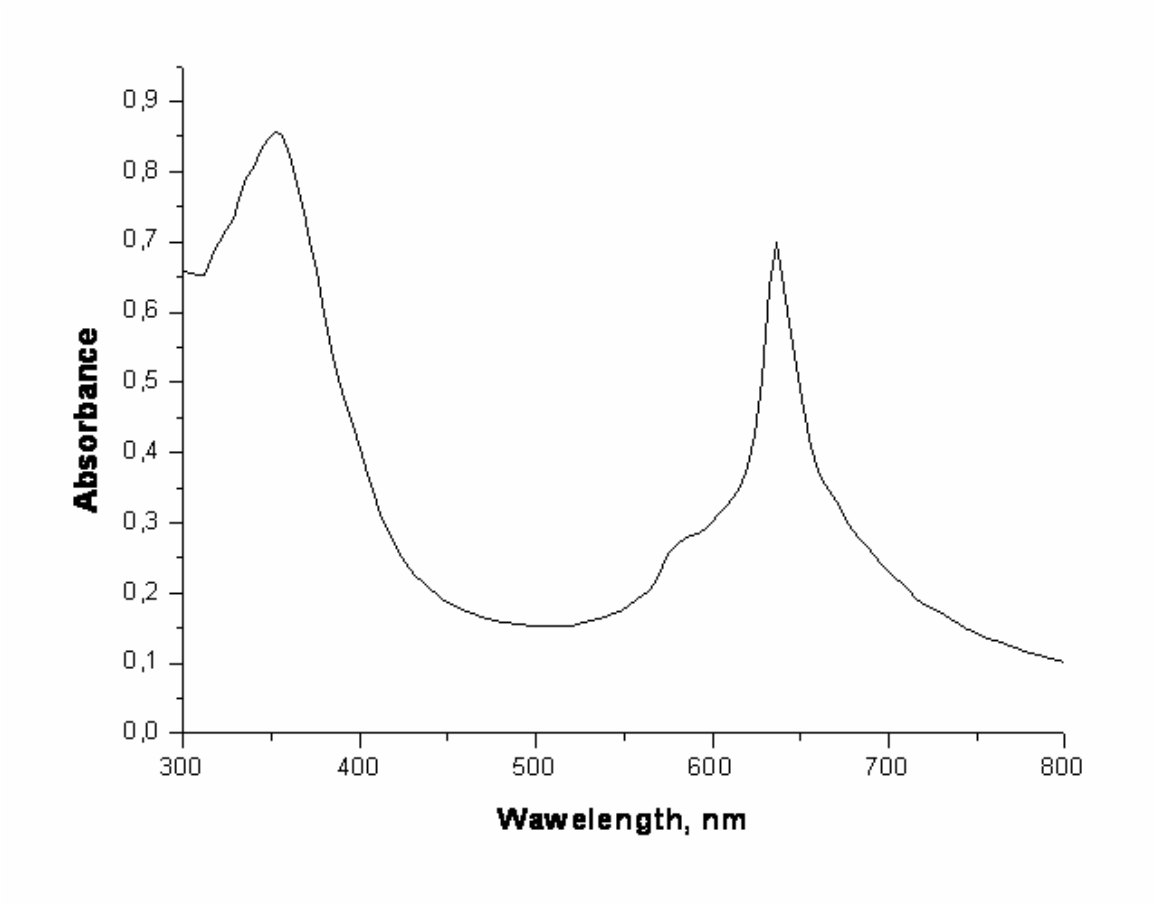

UV-VISIBLE Spectrum of TCPyzPz (5a) in DMSO

APPENDIX O

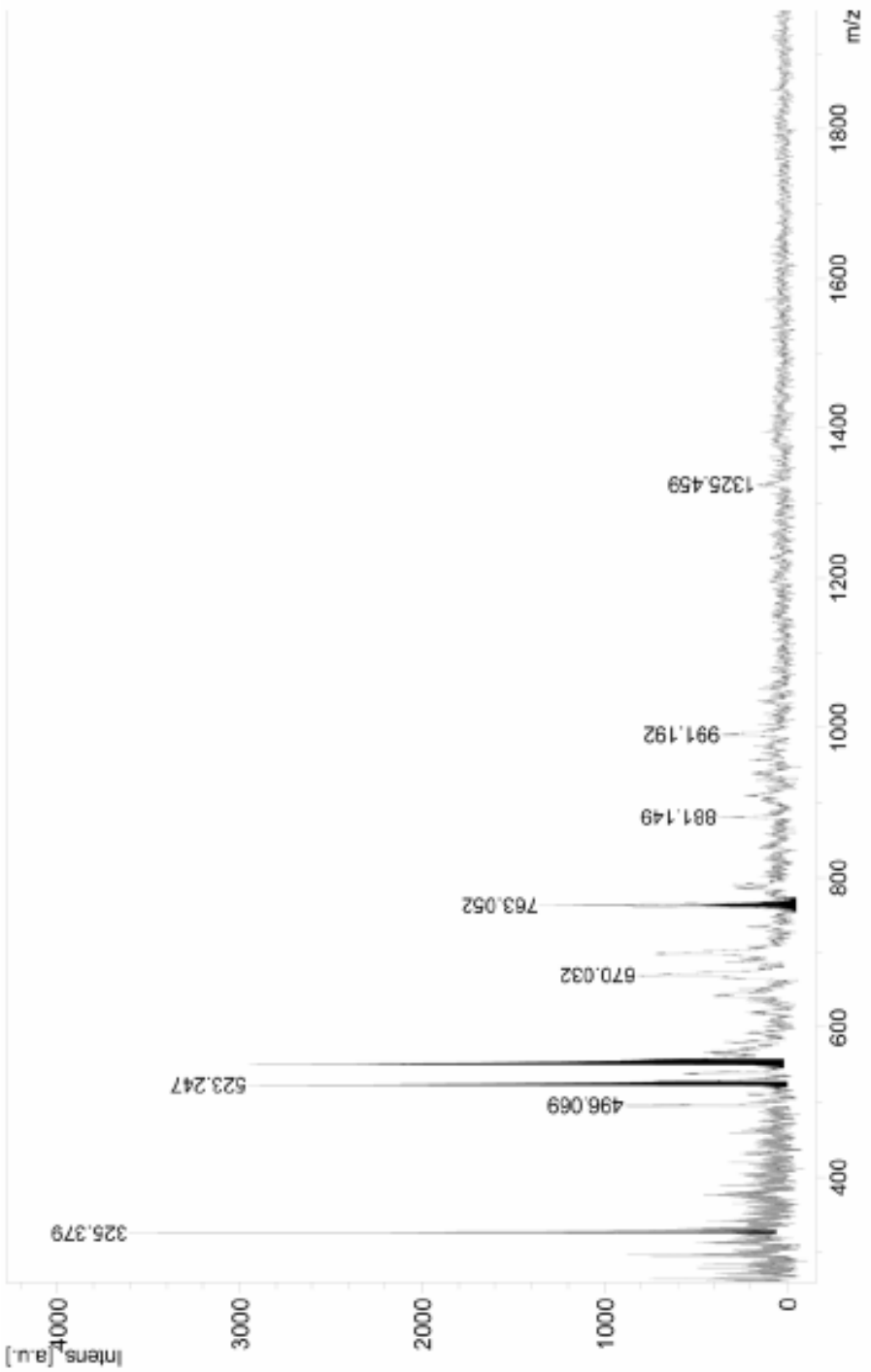

MALDI-MS Spectrum of TCPyzPz (5a)

APPENDIX P

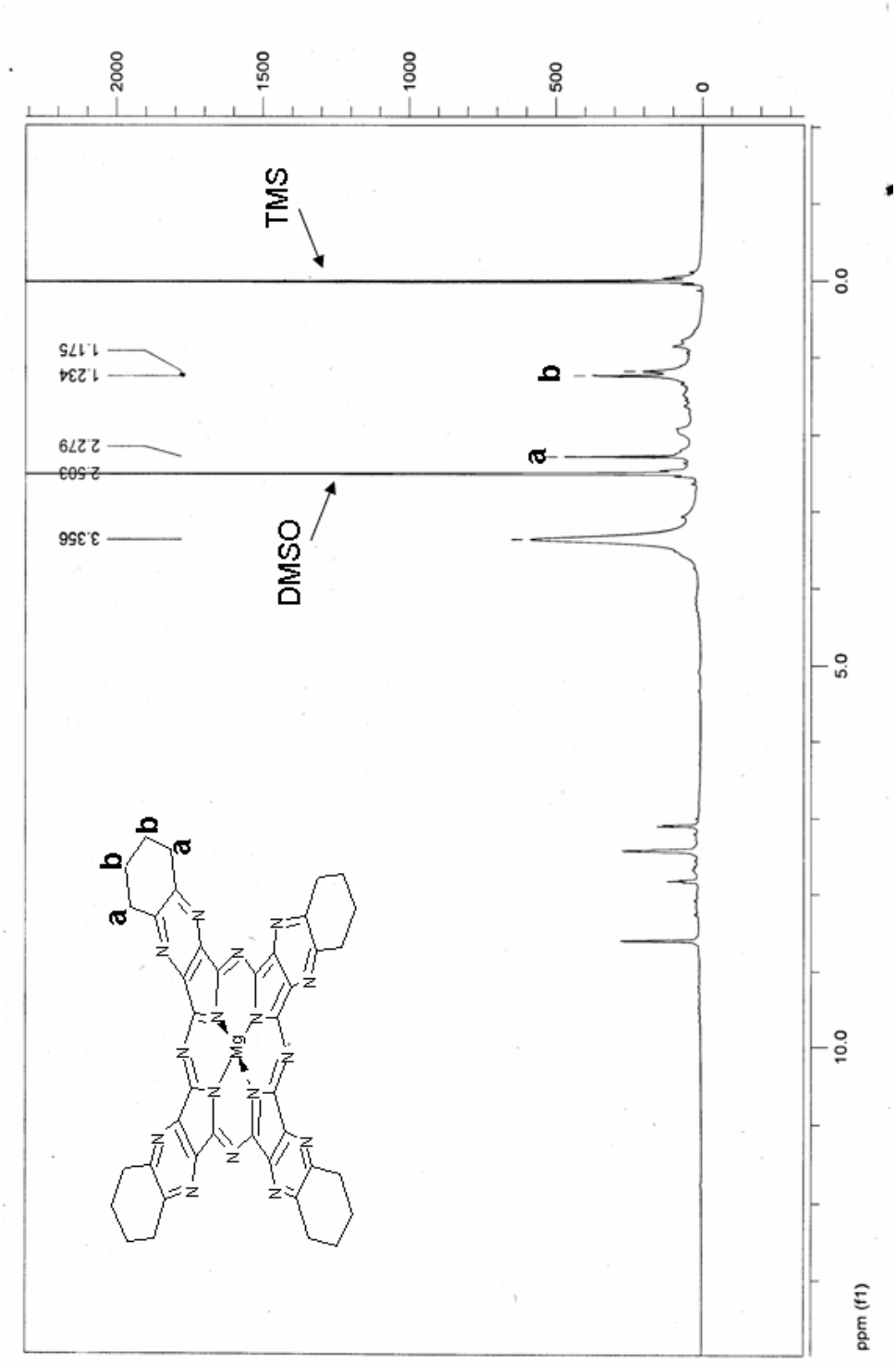

^{1}H-NMR-Spectrum of TCPyzPz (5a)

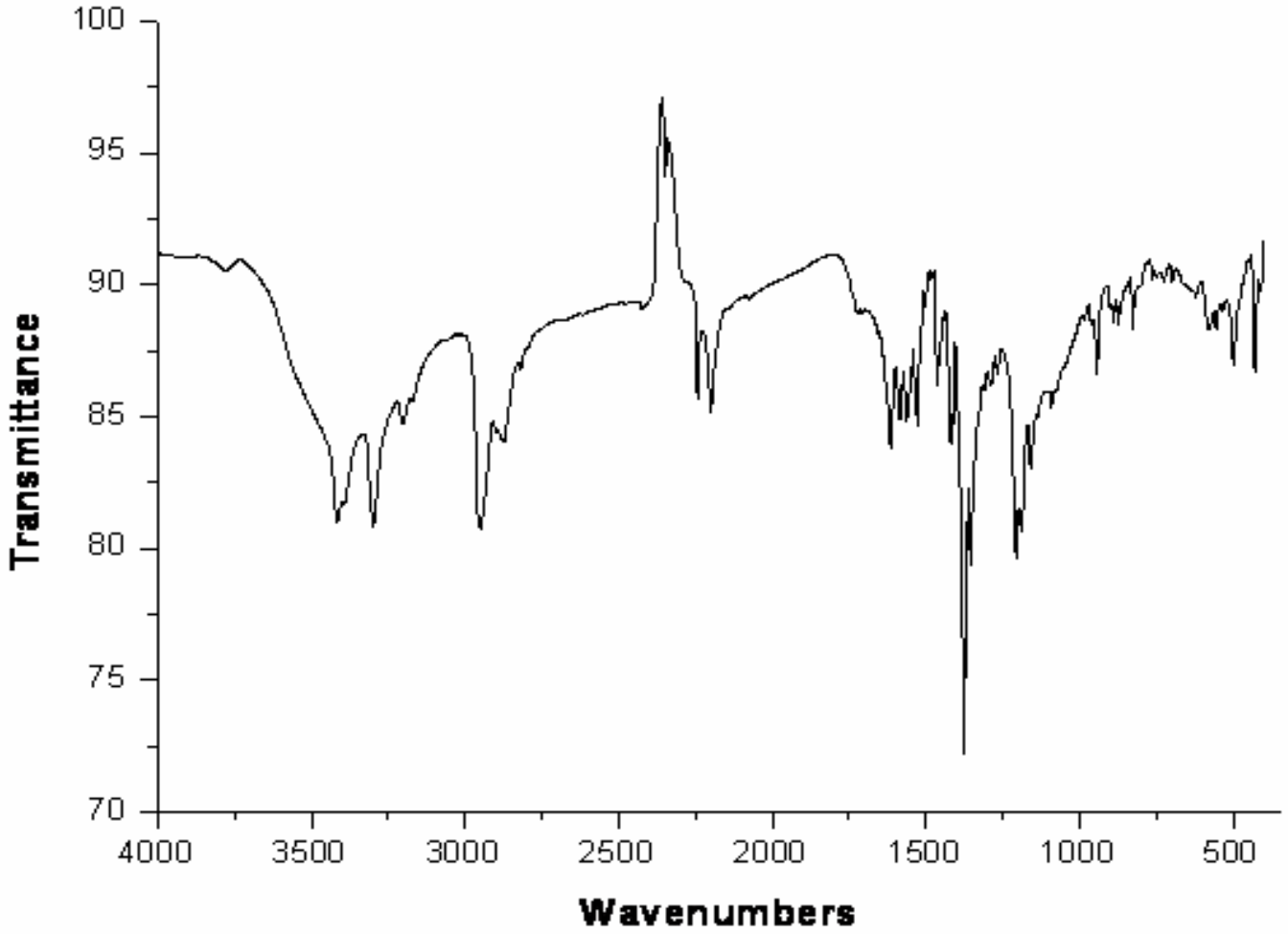

IR Spectrum of 2,3-dicyano-5,6-cyclohexapyrazine (6)

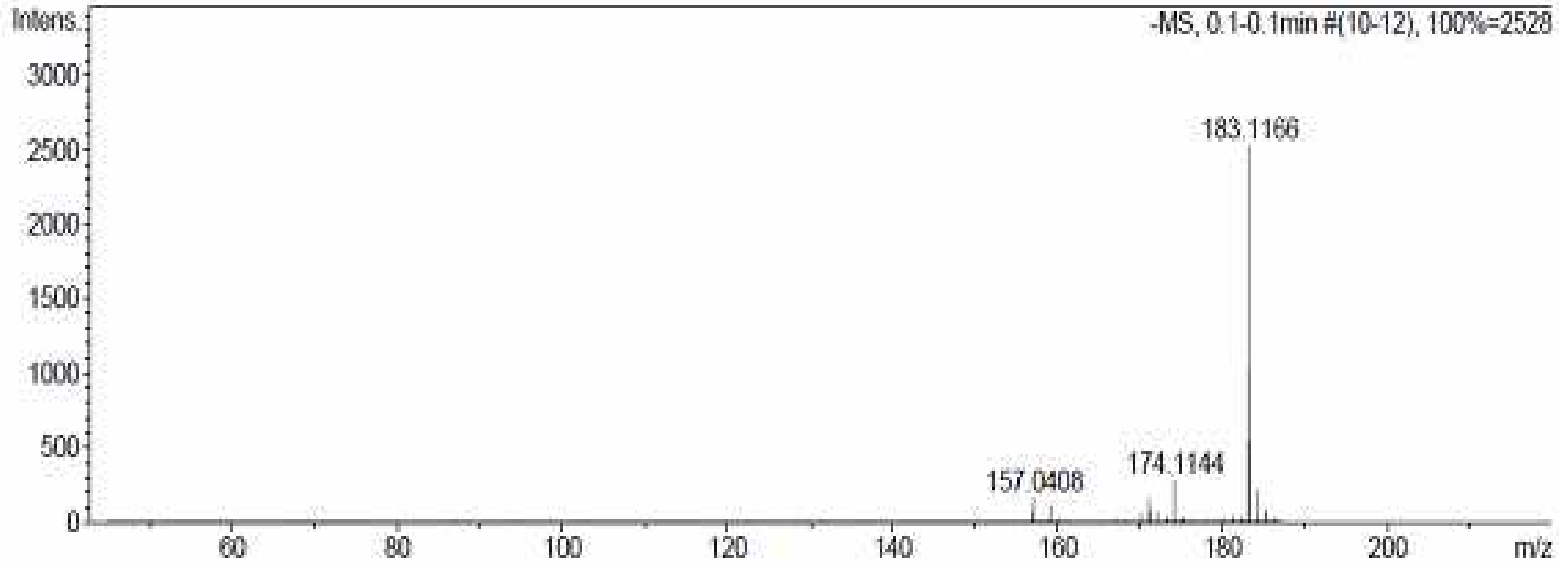

MALDI-MS Spectrum of 2,3-dicyano-5,6-cyclohexapyrazine (6)

APPENDIX S

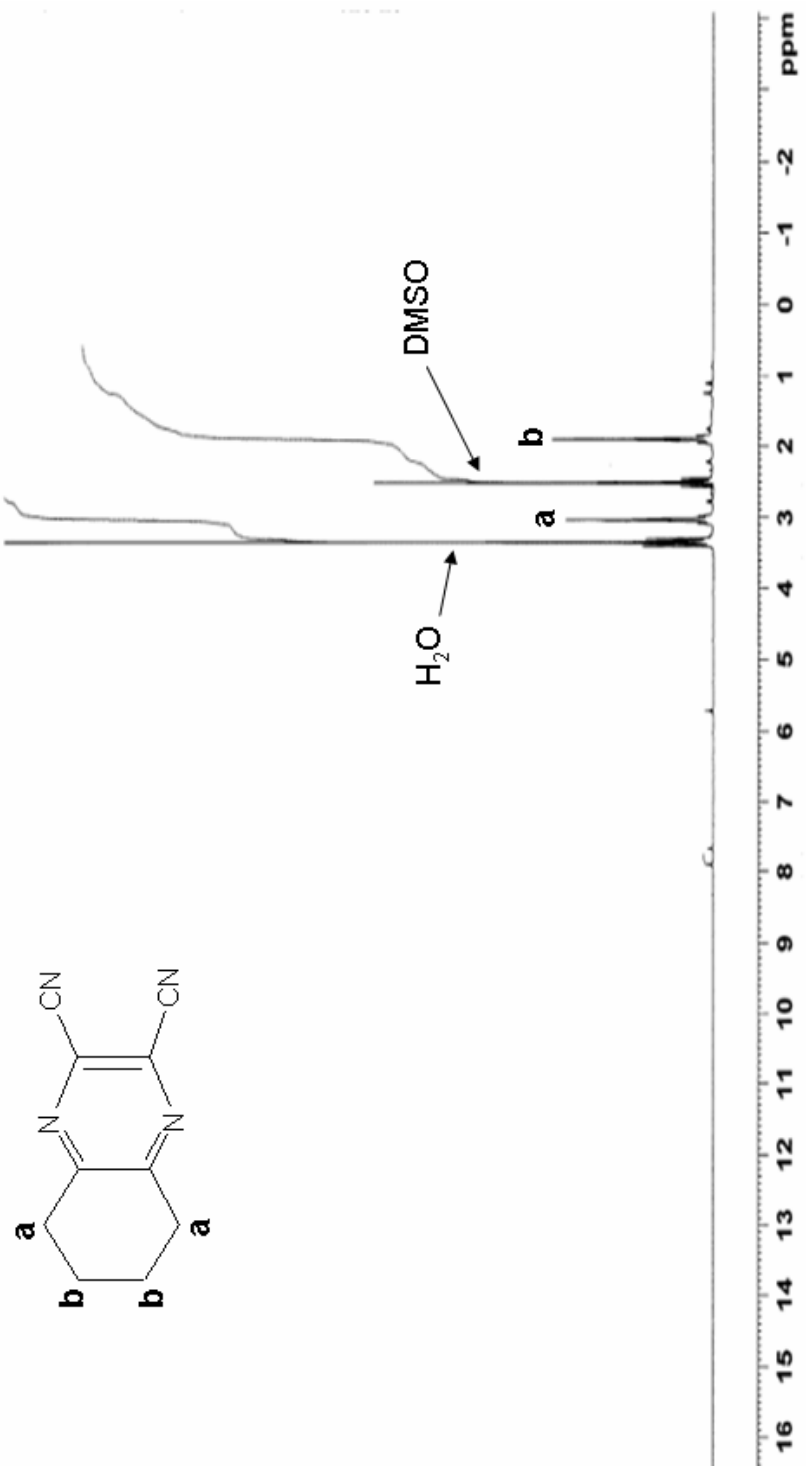

^{1}H-NMR-Spectrum of 2,3-dicyano-5,6-cyclohexapyrazine (6)

APPENDIX T

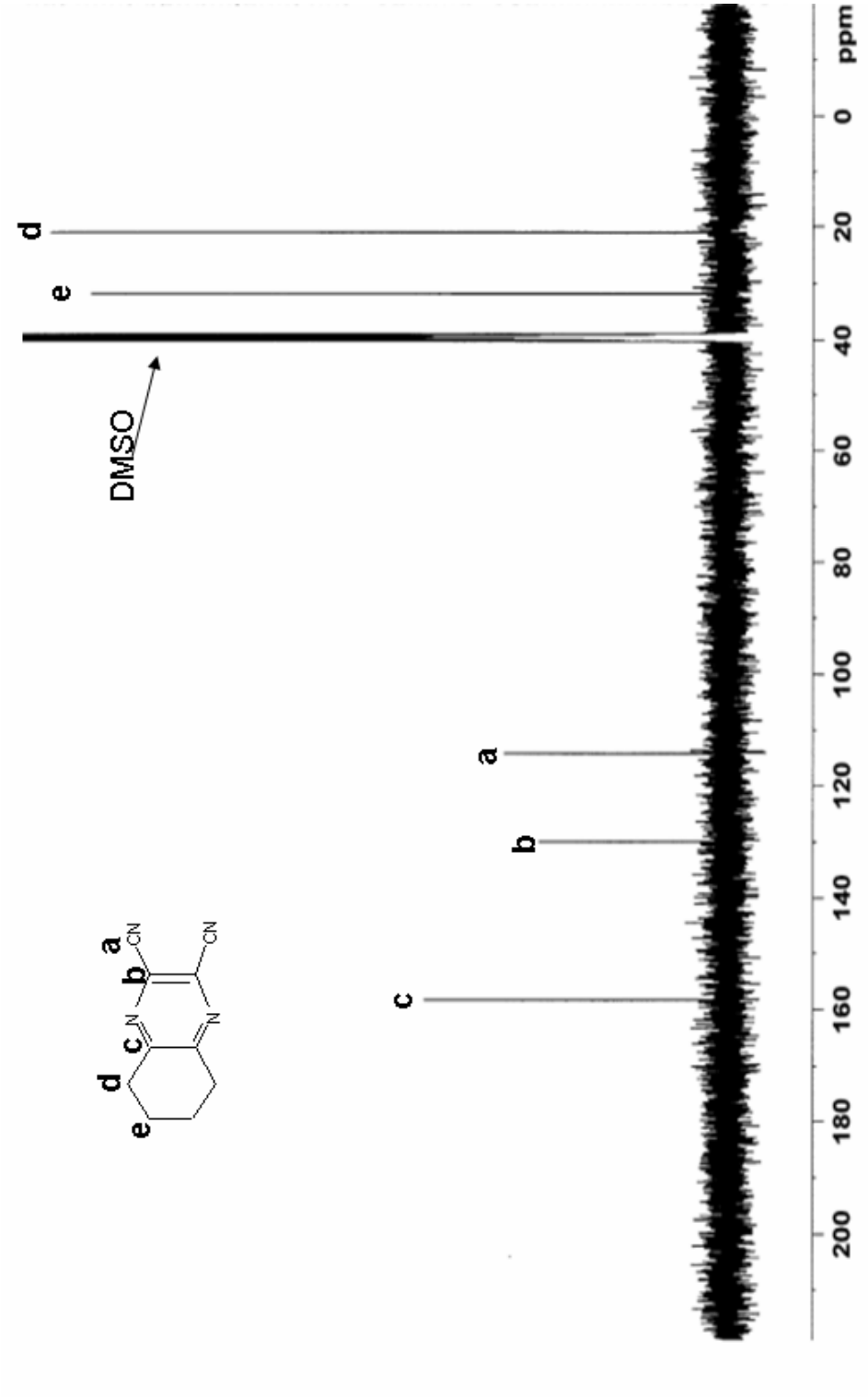

^{13}C-NMR-Spectrum of 2,3-dicyano-5,6-cyclohexapyrazine (6)

APPENDIX U

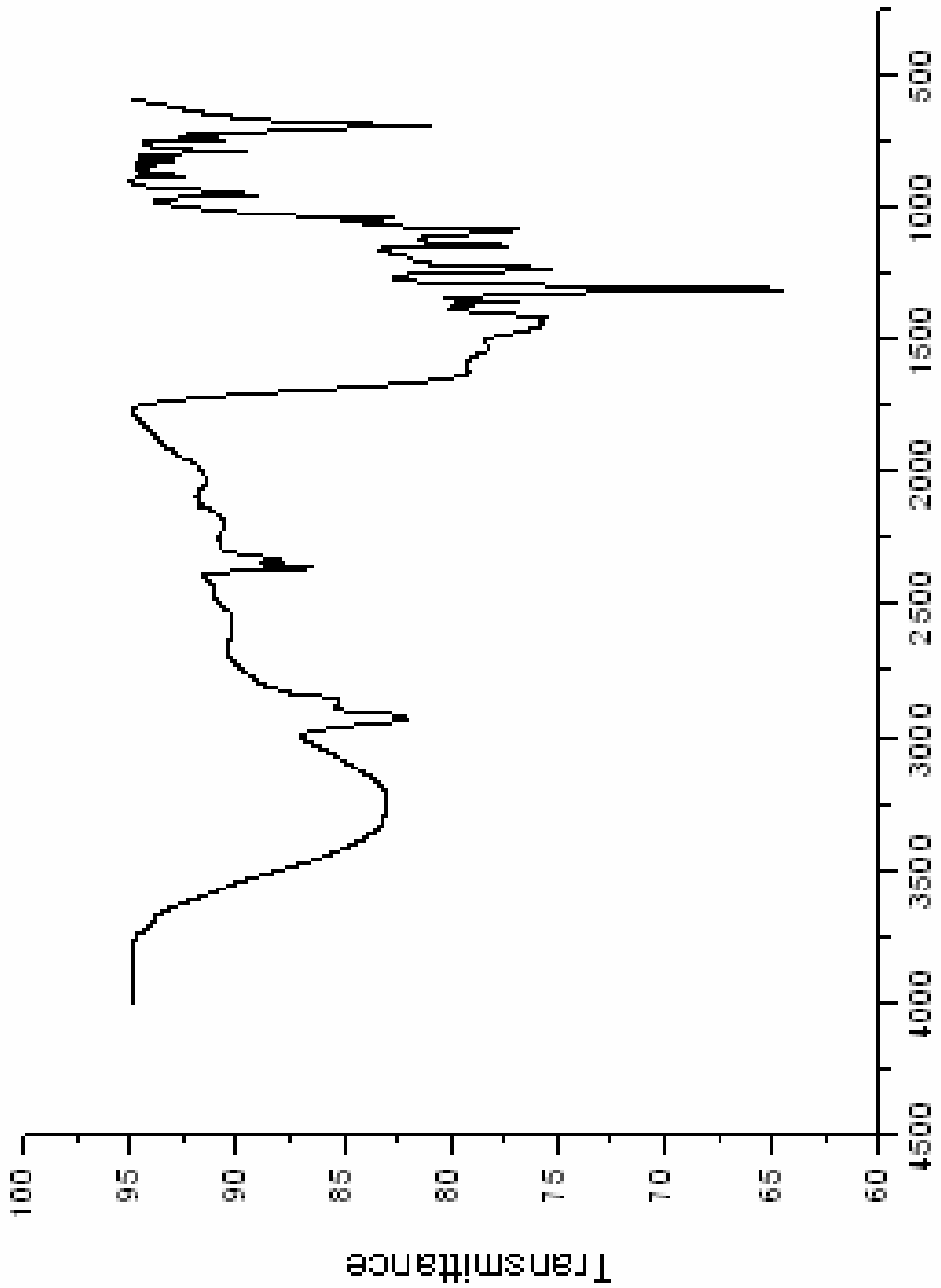

IR Spectrum of TCPyzPz (5b)

APPENDIX V

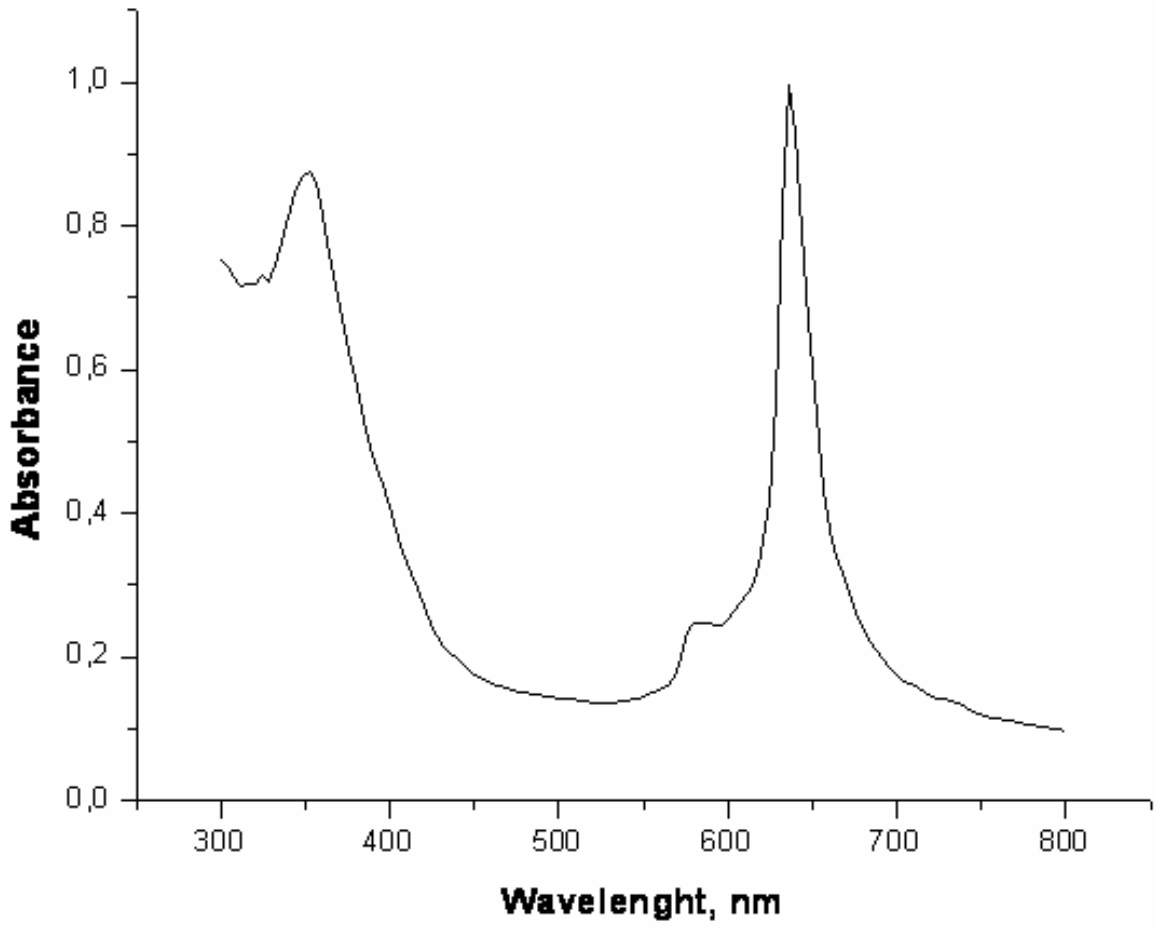

UV-VISIBLE Spectrum of TCPyzPz (5b) in DMSO

APPENDIX W

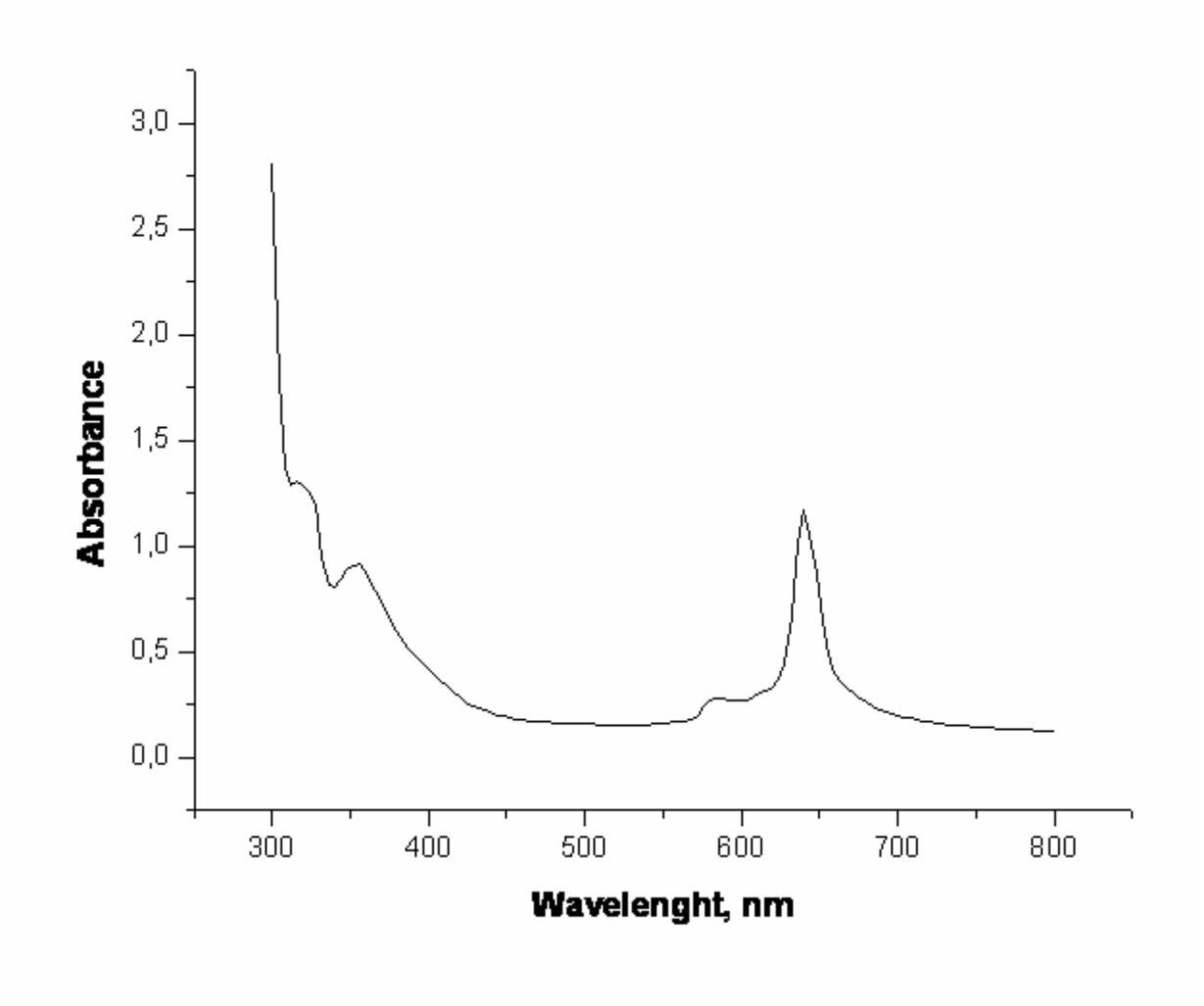

UV-VISIBLE Spectrum of TCPyzPz (5b) in Pyridine

APPENDIX X

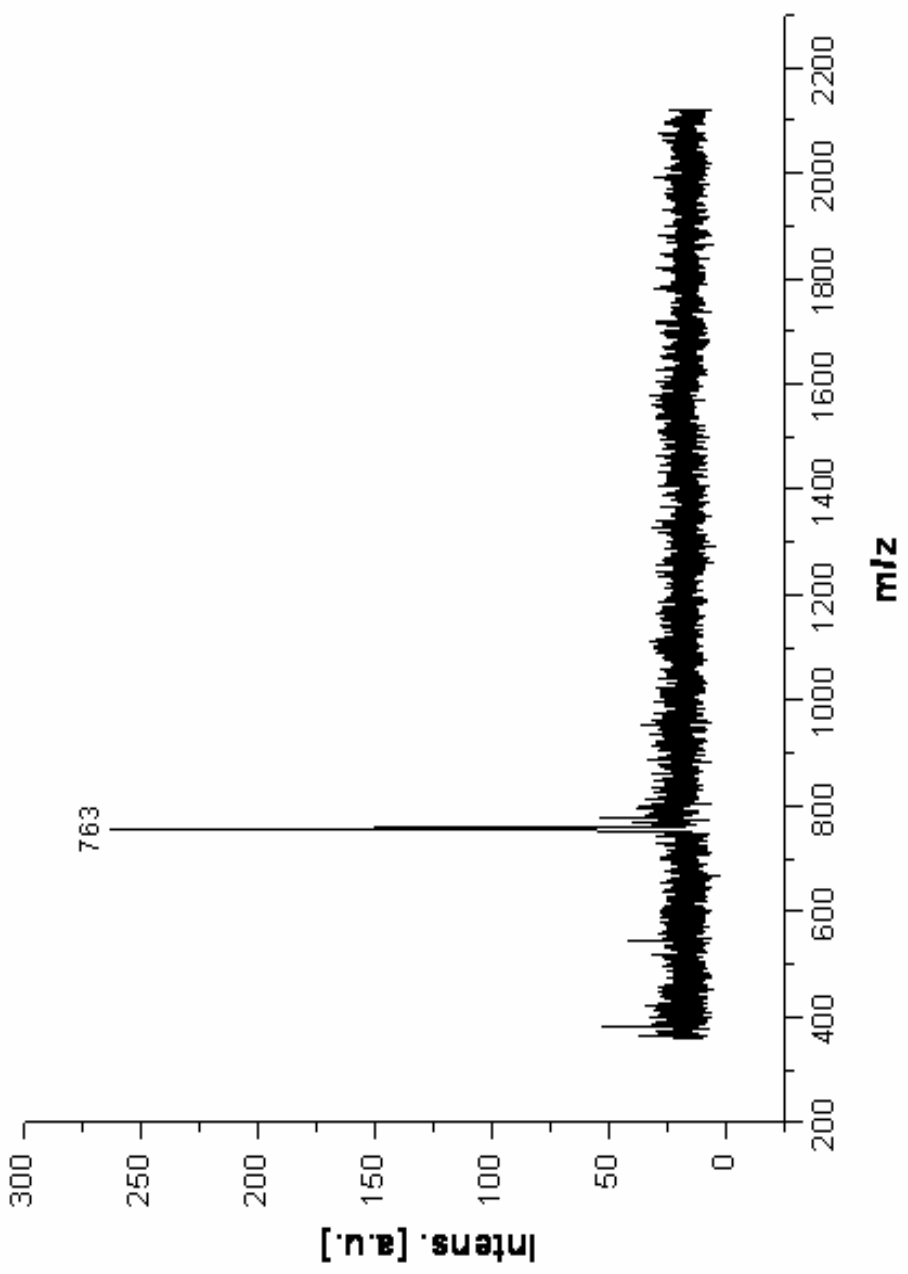

MALDI-MS Spectrum of TCPyzPz (5b)

APPENDIX Y

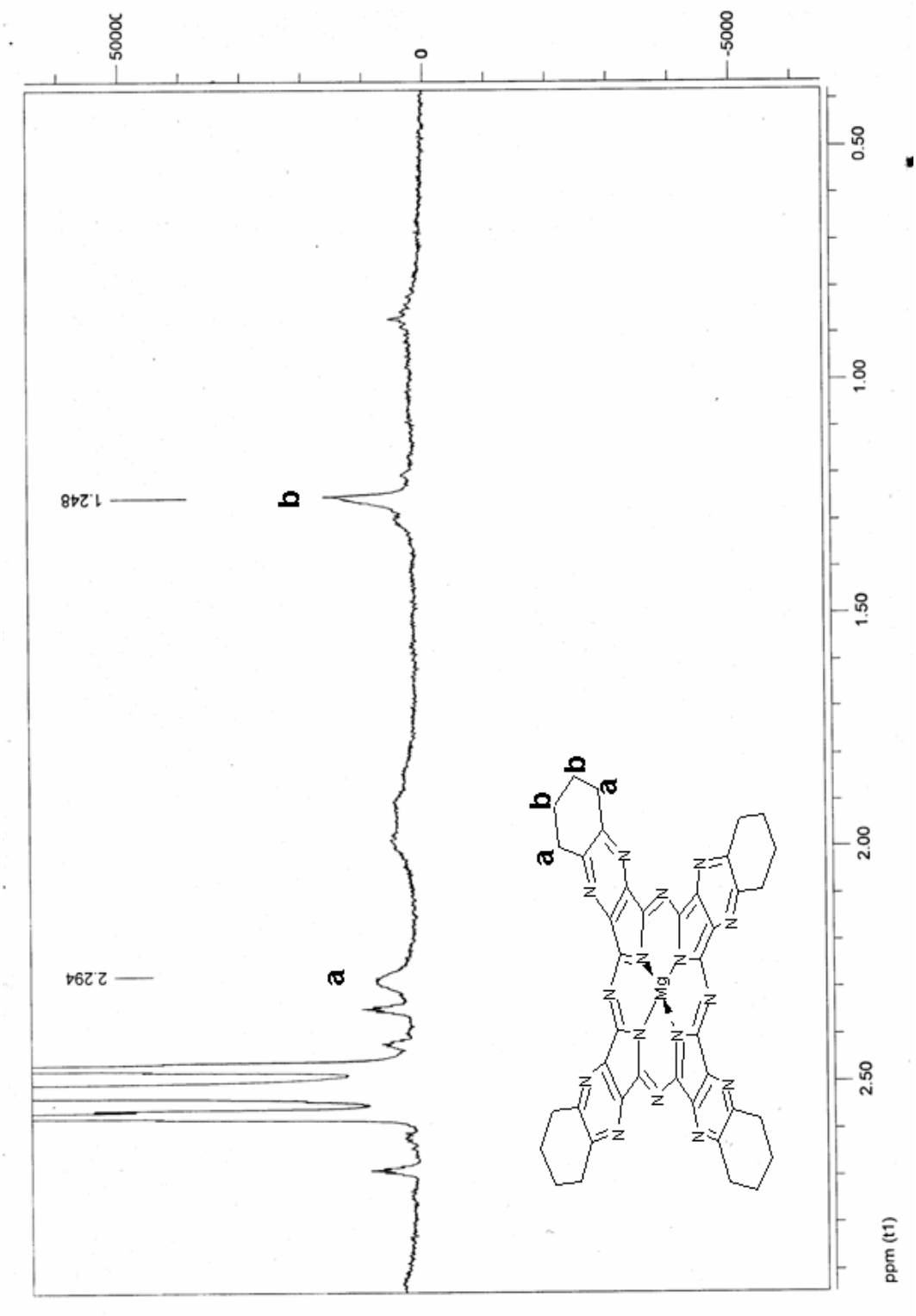

^{1}H-NMR-Spectrum of TCPyzPz (5b)